

## XXXIX Reunión de la Sociedad Española de Mineralogía XXVI Reunión de la Sociedad Española de Arcillas



**Continental sediment metal contamination by  
agricultural, industrial and mining activities:  
mineral processes and bioavailability**

**Baeza, 28 y 29 de junio de 2022**

**Editores:**

Rosario Jiménez Espinosa

Juan Jiménez Millán



**Seminarios de la Sociedad Española de  
Mineralogía  
Volumen 15**

---

**Continental sediment metal  
contamination by agricultural,  
industrial and mining activities:  
mineral processes and bioavailability**

**Seminario celebrado en la Sede Antonio Machado de la  
Universidad Internacional de Andalucía de la ciudad de  
Baeza (Jaén) el 28 y 29 de junio de 2022**

Editores:  
**Rosario Jiménez Espinosa  
Juan Jiménez Millán**

---



### Seminarios de la Sociedad de Española de Mineralogía

© Sociedad Española de Mineralogía  
Museo Geominero del Instituto  
Geológico y Minero de España  
Ríos Rosas, 23  
28003 Madrid

<http://www.semineral.es>

#### Editores

Rosario Jiménez Espinosa  
Juan Jiménez Millán

#### Diseño

Soma Dixital, S.L.

#### Maquetación

Nuria Sánchez Pastor

#### ISSN

2659-9872

#### NOTA EDITORIAL:

Las opiniones y los contenidos de los resúmenes publicados en este volumen son de responsabilidad exclusiva de los autores. Asimismo, éstos son responsables de obtener el permiso correspondiente para incluir material publicado en otro lugar, así como de citar convenientemente las fuentes utilizadas, exonerando a la Sociedad Española de Mineralogía y a los editores del Seminario de las responsabilidades que al respecto se puedan generar.



Drone photograph of the Laguna Honda saline wetland (Jaén) surrounded by olive groves.

Fotografía tomada con dron del humedal salino de Laguna Honda (Jaén) rodeada de olivares.

# Foreword

---

This volume presents the key notes of six invited lecturers to the Workshop on "Continental sediment metal contamination by agricultural, industrial and mining activities: mineral processes and bioavailability " held in the Antonio Machado Campus of the International University of Andalucía in Baeza (Jaén, Spain) on June 28 and 29, 2022, during the SEM-SEA 2022 congress, a joint meeting of the Spanish Mineralogical Society (SEM) and the Spanish Clay Society (SEA) organized by both societies, the International University of Andalucía and the University of Jaén. The meeting was coordinated by Isabel Abad and África Yebra (University of Jaén).

Sediments and soils from continental basins with intense human activity are a favorable environment for the concentration of natural nanomaterials (clays, oxides, sulfides), industrially designed nanomaterials (metallic nanoparticles of phytosanitary products, such as fungicides, herbicides...) and incidental nanomaterials formed by the reaction of anthropic nanomaterials with the environment (e.g. metal sulphides from industrial nanomaterials). This workshop aims to cover the important gaps in the knowledge about the interaction between the different types of nanoparticles and the influence of environmental conditions on the solubility, aggregation and mineral fixation of metal nanoparticle contaminants. The contributions integrating this volume evaluate if continental sediments have a relevant role in the natural attenuation of pollution and the design of solutions based on nature for the remediation of environmental pollution problems.

Michael Hochella Jr. reviewed in his plenary talk sources and impacts of natural nanomaterials, which are not created directly through human actions, incidental nanomaterials, which form unintentionally during human activities and engineered nanomaterials, which are created for specific applications. Knowledge of the properties of all three types as they cycle through the Earth system is essential for understanding and mitigating their long-term impacts on the environment and human health.

Rosario Jiménez Espinosa and Juan Jiménez Millán aim to show the influence of the microorganisms on the main reactions involving clays and other minerals associated to the metal nanoparticle fixation, reviewing the sources of salinity and metal enrichment in wetlands from the Chicamocha Basin (Colombia) and the most important bacterial communities developed in the organic matter rich sediments deposited in these environments.

The contribution by Julián Martínez, Rosendo Mendoza, María José De La Torre, Vicente López Sánchez-Vizcaíno, María José Campos Suñol and Rosario Jiménez Espinosa describes the metal pollution on the hydrographic network of the abandoned Linares Mining District (Spain), which was visited in a field trip integrated in the workshop.

The lecture of Tibor Németh gives an insight through some examples into the change of metal sorption with the alteration of clay minerals in soils and sediments which is useful for researchers working on metal contamination issues.

# Foreword

---

The manuscript by Rafael Pérez-López, Sergio Carrero, Ricardo Millán-Becerro, María D. Basallote, Francisco Macías, Carlos R. Cánovas and José M. Nieto focuses on the geochemical processes involving metal mobility in acid mine drainage-impacted waters occurring in the Tinto and Odiel rivers as well as in the Huelva Estuary (Spain), which are extensible to other mining districts in the world where AMD-affected fluvial courses reach seawater.

Beata Smieja-Król summarizes the current state of knowledge on the biogenic sulfide formation in wetlands and its role in metal sequestration, as well as the implications of sulfide formation in the water-saturated contaminated sites producing anthropogenic metal accumulations similar to known from geological records.

We want to acknowledge the collaboration and enthusiasm of the authors to provide us their communications and make possible the publication of this volume.

**Rosario Jiménez Espinosa**  
**Juan Jiménez Millán**

# Index / Índice

---

1

**The impact of nanomaterials on the Earth systems**

**El impacto de los nanomateriales en los sistemas de la Tierra**

*Michael F. Hochella Jr.*

3

**Reactivity of clays and metal nanomaterials in waters and sediments from saline wetlands: the role of the bacterial communities**

**Reactividad de arcillas y nanomateriales metálicos en aguas y sedimentos de humedales salinos: el papel de las comunidades bacterianas**

*Rosario Jiménez Espinosa, Juan Jiménez Millán*

16

**Metal pollution in hydrographic networks of abandoned mining basins: The case of Linares Mining District (SE Spain)**

**Contaminación por metales en redes hidrográficas de cuencas mineras abandonadas: El caso del Distrito Minero de Linares (SE de España)**

*Julián Martínez, Rosendo Mendoza, María José De La Torre, Vicente López Sánchez-Vizcaíno, María José Campos Suñol, Rosario Jiménez Espinosa*

25

**Metal sorption processes by clay minerals in soil and sediments**

**Procesos de adsorción de metales por minerales arcillosos en suelos y sedimentos**

*Tibor Nemeth*

30

**Metal mobility in acid mine drainage-impacted waters: from rivers to oceans**

**Movilidad de metales en aguas impactadas por drenaje ácido de minas: de ríos a océanos**

*Rafael Pérez-López, Sergio Carrero, Ricardo Millán-Becerro, María D. Basallote, Francisco Macías, Carlos R. Cánovas, José M. Nieto*

43

**Industrial trace element contamination in wetlands: the effect of the precipitation of biogenic sulfides**

**Contaminación por elementos traza industriales en humedales: el efecto de la precipitación de sulfuros biogénicos**

*Beata Smieja-Król*

# The impact of nanomaterials on Earth systems

Michael F. Hochella, Jr. (1)

(1) University Distinguished Professor (Emeritus), Department of Geosciences, Virginia Tech, Blacksburg, VA, USA.

## *Abstract*

As our group has written about before, particularly in our highly cited Science article (Hochella et al., 2019), nanomaterials are critical components in the Earth system's past, present, and future characteristics and behavior. They have been present since Earth's origin in great abundance. Life, from the earliest cells to modern humans, has evolved in intimate association with naturally occurring nanomaterials. This synergy began to shift considerably with human industrialization. Particularly since the Industrial Revolution some two-and-a-half centuries ago, incidental nanomaterials (produced unintentionally by human activity) have been continuously produced and distributed worldwide. In some areas, they now rival the amount of naturally occurring nanomaterials. In the past half-century, engineered nanomaterials have been produced in very small amounts relative to the other two types of nanomaterials, but still in large enough quantities to make them a consequential component of the planet. All nanomaterials, regardless of their origin, have distinct chemical and physical properties throughout their size range, clearly setting them apart from their macroscopic equivalents and necessitating careful study. Following major advances in experimental, computational, analytical, and field approaches, it is becoming possible to better assess and understand all types and origins of nanomaterials in the Earth system. It is also now possible to frame their immediate and long-term impact on environmental and human health at local, regional, and global scales.

For this symposium on the topic of metal contamination by agricultural, industrial and mining activities, and especially mineral processes and bioavailability, I have chosen two examples from our work that are particularly relevant to this theme. The first example is from the Clark Fork River Superfund Complex (western Montana, USA) which is the largest contaminated site in the United States apart from the nuclear fuel/weapons-contaminated sites managed by the U.S. Department of Energy. The Clark Fork contamination is due to base-metal mining that started in this area in the 1860's. Considerable amounts of metals (mainly Pb, Zn, Cu, and As) at toxic concentrations were spread atmospherically, and also distributed down hydrologic gradient from the original mining areas. Extensive transmission electron microscopy (TEM) observations revealed for the first time the key secondary mineral formation as a result of the breakdown of sulfides and silicates in oxic, acidic soil-sediment-solution environments. It was determined that the contaminant metals were taken up by several nanoscale secondary iron and manganese oxide minerals and amorphous aluminosilicates. Clays also carried significant amounts of Cu and Zn.

In a second example of the nanoscience principals given above, we have discovered that burning coal generates large quantities of otherwise rare Magnéli phase titanium suboxides in the nanosize domain from macroscopic TiO<sub>2</sub> minerals naturally present in coal. These nanoscale Magnéli phases, which we have shown now to be spread globally via atmospheric transport, are toxic to mammalian airways and lungs, including in humans. Therefore, these incidental nanophases are likely a significant environmental pollutant, especially in geographic regions where coal combustion is a major contributor to atmospheric particulate matter. It is clear that further toxicology studies are necessary and future assessments of the impact of these nanoparticles on human health is warranted.

## *Resumen*

Tal y como ha publicado previamente nuestro grupo, particularmente en nuestro artículo altamente citado de Science (Hochella et al., 2019), los nanomateriales son componentes críticos para las características y el comportamiento pasado, presente y futuro del sistema de la Tierra. Han estado presentes desde el origen de la Tierra en gran abundancia. La vida, desde las primeras células hasta los humanos modernos, ha evolucionado en íntima asociación con los nanomateriales naturales. Esta sinergia comenzó a cambiar considerablemente con la industrialización humana. Particularmente, desde la Revolución Industrial hace unos dos siglos y medio, los nanomateriales incidentales (producidos de forma no intencional por la actividad humana) se han producido y distribuido continuamente en todo el mundo. En algunas áreas, ahora rivalizan en cantidad con los nanomateriales naturales. En el último medio siglo, los nanomateriales de ingeniería se han producido en cantidades muy pequeñas en relación

a los otros dos tipos de nanomateriales, pero en cantidades lo suficientemente importantes como para convertirlos en un componente importante del planeta. Todos los nanomateriales, independientemente de su origen, tienen distintas propiedades químicas y físicas en todo su rango de tamaño, lo que los distingue claramente de sus equivalentes macroscópicos y requiere un estudio cuidadoso. Tras los importantes avances en los enfoques experimentales, computacionales, analíticos y de campo, cada vez es posible evaluar y comprender mejor todos los tipos y orígenes de los nanomateriales en el sistema terrestre. Ahora también es posible enmarcar su impacto inmediato y a largo plazo en la salud ambiental y humana a escala local, regional y mundial.

Para este simposio sobre el tema de la contaminación de metales por actividades agrícolas, industriales y mineras, y especialmente los procesos minerales y la biodisponibilidad, he elegido dos ejemplos de nuestro trabajo que son particularmente relevantes para este tema. El primer ejemplo es del complejo Superfund del río Clark Fork (oeste de Montana, EE. UU.), que es el mayor lugar contaminado de los Estados Unidos, sin considerar los lugares contaminados con armas o combustibles nucleares administrados por el Departamento de Energía de los EE. UU. La contaminación de Clark Fork se debe a la minería de metales básicos que comenzó en esta área en la década de 1860. Cantidades considerables de metales (principalmente Pb, Zn, Cu y As) en concentraciones tóxicas se dispersaron atmosféricamente y también se distribuyeron por gradiente hidrológico desde las áreas mineras originales. Las observaciones de microscopía electrónica de transmisión (TEM) revelaron por primera vez la formación de minerales secundarios clave como resultado de la descomposición de sulfuros y silicatos en soluciones suelo-sedimento con ambientes oxidantes y ácidos. Se determinó que los metales contaminantes fueron absorbidos a nanoescala por varios minerales secundarios del grupo de los óxidos de hierro y manganeso y aluminosilicatos amorfos. Las arcillas también contenían cantidades significativas de Cu y Zn.

En un segundo ejemplo de los principios de la nanociencia comentados anteriormente, hemos descubierto que la quema de carbón genera grandes cantidades de subóxidos de titanio de fase Magnéli, que de otro modo serían raros, en el dominio de tamaño nanométrico a partir de minerales macroscópicos de  $\text{TiO}_2$  presentes de forma natural en el carbón. Estas fases Magnéli a nanoescala, que ahora hemos demostrado que se propagan globalmente a través del transporte atmosférico, son tóxicas para las vías respiratorias y los pulmones de los mamíferos, incluidos los humanos. Por lo tanto, estas nanofases incidentales son probablemente un importante contaminante ambiental, especialmente en regiones geográficas donde la combustión del carbón es un importante contribuyente a las partículas atmosféricas. Está claro que se necesitan más estudios de toxicología y se justifican evaluaciones futuras del impacto de estas nanopartículas en la salud humana.

*Key-words: Natural, incidental, and engineered nanomaterials, Clark Fork, metal adsorption, Magnéli phase nanoparticles.*

## Reference

Hochella Jr., M.F., Mogk DW, Ranville, J., Allen, I.C. y 10 más (2019) Natural, incidental, and engineered nanomaterials and their impacts on the Earth system. *Science*, **363**, eaau8299. DOI:10.1126/science.aau8299

# Reactivity of clays and metal nanomaterials in waters and sediments from saline wetlands: the role of the bacterial communities

Rosario Jiménez Espinosa (1), Juan Jiménez Millán (1)

(1) Departamento de Geología and CEACTEMA, Universidad de Jaén. Campus Las Lagunillas, 23071, Jaén (España)

## *Abstract*

Saline fluids in eutrophic environments promote multiple mineral reactions coupled with biological activity in wetland sediments from river basins. Microbial redox reactions involving Fe and other metals control mineral authigenic sedimentary processes in these environments affecting the stability of clays, sulfides, oxides and phosphates in sediments. This contribution shows how the wetlands from the Chicamocha river Basin (Colombia) is an excellent natural laboratory to study factors controlling these reactions mediated by microorganisms. Most of the bacterial activity in wetland sediments is associated with organic matter degradation processes. These groups play the role of biogeochemical linkers that relate the reactions of C and S in sediments, favoring elemental mobility that affect the cycle of Fe and other metals of the sediments and the activity of iron- and sulfur-cycling bacteria, sulfur- and sulfate-reducing bacteria (SRB), sulfide-oxidizing bacteria (SOB), iron-reducing bacteria (IRB) and iron-oxidizing bacteria (IOB). Authigenesis and clay mineral reactivity is influenced by cation availability, frequently mediated by the microbial activity, and the presence of an appropriate mineral precursor. Fe-rich environment by hydrothermal and anthropic inputs in the Chicamocha Basin wetlands and the reducing conditions generated by the decay of abundant organic matter caused Fe mobilization mediated by the presence of SRB and SOB communities, which favored the processes of transformation of detrital clays. High concentration hydrothermal K in the waters of the lake and Fe uptake in the octahedral sheet promoted the illitization of the precursor clays (smectites or I-DV). Bacterial activity in organic matter rich sediments also favors the availability of sulfide (stimulated by SRB and their syntrophic partners that produce  $H_2$ ) and  $Fe^{2+}$  (promoted by IRB and SRB) and other metals, such as Zn, that can be fixed as insoluble monosulfides encrusting microbial cells. IRB enrichment of the sediments stimulates a greater availability of  $Fe^{2+}$  and favors the reaction of  $Fe^{2+}$  with  $PO_4^{3-}$  to form vivianite. The stage of monosulfide and/or phosphate precipitation is followed by a dissolution step and a recrystallization process that produce pyrite framboids enhanced by the SOB activity, which also facilitate the oxidation of the reduced sulfides to  $S^0$  and the release of toxic heavy metals again into the environment that can be increased by IOB oxidation reactions even in anoxic environments.

## *Resumen*

Los fluidos salinos en ambientes eutróficos y la actividad biológica asociada promueven múltiples reacciones minerales en los sedimentos de los humedales de las cuencas fluviales. Las reacciones redox microbianas que implican al Fe y a otros metales controlan los procesos sedimentarios de formación de minerales en estos ambientes y afectan a la estabilidad de las arcillas, sulfuros, óxidos y fosfatos presentes en los mismos. Este trabajo muestra que los humedales de la cuenca del río Chicamocha (Colombia) son un excelente laboratorio natural para estudiar los factores que controlan estas reacciones mediadas por microorganismos. La mayor parte de la actividad bacteriana en los sedimentos de los humedales está asociada con los procesos de degradación de la materia orgánica. Estos grupos conectan biogeoquímicamente las reacciones del carbono y del azufre en los sedimentos, favoreciendo la movilidad elemental del hierro y de otros metales de los sedimentos, así como la actividad de las bacterias implicadas en los ciclos del hierro y el azufre: bacterias reductoras del azufre (SRB), bacterias oxidantes del azufre (SOB), bacterias reductoras del hierro (IRB) y bacterias oxidantes del hierro (IOB). La autigénesis y la reactividad de los minerales arcillosos están influidas por la disponibilidad de cationes, frecuentemente mediada por la actividad microbiana, y la presencia de un precursor mineral apropiado. El ambiente rico en hierro por aportes hidrotermales y antrópicos en los humedales de la Cuenca del Chicamocha y las condiciones reductoras generadas por la descomposición de abundante materia orgánica provocaron la movilización de hierro mediada por la presencia de

comunidades de SRB y SOB, que favorecieron los procesos de transformación de las arcillas detríticas. La alta concentración hidrotermal de K en las aguas del lago y la captación de hierro en la capa octaédrica promovieron la illitización de las arcillas precursoras (I-DV). La actividad bacteriana en sedimentos ricos en materia orgánica también favorece la disponibilidad de sulfuro (estimulada por SRB y sus socios sintróficos que producen H<sub>2</sub>), Fe<sup>2+</sup> (promovida por las IRB y SRB) y otros metales, como Zn<sup>2+</sup>, que pueden fijarse como monosulfuros insolubles en incrustaciones de la pared de células microbianas. El enriquecimiento en IRB de los sedimentos estimula una mayor disponibilidad de Fe<sup>2+</sup> y favorece la reacción de Fe<sup>2+</sup> con PO<sub>4</sub><sup>3-</sup> para formar vivianita. A la etapa de precipitación de monosulfuro y/o fosfato, le sigue una etapa de disolución y un proceso de recristalización que produce framboides de pirita potenciados por la actividad de las SOB, que también facilitan la oxidación de los sulfuros reducidos a S<sup>0</sup> y la liberación de metales pesados tóxicos que puede incrementarse por reacciones de oxidación de las IOB incluso en ambientes anóxicos.

*Key-words:* SRB, IRB, SOB, IOB, illite, mackinavite, pyrite.

## 1. Introduction

Water salinity of hydrologically-restricted environments such as continental wetlands can commonly increase due to natural inputs or pollutants affecting the chemical and composition of the sediments. Natural inputs are frequently associated to dissolution processes producing trace element-rich hydrothermal fluids, especially in geothermal or evaporitic areas (see e.g. references in Cifuentes et al., 2020, 2021a). Agricultural activities, smelting and urban wastewaters have been considered as some of the main types of anthropic activities promoting potential pollution in waters and sediments of wetlands (see e.g. references in Quevedo et al., 2020a). Moreover, fertilization techniques and organic matter from urban wastewaters contribute to environmental eutrophication.

Saline fluids in eutrophic environments can promote multiple mineral reactions coupled with biological activity in the sediments (Cuadros et al., 2017; Aghasian et al., 2019; Zhang et al., 2019). Microbial redox reactions involving Fe and other metals control mineral authigenic sedimentary processes in these environments affecting the stability of clays, sulfides, oxides and phosphates in sediments (Andrade et al., 2018).

The Chicamocha river Basin (Colombia) is an excellent natural laboratory to study the influence of natural and anthropic inputs on the composition of organic matter rich sediments deposited in saline wetlands (Cifuentes et al., 2020, 2001a, b and c; Quevedo et al. 2020a and b, 2021). Two main wetlands regulate the surface water outflow of the basin (Figure 1): the La Playa dam and the Sochagota Lake dam. These wetlands store water to meet various demands, such as ranching, agriculture, tourism and industry, and their impoundments receive anthropogenic input from farm activities and wastewater (La Playa reservoir) as well as input from natural hydrothermal waters (Sochagota Lake) that produce high salinity waters, intense eutrophication and organic-rich sediments.

This article reviews the sources of salinity and metal enrichment in wetlands from the Chicamocha Basin and the most important bacterial communities developed in the organic matter rich sediments deposited in these environments with the aim to show the influence of the microorganisms on the main reactions involving clays and other minerals associated to the metal nanoparticle fixation.

### 1. Sources of salinity and metal enrichment in wetlands

Wetlands are hydrologically-restricted environments where water salinity and metal concentrations can increase due to natural inputs or pollutants. Water wetlands salinity increase is frequently controlled by geological factors, such as the presence of regional evaporitic sediments or hydrothermal SO<sub>4</sub><sup>2-</sup>-Na inputs. However, anthropogenic inputs from farm activities (using fertilizers and pesticides) and wastewaters (mainly urban sewage) can also produce high-salinity waters.

High heavy metals concentration is of particular concern for humans because of their detrimental health effects on people in excessive quantities. Polluted wetlands, can create potential risk of metal exposure to humans. The origin of heavy metal enrichment can also be associated to natural and anthropogenic processes.

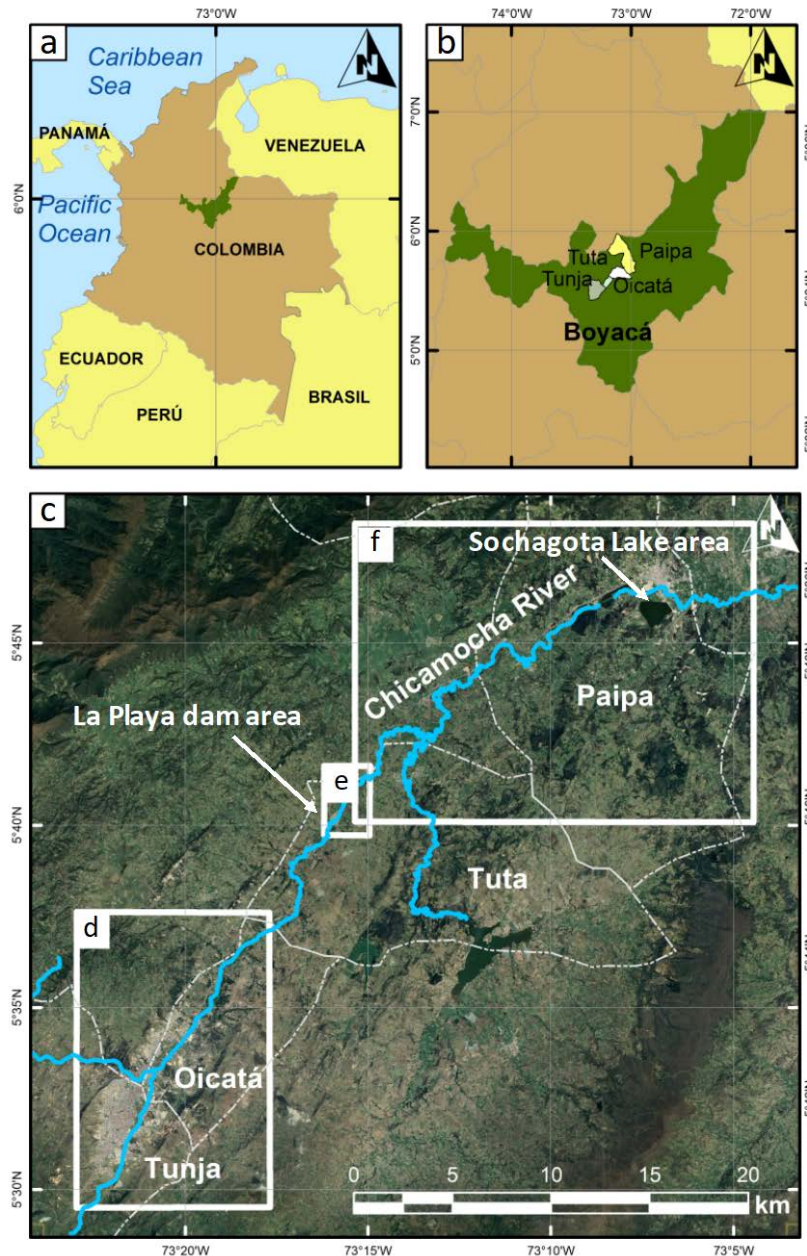


**Fig.1.** Geographical setting of the Chicamocha river Basin (Colombia). (a) Global context of the area; (b) Regional map; (c) Sectors of the Chicamocha River between Tunja and Paipa, Boyacá Province indicating the location of the La Playa dam and the Sochagota Lake. Modified from Quevedo et al. (2020a).

### 1.1. Natural hydrothermal inputs. The Sochagota Lake

The Sochagota Lake is an exceptional case study to show the influence of natural inputs on the composition of waters and sediments. An increase of water salinity and metal concentrations associated to natural inputs can be observed in this wetland located at the lowest segment of the Chicamocha Basin. This is an artificial lake constructed from a previous natural wetland (Figure 2). From a geological point of view, it is located in the main Andean geothermal system in Colombia with hydrothermal systems associated to the area's volcanoes (Alfaro et al., 2005). The rhyolitic Paipa volcano, which is characterized by a collapsed caldera (3 km wide) with several hydrothermal vents, is the nearest volcanic building to the lake. The hydrothermal waters flow through the El Salitre River (a tributary of the Chicamocha River) and are mixed with rain waters in Sochagota Lake (Cifuentes et al., 2021a).

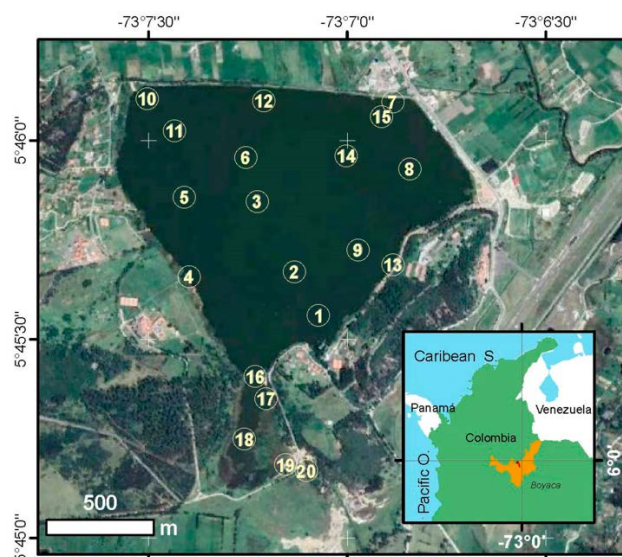


**Fig.2.** Location of the Sochagota Lake. Numbers indicate sample positions. The small map represents the regional context of the global area, i.e., situation of the Paipa province (Boyaca region) in Colombia. Taken from Cifuentes et al. (2021a).

Geothermal waters contribute to the chemical composition of the water of the El Salitre river as follows (see specific data in Cifuentes et al., 2021a): (i)  $\text{SO}_4^{2-}$ - $(\text{Cl}^-)$   $\text{Na}^+$ - $\text{K}$ -rich hot waters; and (ii) Fe-rich,  $\text{HCO}_3^-$  ( $\text{Cl}^-$ - $\text{SO}_4^{2-}$ ) cold waters. Hydrothermal fluids associated with geothermal systems contain potentially pollutant chemicals (e.g., S, Fe, As, Pb, Zn, Mn) in the liquid fraction that may be present in harmful concentrations and can cause environmental chemical pollution. The water isotopic composition of the Sochagota Lake waters (6.4‰ for  $\delta^{34}\text{S}$  and 8.1 for  $\delta^{18}\text{O}$ , which is comparable to several hydrothermal liquids), and the lack of evaporitic rocks in the stratigraphic sequence indicated that the high mineralization of the lake water was a result of hydrothermal contributions of S-bearing fluids from springs feeding the Salitre River. The good correlations of  $\text{SO}_4^{2-}$  with metals in the lake waters also supported that its origin is associated with hydrothermal inputs to the Salitre River. The hydrochemistry of the cold waters can be related to the water–rock interaction of an alluvial shallow aquifer made of volcanic and sedimentary particles and recharged by rain. A mixing of thermal and saline waters with cooler groundwater is produced at the Salitre River bed, causing the  $\text{SO}_4^{2-}$ - $\text{Na}^+$ - $\text{K}^+$ -Fe-rich waters which are accumulated at the south entrance of the lake.

High electrical conductivity and sulfate-rich waters from the south lake entrance are characterized by high contents of  $\text{Cl}^-$ , Li, Be, Al, K, Fe, Co, Ni, Cu, Zn, As, Rb, Cs, and Pb. The concentrations of  $\text{SO}_4^{2-}$ ,  $\text{Cl}^-$ , Fe and As exceeded the regulatory framework for contaminants in waters (250 mg/L for  $\text{SO}_4^{2-}$  and  $\text{Cl}^-$ , 0.3 and 0.01 mg/L, respectively) or electrical conductivity (1000  $\mu\text{S}/\text{cm}$ ). On the other hand, in the centre and north areas of the lake, conductivity,  $\text{SO}_4^{2-}$  and  $\text{Cl}^-$  were clearly lower than in the waters from the south entrance, although these contents slightly exceeded the Colombian regulations for pollutants in waters.

Two main types of sediments can be distinguished in the Sochagota Lake (see specific data in Cifuentes et al., 2020). Sediments from the southern part of the lake, deposited at the entrance of the hydrothermal inputs (El Salitre) under fast-flowing conditions, were found to contain negligible organic matter (TOC 0.7%). In this area, the deposition of organic matter is not favored by the hydrodynamic conditions, thereby promoting the oxygenation of the sediments (measured redox potential around 90 mV). By contrast, the central and northern parts of the lake, under slower-flowing conditions, are characterized by the deposition of the finest clay-rich sediments and organic matter (TOC up to 11.10%) with reduced conditions (redox potential around -150 mV).

The spatial distribution of trace elements in the sediments of Sochagota Lake seems to be associated with the distribution of organic matter content and mineral assemblages (see specific data in Cifuentes et al., 2021b). Organic matter-poor sediments from the southern part of the lake were found to be enriched in Zr (mean 567 mg/kg) and their mineral assemblages did not contain illite, I-DV or S-bearing minerals. The large contents of Zr,  $\text{SiO}_2$  and  $\text{TiO}_2$  in these sediments can be associated with the deposition of terrigenous zircon, quartz and rutile. On the other hand, organic matter-rich sediments with a fine-grain sized matrix rich in illite and I-DV located in the northern and central segments of the lake were found to be enriched in heavy metals (Cu, Zn, Cr, Ni, Co, Pb, Mo), Rb, Ba and

As. These sediments were characterized by the crystallization of S-bearing minerals (mackinawite, pyrite, and  $S^0$ ) (Cifuentes et al., 2020). The concentrations of heavy metals in these sediments exceeded the world standard averages, and the mean level of some of these elements was clearly higher than the value of unpolluted reference sediments from the Chicamocha River area (Quevedo et al., 2020a).

## 1.2. Anthropogenic pollution inputs. La Playa dam

La Playa dam, the most relevant anthropic change in the Chicamocha Basin, offers the opportunity of showing the influence of human activity inputs on several biogeochemical cycles. The reservoir of the La Playa dam receives wastewaters (urban sewage) from the towns of the region and waters of the agricultural activities, which generate a high nutrient load and intense eutrophication. Moreover, the La Playa dam is located less than 3 km east of an important smelter that produce smelting slags with high Zn contents.

Waters and sediments from La Playa reservoir reflect the effect of these anthropic inputs. Water composition is characterized by high heavy metals concentrations, especially for Zn (mean value 268  $\mu\text{g/L}$ ) as compared with waters from other segments of the Chicamocha River, and high P contents (mean value 6847  $\mu\text{g/L}$ ). Water salinity is very high (1478  $\mu\text{S/cm}$ ) and redox potential is low (-27 mV) (see specific data in Quevedo et al., 2020a).

The sediments from the La Playa dam are characterized by alternating bands of microlaminated organic-matter-rich layers and clay-rich layers, showing a high organic matter content (TOC of up to 11.1%), low redox potential (around -230 mV) and high electrical conductivity (2625  $\mu\text{S/cm}$ ) (see specific data in Quevedo et al., 2020a, b, 2021). Clay mineral assemblage in the sediments trapped in La Playa dam in the upper part of the basin is characterized by the presence of detrital kaolinite and I-DV and authigenic Fe-bearing smectite (up to 0.4 atoms per formula unit (a.p.f.u.)). Fe and Zn-bearing minerals (pyrite, ZnS, vivianite, goethite) are exclusively found in sediments from the La Playa dam and are absent from the rest of the alluvial sediments from the Chicamocha river basin. Periodical water discharges in La Playa dam create areas with intermittently emerged sediments, whereas other areas contain permanently flooded sediments, producing important changes in the redox conditions of sediments (Figure 3). Pyrite is present in all of the sediments deposited in the reservoir. Permanently flooded sediments that are richer in organic matter and have a lower redox potential (around -230mV) from the northern part of the reservoir are characterized by the presence of vivianite and ZnS, and, by contrast, periodically emerged sediments from the southern part of the reservoir with lower organic matter contents (4.29%) and higher Eh values (-10mV) contain goethite.

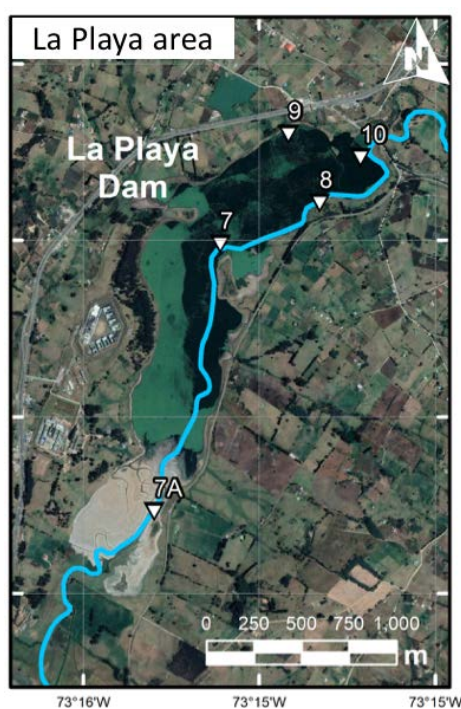


**Fig.3.** Location of the La Playa dam. Numbers indicate sample positions. Taken from Quevedo et al. (2020).

From the geochemical point of view, clay-rich sediments from la Playa reservoir have lower SiO<sub>2</sub> contents (mean 61.24%) and higher Al<sub>2</sub>O<sub>3</sub> contents (mean 17.17%) than quartz-rich sediments from the rest of segments of the Chicamocha Basin. The La Playa sediments are also characterized by the highest content in organic matter (TOC up to 13.84%), and LOI values (up to 15.43%). A significant enrichment in the P<sub>2</sub>O<sub>5</sub> content (mean value of 0.58%) and heavy metals (Zn > Cu > Cr > Ni > Pb) of these sediments can also be observed.

## 2. Bacterial communities in organic matter rich saline environments

Several environmental variables, such as hydrodynamic conditions, organic matter content, salinity or cycles of wetting and drying, favor the presence of specific microorganism communities controlling some of the most important biogeochemical cycles in wetlands. Processes of organic matter degradation and mineral transformation in the C, Fe, P and S cycles are associated with the bacterial activity of the sediments of these environments. Thus, the presence of a diverse bacterial community composition made of the following groups can be identified (Cifuentes et al., 2021b; Quevedo et al., 2021).

### 2.1. Bacterial groups involved in the degradation of the organic matter

Most of the bacterial activity in wetland sediments is associated with organic matter degradation processes. In the Chicamocha Basin, the main bacterial communities belong to fermentative genera from anoxic zones from *Bacteroidetes*, *Chloroflexi* and *Firmicutes* phyla, which digest, grow on and degrade organic substrates (Rui et al., 2009; Zhou et al., 2016). *Sphingobacteriales* can play an important role during the initial degradation stages of organic matter whereas other groups like *Bacteroidetes\_vadinHA17* and *Dehalococcoidia* and *Anaerolineae* are more important during the final degradation stages of organosulfur compounds in sulfidic zones. Other groups, such as *Ignavibacteriales* order, have the function of CO<sub>2</sub> fixation. *Rikenellaceae* family (*Bacteroidetes*) in these sediments can be associated with being responsible for the decomposition of harmful algal bloom in ponds. Other *Bacteroidetes* genera, such as WCHB1-32, BVS13 and *Macellibacteroides* (Ji et al., 2018), have been thought to be important in the formation of methanogenic precursors from organic matter degradation. Some members of the phylum *Firmicutes*, such as the *Christensenellaceae* family, are frequently reported in human feces and other animal feces, and show a fairly high capability for degrading carbohydrates and carboxylic acids. Finally, several communities, i.e. *Syntrophomonadaceae* members (*Firmicutes*) or *Anaerolineaceae* (*Chloroflexi*) can contribute to produce H<sub>2</sub> used by sulfate-reducing bacteria (SRB) acting as syntrophic partners (Timmers et al., 2018). Thus, these groups play the role of biogeochemical linkers that relate the reactions of C and S in sediments, favoring the mobility of these elements in the system, which can affect the cycle of Fe and other metals of the sediments and the activity of iron- and sulfur-cycling bacteria, sulfur- and sulfate-reducing bacteria (SRB), sulfide-oxidizing bacteria (SOB), iron-reducing bacteria (IRB) and iron-oxidizing bacteria (IOB).

### 2.2. SRB and IRB communities

SRB and IRB have direct effects on the availability of dissolved metals, which can be incorporated into the precipitated minerals (e.g., sulfides or phosphates).

An important SRB community was identified in the wetland sediments of the Chicamocha Basin (Cifuentes et al., 2021b; Quevedo et al., 2021). This community was dominated by *Desulfatiglans*, *Pseudomonas*, *Syntrophobacter*, and *Thermodesulfovibrionia* although other SRB microbial communities of *Desulfobacterales* (Fam. *Desulfobacteraceae*, G. *Sva0081 sediment group*), *Sva0485*, *Desulfomicrobium* and *Desulfobulbus* and *Desulfobacca* genera. were also identified. These bacterial groups are characterized by its elevated levels of metal resistance (*Pseudomonas*, Zampieri et al., 2020), its ability to colonize in sludge and sewage (*Desulfobacca*) in sulfate-rich wetlands (*Syntrophobacter*) where play a crucial role in the cycles of nitrogen and sulfur (*Thermodesulfovibrionia*) and promoting P release at contaminated sediments (*Desulfomicrobium* and *Desulfobulbus*).

The presence of a significant proportion of iron-reducing *Latescibacteria*, *Geobacter*, *Dechloromonas*, *Paludibacter* and *Acidibacter* (Cifuentes et al., 2021b; Quevedo et al., 2021) suggests that these communities could have also contributed to the direct reduction of Fe<sup>3+</sup>. *Geobacter* and *Paludibacter* was associated with organic-matter-rich sediments with humic acids, playing an essential function in the release of Fe<sup>2+</sup> to the interstitial waters of sediments

under anaerobic conditions. *Dechloromonas* has been found to be related to the reduction of  $\text{Fe}^{3+}$  to  $\text{Fe}^{2+}$  in sludges that contain P and Fe. *Paludibacter* has been described as a fermentative microorganism in high sulfate and metal concentration environments that is able to transfer electrons from anaerobic oxidations to promote the reduction of iron. *Acidibacter* has the capability of reducing dissolved  $\text{Fe}^{3+}$  in low pH and high Fe environments (Chen et al., 2020).

### 2.3. SOB communities

Some groups of *Gammaproteobacteria* and *Epsilonbacteraeota* are believed to be the functional SOB of the wetlands from the Chicamocha Basin (Cifuentes et al., 2021b; Quevedo et al., 2021), producing the transformation of Fe sulfides and contributing to the possible release of metals and producing the presence of sulfates and  $\text{S}^0$  associated with areas with pyrite framboids.

*Thioalkalimicrobium* and *Thiobacillus* were the dominant SOB belonging to the *Gammaproteobacteria* group, whereas *Sulfurovum*, *Sulfuricurvum*, *Arcobacter* and *Sulfurimonas* are the main components of the *Epsilonbacteraeota* group. These two SOB communities use diverse strategies for the oxidation of sulfur. *Epsilonbacteraeota* need a continuous supply of reduced sulfur and oxygen, but *Gammaproteobacteria* are able to adapt their energy metabolisms to different reduced environmental conditions. *Thiobacillus*, *Sulfurimonas* and *Arcobacter* are commonly involved in the autotrophic denitrification of saline sewages and can be used as an indicator of sewer and human fecal pollution (especially *Arcobacter*). *Sulfuricurvum* is frequently the dominant SOB under elevated free sulfide concentrations.

### 2.4. IOB communities

Although IOB are commonly absent in reduced sediments of the Chicamocha Basin. The alternation of wetting and drying periods can favor an increase of the IOB amount. Thus, Gallionellaceae family and Sideroxydans genus are very well represented in the periodically emerged sediments of the La Playa dam (Quevedo et al., 2021). These groups can play an important role in the oxidation of  $\text{Fe}^{2+}$  in sediments with low oxygen levels.

## 3. Clay mineral reactions

Many mineral reactions at low temperature are not controlled by thermodynamics but kinetics. In organic matter rich sediments, authigenesis and clay mineral reactivity is influenced by cation availability, frequently mediated by the microbial activity, and the presence of an appropriate mineral precursor.

Regarding cation availability, continental saline environments are characterized by Fe-enrichment due to natural or anthropic input sources. The abundance of organic matter promotes reducing conditions generated by its decay and the proliferation of IRB and SRB. These bacterial communities cause Fe mobilization that can eventually be fixed as sulfide or phosphate minerals. However, the common coexistence of SOB in this type of sediments can favor sulfur oxidation and Fe-release. These processes can facilitate the presence of abundant dissolved and colloidal  $\text{Fe}^{2+}$  and  $\text{Fe}^{3+}$  in the interstitial water that promote formation of reactive Fe phases in constant transformation favoring silicate mineral neof ormation and reactions (Andrade et al. 2018; Quevedo et al, 2020b). The authigenic formation of clay minerals, such as smectites, is frequently revealed the presence of small flakes forming rose-shaped aggregates that fill pores in the sediment, such those observed in the La Playa dam (Quevedo et al, 2020b). The existence of Fe easily mobilized by bacteria mediated oxidation–reduction reactions favored that, under the influence of the reducing environment produced by anthropic contamination, clay minerals uptake Fe and incorporate it into authigenic clays. The presence of up to 0.4 a.p.f.u. of Fe in the TEM-EDX analysis of smectite from La Playa sediments suggested that Fe was incorporated in the octahedral sheet (Quevedo et al, 2020b).

The crystallization of illite is a common feature of the end of the processes of authigenesis and clay mineral reactions in saline sediments rich in organic matter. The presence of an appropriate mineral precursor and cation availability (Fe and K) and are the two main factors controlling the illitization process in these environments (Cuadros et al., 2017).

Smectite or illite–smectite mixed layers are the most frequently proposed clay precursors for illite formation in sedimentary basins but the transformation to illite can also be produced through illite–dioctahedral vermiculite (I-

DV) interstratification, as in the Sochagota Lake (Cifuentes et al., 2021c). Climatic conditions in the Sochagota Lake area produced a partial transformation of primary minerals to kaolinite and vermiculitic minerals as the main clay minerals in the source materials draining the basin, favoring the deposit of small-sized metastable intermediates of I-DV minerals, which acted the mineral detrital precursor of the illitization process. TEM-EDS data revealed that well-crystallized neoformed illite (Figure 4) has more Fe than I-DV, revealing that the uptake of Fe played an important role during the illitization process. The chemistry of the lake water, which is enriched in Fe by hydrothermal input, and the reducing conditions generated by the decay of abundant organic matter caused Fe mobilization mediated by the presence of SRB and SOB communities. High concentration hydrothermal K in the waters of the lake and Fe uptake in the octahedral sheet can promote the illitization of the precursor clays (I-DV). The incorporation of Fe during illitization should be produced by the coupled substitutions of Al for Si in the tetrahedral sheet and of Mg and Fe for Al in the octahedral sheet, promoting the incorporation of K to the interlayer. This low-temperature illitization process highlights the importance of clays in the uptake of K from hydrothermal waters in geothermal areas.

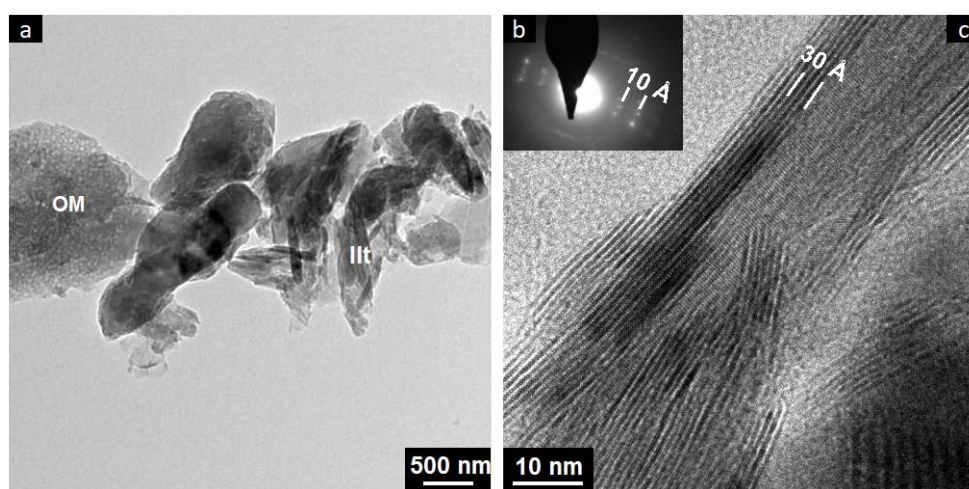


**Fig.4.** TEM images of illite in samples from the Sochagota Lake. (a) Textural image of illite in clay aggregates. (b) SAED pattern of illite. (c) HRTEM image of illite showing wide areas of well-defined 10 Å lattice fringes. OM: organic matter, Illt: illite. From Cifuentes et al. (2021c).

#### 4. Bacteria mediated reactions of metal-rich minerals

The redox reactions of metal-bearing minerals in organic matter-rich sediments have a strong effect on the speciation, mobility and bio-availability of pollutants. The precipitation of Fe and other metals in different minerals depends on the environmental conditions. Redox conditions are one of the main factors controlling the precipitation of Fe-bearing minerals, favoring the precipitation of Fe<sup>2+</sup>-minerals (mainly phosphates and sulfides) under low redox potential conditions and Fe<sup>3+</sup>-minerals (mainly oxides and oxyhydroxides) under high redox potential conditions. In anoxic environments rich in P and S, microbial processes can promote the formation of vivianite (Fe<sub>3</sub>(PO<sub>4</sub>)<sub>2</sub> · 8H<sub>2</sub>O) and iron and other metal sulfide minerals, such as mackinawite ((Fe,Ni)S), ZnS or pyrite (FeS<sub>2</sub>). The crystallization of sulfide minerals can widely affect all of these reactions.

The importance of a decaying organic matter-rich environment for the crystallization of metal sulfides have been frequently described as important factor controlling the mineral assemblage of sediments (see e.g., Folk, 2005; Love, 1967; Love et al., 1984; MacLean et al., 2008). High metal concentrations in sediments is frequently related to the process of sulfide crystallization in these carbonaceous matter-rich environments.

Bacterial communities of this types of sediments in the Chicamocha Basin (Cifuentes et al., 2021b, Quevedo et al., 2021) are characterized by the presence of groups able to reduce sulfate (SRB, such as *Desulfatiglans*, *Desulfobacterales* and Sva0485 in the Sochagota Lake; *Pseudomonas*, *Desulfomicrobium* and *Desulfobulbus* in the La Playa dam) and Fe<sup>3+</sup> (IRB, *Latescibacteria* in the Sochagota Lake; *Geobacter*, *Dechloromonas*, *Pseudomonas* and *Paludibacter* in the La Playa dam). The activity of these bacterial groups in the flooded sediments can be reinforced by syntrophic partners to produce H<sub>2</sub> used by SRB (such as *Syntrophomonadaceae*) and increase the sulfide availability. Therefore,

bacterial activity in organic matter rich sediments favors the availability of sulfide (stimulated by SRB and their syntrophic partners that produce  $H_2$ ) and  $Fe^{2+}$  (promoted by IRB and SRB) and other metals, such as Zn, that can be fixed as insoluble sulfides. SEM images showing cell-shaped aggregates with metal sulfide composition support the importance of the bacterial communities in the nucleation and transformation of sulfide minerals (Figure 5). HRTEM images of the nanoparticles encrusting bacterial cells frequently show (001) lattice fringes of  $\approx 5 \text{ \AA}$  (Cifuentes et al., 2021b) suggesting mackinawite precipitation during the initial step of the sedimentary sulfide formation in the Sochagota Lake. Raman microspectrometry has confirmed the accumulation of these mackinawite particles at the inner part of plant fragments (Figure 5c).

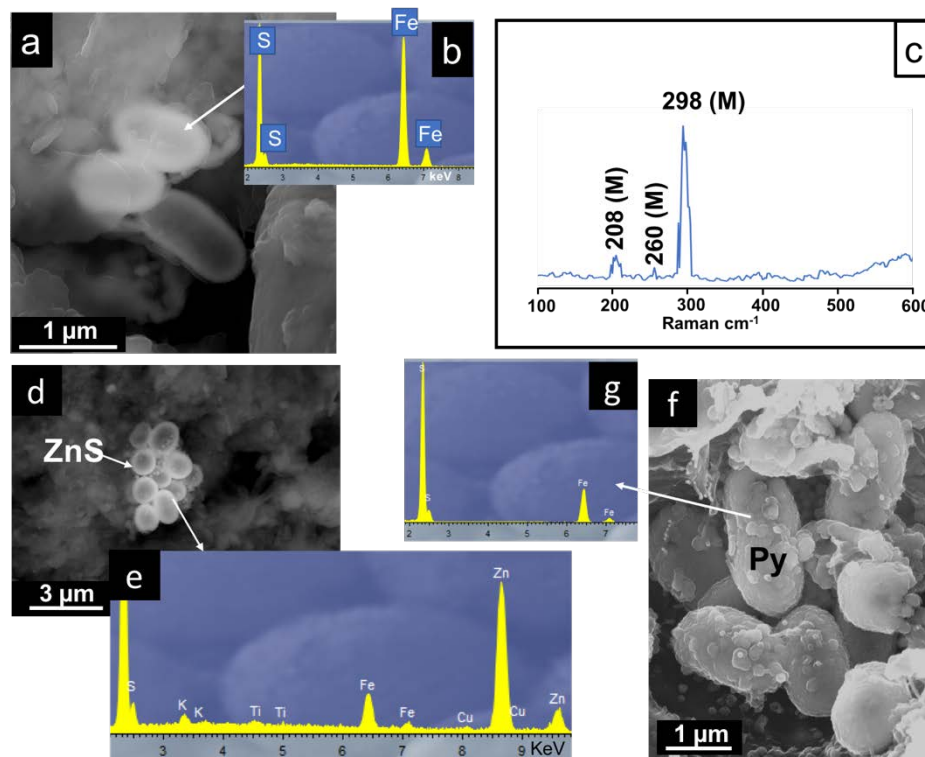


**Fig.5.** Metal sulfide nanoparticles forming aggregates which oval and spherical shape and size closely resemble bacterial cell morphology. (a) FeS nanoparticles aggregates with bacterial cell morphology in the Sochagota Lake sediments. (b) EDX spectrum of the FeS minerals. (c) Raman spectrum of the FeS minerals confirming the presence of mackinawite. (d) ZnS cell-shaped aggregate in La Playa dam. (e) EDX spectrum of the ZnS minerals. (f) Pyrite cell-shape aggregates in La Playa dam. (g) EDX spectrum of pyrite M: mackinawite. Py: pyrite. Modified from Cifuentes et al. (2020) and Quevedo et al. (2020a, 2021).

The monosulfide nucleation promoted by microbial cells can also enhance the accumulation of trace elements to the sediments. The Zn-enrichment of the sediments from the La Playa dam can be associated to the crystallization of ZnS nanoparticles encrusting SRB cells (Figure 5d), probably from the *Pseudomonas* group is a very good example of metal fixation by monosulfide precipitation.

Sulfide formation can compete with the precipitation of  $Fe^{2+}$ -bearing phosphate (vivianite) for the available reduced Fe of the environment. The formation of vivianite is frequently restricted to environments where an excess of Fe in dissolution is available after the crystallization of sulfides. However, microorganisms can play an important role in the availability of these substances and, therefore, in the concomitant crystallization of phosphates and sulfides.

IRB enrichment of the sediments (such as in the permanently flooded sediments of the La Playa dam which contain *Geobacter*, *Dechloromonas*, *Pseudomonas* and *Paludibacter*) can promote a greater availability of  $Fe^{2+}$ , which favors the precipitation of vivianite by the contribution of microbial iron- and sulfur-reducing processes, as in the La Playa dam (Figure 6). These bacterial communities play an essential function in the release of  $Fe^{2+}$  to the interstitial waters of sediments under anaerobic conditions and they have been found to be related to the reduction of Fe in sludges that contain P and Fe, promoting the reaction of  $Fe^{2+}$  with  $PO_4^{3-}$  to form vivianite (Wu et al., 2021).

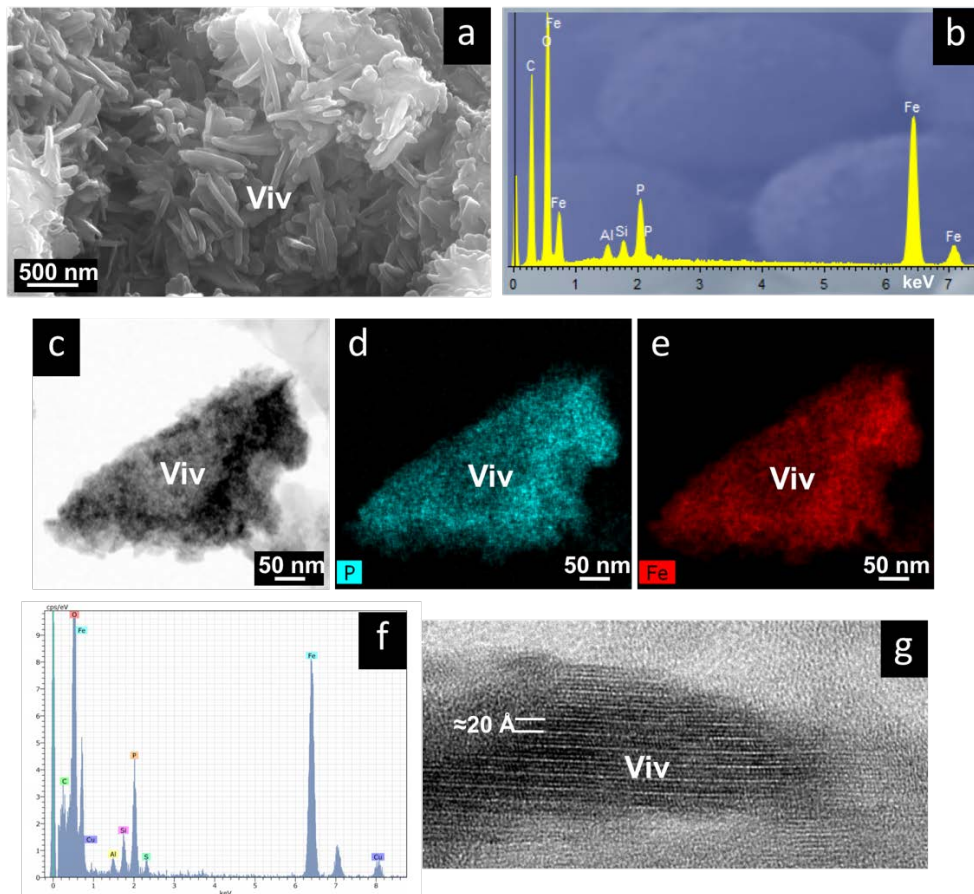


**Fig.6.** *Vivianite* from sediments of La Playa dam: (a) prismatic to flat nanocrystals of *vivianite* frequently associated with the occurrence of plant fragments (SE image); (b) EDX spectrum; (c) HRTEM image (bright field) of a *vivianite* crystal; (d) EDX elemental map of P; (E) EDX elemental map of Fe; (f) EDX spectrum of *vivianite* from image c; (g) lattice fringe image of *vivianite* crystal from image c. *Viv*: *vivianite*. From Quevedo et al. (2021).

The initial stage of monosulfide and/or phosphate precipitation is in many cases followed by a dissolution step under free sulfide excess conditions and a recrystallization process that produce pyrite framboids. This stage can be enhanced by the SOB activity. Several SOB communities, such as *Sulfuricurvum* or *Arcobacter* are the dominant SOB under elevated free sulfide concentrations increasing the pyrite crystallization rate. Morphology of the pyrite crystals in the framboids reveals physicochemical conditions controlled in some cases by the bacterial activity. In the La Playa dam, the formation of microframboids, including hopper pyrite crystals (Figure 7), suggests transformation processes under high supersaturation values of Fe and sulfide, which promote the fast accumulation of growth units at the crystal edges, causing the typical faces of hopper grains (García Ruiz et al., 2015).

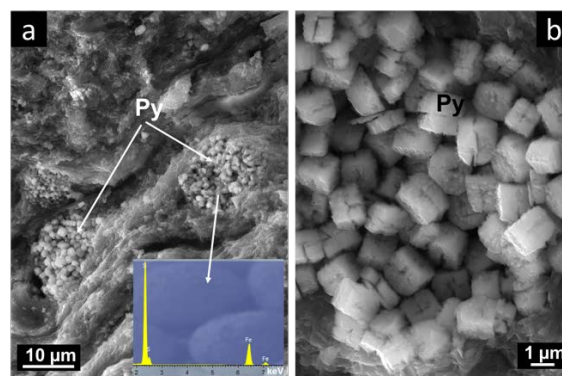


**Fig.7.** SE images of pyrite from sediments of La Playa dam: (a) pyrite framboids; (b) pyrite hopper crystals forming framboids. *Py*: pyrite. Modified from Quevedo et al. (2021).

During this stage, the presence of Cu-pyrite crystals (Sochagota Lake) and other Cu-bearing sulfides (Laguna Honda) in sediments from wetlands evidence the importance of the process of metal sulfidation on the metal take up into low-solubility minerals.

However, the persistent action of the SOB can facilitate the oxidation of the reduced sulfides to  $S^0$  (Figure 8) and sulfates such as barite. In the Sochagota Lake, the SOB communities (*Thioalkalimicrobium*, *Sulfurovum*, *Arcobacter* and *Sulfurimonas*) might have played an important role during this oxidation stage. The oxidation processes of the reduced sulfide may promote the release of toxic heavy metals again into the environment.

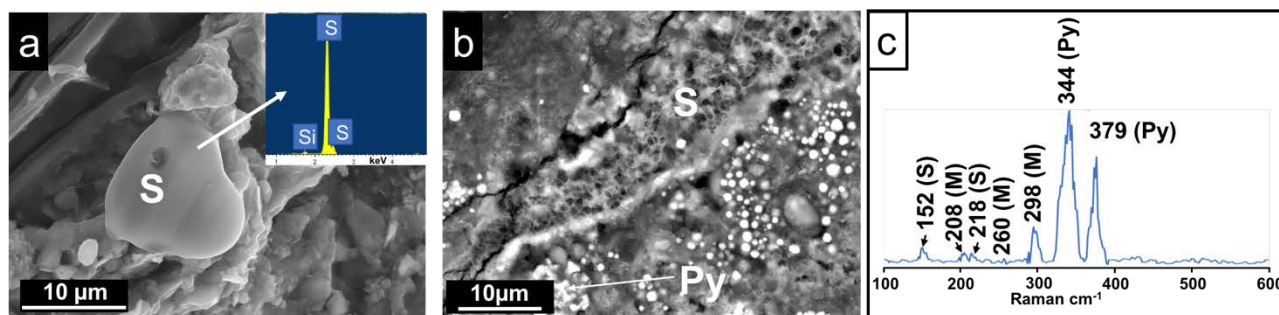


**Fig.8.** Electron microscope image and spectroscopy data (EDS and Raman) of  $S^0$  in sediments of the Sochagota Lake: (a) SE image of an individual grain of native sulfur near pyrite-rich zones; (b) BSE image of a  $S$ -aggregate formed by microfilaments that generate a vesicular texture; (c) Raman spectrum of pyrite-rich region. Py: pyrite, S: elemental sulfur. Modified from Cifuentes et al. (2020).

The presence of IOB can promote this type of oxidation reactions even in anoxic environments. The high representation of Members of the Gallionellaceae family and the Sideroxydans genus in the periodically emerged of La Playa dam with Eh negative values reveal that these groups can be adapted to low oxygen levels, enhancing goethite precipitation in these sediments (Figure 9). Watanabe et al. (2021) revealed the importance of bacteria that belong to the Gallionellaceae family and the Sideroxydans genus on the oxidation of  $Fe^{2+}$  in soils that alternate wetting and drying periods.

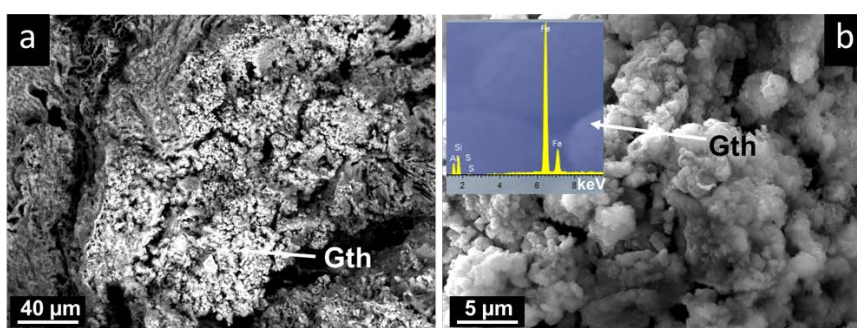


**Fig.9.** SEM and EDX images of goethite sediments of La Playa dam. From Quevedo et al. (2021).

## Conclusions

Organic matter-rich sediments from wetlands of the Chicamocha Basin are characterized by the presence of bacterial communities producing biodegradation associated with eutrophication. These sediments show relevant SRB communities involved in the precipitation of Fe-sulfides. SEM images showing cell-shaped aggregates with metal sulfide composition support the importance of the bacterial communities in the nucleation and transformation of sulfide minerals (mackinawite,  $ZnS$ ). The activity of these bacterial groups can be reinforced by syntrophic partners involved in the organic matter biodegradation, which produce  $H_2$  used by SRB and increase the sulfide availability. IRB enrichment favors the precipitation of vivianite by the contribution of microbial iron- and sulfur-reducing processes producing the accumulation of metals into the sediments.

The presence SOB in the sediments can favor both pyrite crystallization under a high sulfide availability and the oxidation of microbially precipitated monosulfides releasing metals into the environment and promoting the precipitation of  $S^0$  and sulfates. The Fe mobilization mediated by the presence of SRB and SOB communities

avored the processes of transformation of detrital clays. High concentration hydrothermal K in the waters of the lake and Fe uptake in the octahedral sheet promoted the illitization of the precursor clays (smectites or I-DV).

## Acknowledgements

This contribution includes ideas and data provided by Gabriel Ricardo Cifuentes, Claudia Patricia Quevedo, Fernando Nieto, Javier Cuadros, Antonio Gálvez and José Castellano. We sincerely thank all their efforts and creativity. Our investigations are in the framework of the projects “Solubilidad, agregación y fijación mineral de contaminantes agrícolas nanoparticulados de metales: papel de los sedimentos de ambientes lacustres salinos, FEDER UJA 2020 1380934” and “Procesos minerales de fijación y solubilidad de nanopartículas metálicas contaminantes en sedimentos lacustres y fluviales. Referencia: PAIDI 2020 P20\_00990.

## References

- Aghasian, K., Moridi, A., Mirbagheri, A., Abbaspour, M. (2019): Selective withdrawal optimization in a multipurpose water use reservoir. *Int. J. Environ. Sci. Technol.*, **16**, 5559–5568.
- Alfaro, C., Velandia, F., Cepeda, H. (2005): Colombian Geothermal Resources. in “Proceedings of the World Geothermal Congress”, Antalya, Turkey, **24–29**, 1–11.
- Andrade, G.R.P., Cuadros, J., Partiti, C.M.S., Cohen, R., Vidal-Torrado, P. (2018): Sequential mineral transformation from kaolinite to Fe-illite in two Brazilian mangrove soils. *Geoderma*, **309**, 84–99.
- Chen, H., Xiao, T., Ning, Z., Li, Q., Xiao, E., Liu, Y., Xiao, Q., Lan, X., Ma, L., Lu, F. (2020): In-situ remediation of acid mine drainage from abandoned coal mine by filed pilot-scale passive treatment system: Performance and response of microbial communities to low pH and elevated Fe. *Bioresour. Technol.*, **317**, 123985.
- Cifuentes, G.R., Jiménez-Millán, J., Quevedo, C.P., Jiménez-Espinosa, R. (2020): Transformation of S-bearing minerals in organic matter-rich sediments from a saline lake with hydrothermal inputs. *Minerals*, **10**, 525.
- , Jiménez-Espinosa, R., Quevedo, C.P., Jiménez-Millán, J. (2021a): Damming Induced Natural Attenuation of Hydrothermal Waters by Runoff Freshwater Dilution and Sediment Biogeochemical Transformations (Sochagota Lake, Colombia). *Water*, **13**, 3445.
- , Jiménez-Millán, J., Quevedo, C.P., Gálvez, A., Castellanos-Rozo, A., Jiménez-Espinosa, R. (2021b): Trace element fixation in sediments rich in organic matter from a saline lake in tropical latitude with hydrothermal inputs (Sochagota Lake, Colombia): The role of bacterial communities. *Sci. Total Environ.*, **762**, 143113.
- , –, Nieto, F., Cuadros, F., Jiménez-Espinosa, R. (2021c): Low Temperature Illitization through Illite-Dioctahedral Vermiculite Mixed Layers in a Tropical Saline Lake Rich in Hydrothermal Fluids (Sochagota Lake, Colombia). *Minerals*, **10**, 525
- Cuadros, J., Andrade, G., Ferreira, T.O., Partiti, C.S.M., Cohen, R., Vidal-Torrado, P. (2017): The mangrove reactor: Fast clay transformation and potassium sink. *Appl. Clay Sci.*, **140**, 50–58.
- Folk, R.L. (2005): Nannobacteria and the formation of framboidal pyrite: Textural evidence. *J. Earth Syst. Sci.*, **114**, 369–374.
- García-Ruiz, J.M., Otálora, F. (2015): Crystal Growth in Geology: Patterns on the Rocks. in “Handbook of Crystal Growth”, Nishinaga, T., Rudolph, P., eds., Elsevier: Amsterdam, The Netherlands, Volume II, 1–43.
- Ji, Y., Liu, P., Conrad, R. (2018): Response of fermenting bacterial and methanogenic archaeal communities in paddy soil to progressing rice straw degradation. *Soil Biol. Biochem.*, **124**, 70–80.
- Love, L. (1967): Early diagenetic iron sulphide in recent sediments of the Wash (England) *Sedimentology*, **9**, 327–352.
- Love, L.G., Al-Kaisy, A.T.H., Brockley, H. (1984): Mineral and organic material in matrices and coatings of framboidal pyrite from Pennsylvanian sediments, England. *J. Sediment. Res.*, **54**.
- MacLean, L.C.W., Tyliszczak, T., Gilbert, P.U.P.A., Zhou, D., Pray, T.J., Onstott, T.C., Southam, G. (2008): A high-resolution chemical and structural study of framboidal pyrite formed within a low temperature bacterial biofilm. *Geobiology*, **6**, 471–480.
- Quevedo, C.P., Jiménez-Millán, J., Cifuentes, G.R., Jiménez-Espinosa, R. (2020a): Electron microscopy evidence of Zn bioauthigenic sulfides formation in polluted organic matter-rich sediments from the Chicamocha River (Boyacá-Colombia). *Minerals*, **10**, 673.
- , –, –, –, (2020b): Clay mineral transformations in anthropic organic matter-rich sediments under saline water environment. Effect on the detrital mineral assemblages in the upper Chicamocha river basin, Colombia. *Appl. Clay Sci.*, **196**, 105576.

- , —, —, Gálvez, A., Castellanos-Rozo, J., Jiménez-Espinosa, R. (2021): The Potential Role of S-and Fe-Cycling Bacteria on the Formation of Fe-Bearing Mineral (Pyrite and Vivianite) in Alluvial Sediments from the Upper Chicamocha River Basin, Colombia. *Minerals*, **11**, 1148.
- Rui, J., Peng, J., Lu Y. (2009): Succession of bacterial populations during plant residue decomposition in rice field soil *Appl. Environ. Microbiol.*, **75**, 4879-4886
- Timmers, P.H.A., Vavourakis, C.D., Kleerebezem, R., Damsté, J.S.S., Muyzer, G., Stams, A.J.M., Sorokin, D.Y., Plugge, C.M. (2018): Metabolism and Occurrence of Methanogenic and Sulfate-Reducing Syntrophic Acetate Oxidizing Communities in Haloalkaline Environments. *Front. Microbiol.*, **9**, 3039.
- Watanabe, T., Katayanagi, N., Agbisit, R., Llorca, L., Yasukazu, H., Susum, A. (2021): Influence of alternate wetting and drying water-saving irrigation practice on the dynamics of *Gallionella*-related iron-oxidizing bacterial community in paddy field soil. *Soil Biol. Biochem.*, **152**, 108064.
- Wu, M., Liu, J., Gao, B., Sillanpää, M. (2021): Phosphate substances transformation and vivianite formation in P-Fe containing sludge during the transition process of aerobic and anaerobic conditions. *Bioresour. Technol.*, **319**, 124259.
- Zampieri, B.D.B., da Costa Andrade, V., Chinellato, R.M., Garcia, C.A.B., de Oliveira, M.A., Brucha, G., Fernandes Cardoso de Oliveira, A.J. Heavy metal concentrations in Brazilian port areas and their relationships with microorganisms: Can pollution in these areas change the microbial community? *Environ. Monit. Assess.* 2020, **192**, 512.
- Zhang, Q., Chen, H., Huang, D., Xu, C., Zhu, H., Zhu, Q. (2019): Water managements limit heavy metal accumulation in rice: Dual effects of iron-plaque formation and microbial communities. *Sci. Total Environ.*, **687**, 790–799.
- Zhou, G.X., Zhang, J.B., Zhang, C.Z., Feng, Y.Z., Chen, L., Yu, Z., Xin, X., Zhao B. (2016): Effects of changes in straw chemical properties and alkaline soils on bacterial communities engaged in straw decomposition at different temperatures *Sci. Rep.*, **6**, 22186.

# Metal pollution in hydrographic networks of abandoned mining basins: The case of Linares Mining District (SE Spain)

Julián Martínez (1), Rosendo Mendoza (1), María José De La Torre (2), Vicente López Sánchez-Vizcaíno (2), María José Campos Suñol (2), Rosario Jiménez Espinosa (3)

(1) Departamento de Ingeniería Mecánica y Minera, Universidad de Jaén. Campus Científico-Tecnológico de Linares, Avenida de la Universidad s/n, 23700 Linares (España)

(2) Departamento de Geología, Universidad de Jaén. Campus Científico-Tecnológico de Linares, Avenida de la Universidad s/n, 23700 Linares (España))

(3) Departamento de Geología, Universidad de Jaén. Campus Las Lagunillas, Facultad de Ciencias Experimentales. Edificio B3, 23071 Jaén (España)

## *Abstract*

The extractive mining activity and the associated concentration and smelting industries produce different types of solid waste that are accumulated in dumps, flotation tailings dams and slag heaps. These mining waste have high contents of metals and semi-metals, which can cause an environmental risk if they reach the ground and drainage networks. Aware of this risk, administrations have been addressing the problem in recent years, in such a way that many of these tailing dams are being restored and sealed.

In this field trip, we will focus on the area known as Adaro, within the Linares mining district. A review of the geology of the district and types of deposits, the mining techniques used and the concentration processes will be carried out. Based on this knowledge, the hydrogeochemical works carried out for the characterization of surface and groundwater in the studied sector are indicated, analyzing the condition they have evolved since the mining activity ended. The geophysical techniques used for the characterization of mining dams are also described and the effectiveness of the sealing carried out in some of these restored dams is evaluated.

## *Resumen*

La actividad extractiva minera y las industrias de concentración y fundición asociadas producen diferentes tipos de residuos sólidos que se acumulan en escombreras y presas de flotación y lavado. Estos residuos mineros tienen altos contenidos de metales y semimetales, lo que puede ocasionar un riesgo ambiental si llegan al suelo y a las redes de drenaje. Conscientes de este riesgo, las administraciones han venido abordando el problema en los últimos años, de tal forma que muchas de estas presas están siendo restauradas y selladas.

En esta salida de campo nos centraremos en la zona conocida como Adaro, dentro del distrito minero de Linares. Se realizará una revisión de la geología del distrito y los tipos de yacimientos, las técnicas mineras utilizadas y los procesos de concentración. Se muestran los trabajos hidrogeoquímicos realizados para la caracterización de las aguas superficiales y subterráneas en el sector de estudio, analizando su evolución desde que finalizó la actividad minera. También se describen las técnicas geofísicas utilizadas para la caracterización de presas mineras y se evalúa la eficacia del sellado realizado en algunas de estas presas restauradas.

*Key-words:* Linares, Mining activity, Waste mining materials, Metal pollution, Solis, Water.

## **1. Introduction**

The metallogenic district of Linares-La Carolina (SE Spain, province of Jaén) is characterized by the presence of phyllonian deposits with sulfide metallizations, basically galena (PbS) in Paleozoic granites (Azcárate et al, 1977; Lillo 1992a). These mining waste have high contents of metals and semi-metals, which can origin an environmental risk if they reach the drainage networks This extractive activity yield an important accumulation of mining waste material that was deposited in the proximity of the exploitation work. On the other hand, in mineral concentration processes waste was also produced, specifically, the rejection generated in the flotation process was deposited in

dumps, flotation tailings dams and slag heaps. In these areas is possible to find contents of metal sulfides, which behave unstable under the oxidizing conditions, which can give negative effects on the environment. In addition, in cases where there is generation of leachates, these have high contents of sulfates and metallic elements, as has been described both in this sector (Hidalgo et al., 2006; 2010; Cortada et al, 2019).

## 2. Description of the study area

In the mining district of Linares, hydrothermal vein deposits are hosted in a Palaeozoic basement and fossilized by a Triassic sedimentary cover. Bedrock is composed of metamorphic rocks (mainly phyllites with alternating quartzites), intensely deformed during the Hercynian orogeny and affected by a granitic intrusion. This Palaeozoic basement is severely fractured and characterized by the presence of a dense dyke network associated with the granitoid massif (Azcárate, 1977; Lillo, 1992). The exploited ore consists of Pb-Ag and Cu-Fe sulfides. Dominant ore minerals are galena, sphalerite, iron sulfides (pyrrhotite, pyrite, marcasite) and chalcocopyrite. Gangue minerals are ankerite, quartz, calcite, amorphous silica, barite, and minor amounts of kaolinite.

For this activity, the waste deposits of an old flotation plant (Adaro washery, Fig. 1), in the mining district of Linares, were chosen. There are two tailing ponds, one located along the left bank of the Guadiel River (restored in 2011) and another (unrestored) on the right bank (Fig. 2). The aim of this field trip is to visit these dams and showing the characterization of these waste materials and the effectiveness of the sealing techniques employed.

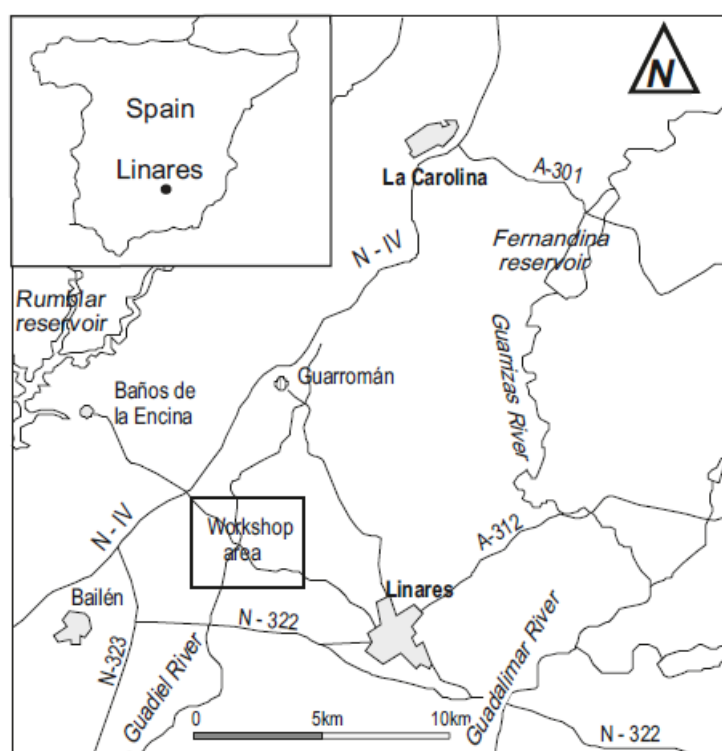


Fig.1. Location of the field trip in the area of Linares.

The mineralogy of the tailings (De la Torre et al., 2012) was studied using XRD analysis. The results of the semi-quantitative analysis indicate that these tailings are mainly composed of quartz, which is very abundant (30–35%), accompanied by phyllosilicates (25–30%), and feldspar, calcite and ankerite, classified as abundant (10–15%) in the tailings samples. Galena, cerussite and lepidocrocite also appear, but only as trace minerals (< 5%). The total contents of metal(loid)s were also analyzed in surface and bottom (Rojas et al., 2012) showing that concentrations were also quite similar in surface and bottom samples, and significant values were found for Fe (25,600–26,900 mg/kg), Pb (3400–1200 mg/kg), Zn (150–100 mg/kg), and As (35–38 mg/kg).

## 3. Hydrochemistry

Based on the work carried out by the RNM-374 research group and the results obtained in Cortada et al. (2017), in a hydrogeochemical study was made in this area in order to detect water pollution. Table 1 show the physicochemical characteristics of surface and groundwater in the environment surrounding the studied dams. The maximum annual mean values (AA) are also included, in accordance with the environmental quality standards of the European Union for priority toxic elements in surface water. In the case of the Guadiel River, there are analytical data obtained from periodic sampling carried out for more than a decade at point R1 (Fig. 2). The first column of Table 2 shows the mean values obtained for water sampled before 2011, the time when the restoration of the main Adaro dam took place. At that time, the river had a calcium bicarbonate-sulfate facies, which reflected the effects of the oxidation of the sulfides present in the mining wastes. In the same way, the electrical conductivity values (968  $\mu\text{S}/\text{cm}$  on average) indicated an increase in the mineralization of the surface waters near the mining area, with notable sulfate contents

(130 mg/L on average) and some trace elements. This is the case of iron (mean value of 0.5 mg/L), manganese (mean value of 0.6 mg/L) and lead (38 µg/L), which, downstream of the dams, exceeded the maximum limits established by environmental laws. During that period, the concentrations of these elements reached particularly alarming maximum values around the Adaro flotation tailing dams (1.3 mg/L Fe, 1.9 mg/L Mn and 0.2 mg/L Pb).

These hydrochemical controls at R1 continued at four-month intervals between 2012 and 2014, after the dam restoration. The average value of the electrical conductivity of the water was 735 µS/cm, which is significantly lower than the value recorded before carrying out the restoration work, also observing an increase in the pH of the water to values above 8, typical of alkaline conditions. In addition, the average sulfate content has been reduced by almost half. A decrease in the mean value of the dissolved concentrations of all the contents of metallic and semi-metallic elements, except As, can be observed (Table 1). Despite this apparent improvement in the chemical quality of the Guadiel river waters, it should be noted that the average Se and Pb contents are still above the annual average values (AA) set by the European Union for surface waters. Furthermore, Fe, Mn and Zn have reached high maximum values in some samples (0.7 mg/L, 0.6 mg/L and 0.6 mg/L, respectively). These results suggest that, despite sealing the landfill, during certain times of the year leachate leaks are generated that can be incorporated into the river, both from the environment surrounding the restored dam and from the unrestored pond on the right bank.

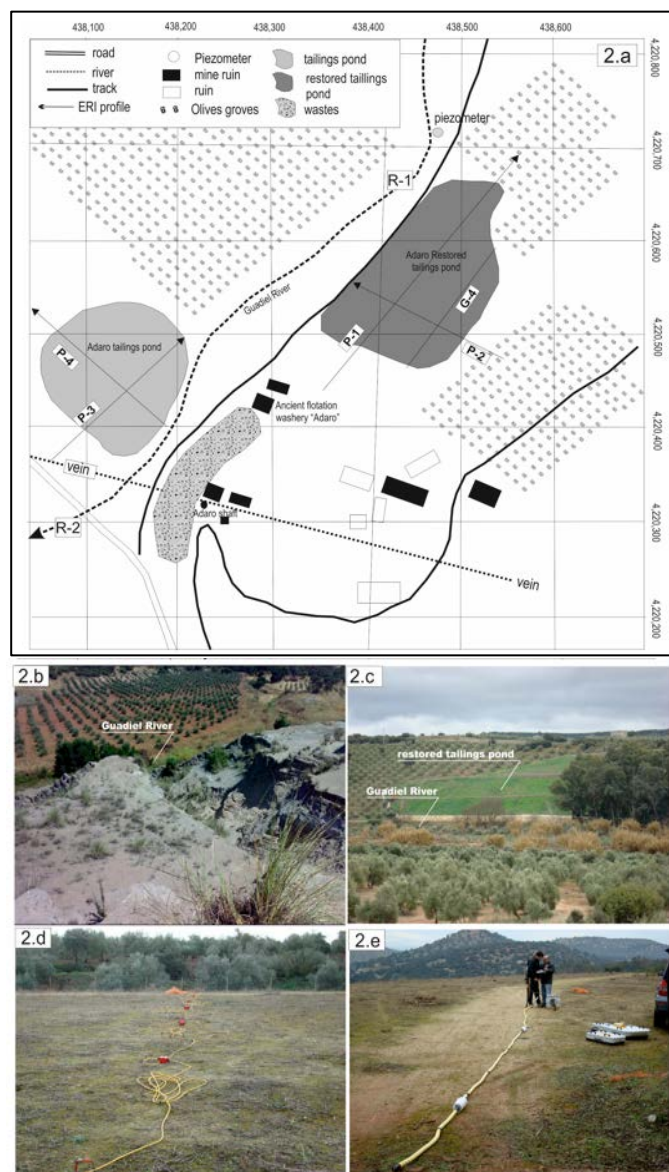


**Fig.2.** Location of the studied tailings ponds with the positions of the piezometer, ERI and GPR profiles (P.1, P.2, P.3, P.4 and G4). R-1 and R-2: surface water sampling points in the Guadiel River (2.a). Tailings pond before restoration affected by a landslide (2.b). Restored tailings pond (2.c). Electrical resistivity imaging profile 2 (2.d). Ground penetrating radar equipment used in this study: 30-MHz Rough Terrain Antennas (RTA) and 100 and 250 MHz screened antennas (2.e) (Cortada et al. 2017).

To analyze the role that abandoned dams and ponds currently play in the chemical quality of the waters of the Guadiel River in the Adaro environment, a new sampling campaign was carried out in the spring of 2016 (Table 2) that included the river in R1 next to the restored dam (Adaro) and a second sampling point downstream of a second restored pond (R2) (La Carlota). The results obtained were compared with the quality of the groundwater from the old Adaro mining well (Well B), flooded after the closure of the mine, and with the waters of a piezometer with a depth of 90 m, located between the restored dam and the riverbed. In the mine water, calcium bicarbonate-sulfate hydrofacies were found with a conductivity greater than 900  $\mu\text{S}/\text{cm}$ , a low content of dissolved oxygen (4 mg/l) and high concentrations of Fe (0.3 mg/l), Pb (0.05 mg/l), Sr (0.5 mg/l) and Zn (0.2 mg/l).

**Table 1:** Physical-chemical characteristics of surface and ground waters. Sample locations shown in Fig. 2. Maximum allowable annual average (AA) values for selected elements are included. Contents exceeding the AAs are in bold.

Parameters and metal(oid)s	Guadiel River - R1		Guadiel River		Spring 2016	
	before 2011	2012-2014	R1	R2	Piezometer	Adaro shaft
Electrical Cond. ( $\mu\text{S}/\text{cm}$ )	968	735	690	712	645	932
Temperature ( $^{\circ}\text{C}$ )	18,1	19	10,5	10,2	19,0	18,6
pH	7,6	8,3	8,2	8,4	6,5	7,2
O <sub>2</sub> (mg/L)	8,7	11,5	8,9	10,5	4,3	4,0
Major constituents (mg/L)						
Ca <sup>2+</sup>	96	78	66	71	66	102
Mg <sup>2+</sup>	32	24	27	21	17	28
Na <sup>+</sup>	58	42	34	40	34	45
K <sup>+</sup>	6	5,3	2	6	3	3
Cl <sup>-</sup>	67	48	53	55	32	45
SO <sub>4</sub> <sup>2-</sup>	133	69	65	81	36	126
HCO <sub>3</sub> <sup>-</sup>	345	272	287	269	236	337
Trace elements ( $\mu\text{g}/\text{L}$ )						
Al	172	31	46	32	27	29
As (50 $\mu\text{g}/\text{l}$ AA)	8	14	26	13	30	13
Ba	256	169	226	202	204	137
Co	1,0	0,6	1,5	0,9	0,5	0,4
Cr (50 $\mu\text{g}/\text{L}$ AA)	2,6	0,7	1,5	0,5	0,7	10
Cu (40 $\mu\text{g}/\text{L}$ AA)	20	3,5	7	6	10	15
Fe	475	395	353	275	219	324
Ga	10	37	18	8	11	7
Mn	632	339	390	482	20	21
Ni (20 $\mu\text{g}/\text{L}$ AA)	<b>31</b>	3,2	5,0	2,8	1,7	3,5
Pb (7.2 $\mu\text{g}/\text{l}$ AA)	<b>38</b>	<b>23</b>	<b>20</b>	<b>10</b>	<b>16</b>	<b>47</b>
Rb	4	2	2	2	8	8
Se (1 $\mu\text{g}/\text{l}$ AA)	<b>1,4</b>	<b>1,2</b>	<b>1,5</b>	<b>1,6</b>	<b>1,4</b>	<b>2,6</b>
Sr	428	256	290	243	288	460
Zn (300 $\mu\text{g}/\text{l}$ AA)	218	161	201	147	148	198

The increase in sulfate content in this hydrogeological context must be linked to an oxidation process of the metal sulfides present in the old mining galleries. The existence of an acid drainage, as could be inferred from this process, is not detected at any point in this area, probably due to the presence of carbonate gangues (ankerite) that balance the pH (Hidalgo et al., 2006). On the other hand, the water collected in the river piezometer is of the calcium

bicarbonate type and has the lowest electrical conductivity (645  $\mu\text{S}/\text{cm}$ ) and pH (6.5) measured in the study area. Its chemical composition is representative of a subsurface flow, which, in periods of high water, can reach the river bed in the vicinity of the dam. The metal(oid) concentrations analyzed in this water sample are, in almost all cases, lower than those detected in the mine water, as expected, with the exception of As and Ba.

For the waters of the Guadiel River, it should be noted that in this last sampling campaign a calcium bicarbonate facies and a moderate conductivity (690-712  $\mu\text{S}/\text{cm}$  in R1 and R2) are maintained, which are very similar to the average values of the 2012 period. 2012-2014. Despite this, the concentrations of dissolved metals are higher than those obtained for the piezometer water in most cases, and for Fe, Mn and Ba, they even exceed those of the mine water analyzed on the same date. A slight increase in the degree of mineralization of the water is recorded between R1 and R2, associated with an increase in the sulfate content. Additionally, in this section of the river, a significant increase in manganese content is observed, reaching 0.5 mg/l, a particularly high value when compared to the concentrations measured in groundwater samples (0.02 mg/l, both in the mine water and in the piezometer water). Therefore, it is reasonable to assume that the origin of the Mn content does not come from underground or subsurface flows towards the river bed.

## 4. Characterization of dams by geophysical techniques

### 4.1. Electrical Resistivity Imaging (ERI) and Induced Polarization (IP)

This geophysical prospecting technique is based on determining the distribution of a physical parameter in the subsoil, based on a very high number of measurements made from the ground surface. In this case, the difficulty (resistivity) offered by a material to the passage of electric current through it is measured (Telford et al., 1990; Store et al., 2000). The different geoelectric behavior allows obtaining 2D profiles, turning out to be a very effective non-destructive tool for the study and characterization of subsurface discontinuities (Sasaki, 1992; Store et al., 2000). In this investigation, profiles have been executed with spacing between electrodes of 5 m in the restored dam and 3 m in the non-restored one (Fig. 2 a and d). The electrical tomography equipment used is the RESECS model, Deutsche Montan Technologie (DMT).

In total, 4 electrical tomography profiles have been made with 64 electrodes (Cortada et al., 2017) located in Figure 2. Two of them have been carried out in the restored pond (P-1 and P-2 in Fig. 2) with a length of 320 m each, and another two in the unrestored pond (P-3 and P-4 in Fig. 2), of 192 m per profile. The interpretations of the electrical tomography profiles have been made from the apparent resistivities obtained in the field work, treated by means of the specific resistivity and induced polarization software RES2DINV (Griffiths and Barker, 1993; Loke and Barker, 1996; Loke and Dahlin, 2002). Figure 3 shows the two profiles made on the restored dam, both with apparent resistivity values (A and B in Fig. 3) and real resistivities (C and D in Fig. 3).

The profiles have been designed to cover the entire dam, in order to characterize the residue and the contact with the substrate. Profile 1, SW-NE direction, was made in one of the berms of the dam. From the resistivity values, two large sets can be differentiated (C in Fig. 3): a superficial one, with low values (less than 150  $\Omega\cdot\text{m}$ ) that is associated with the sludge dam, and another set, with high values. increasing resistivity (which can exceed 2000  $\Omega\cdot\text{m}$ ) associated with granite. Within the granite assemblage, in the highest part, the lowest resistivity values appear, which is associated with the high degree of alteration that this rock presents on the surface. At depth, the resistivity values increase associated with a progressively healthier granite.

In the longitudinal profile of the structure (D in Fig. 3), as in the previous case, two sets could be considered: the granite and the mining deposits. A very irregular topographical base is detected, on which the sludge was deposited, filling two depressions, with changes in power in the fillings that range between 5 and 7 meters in the crest area up to 35 m in the middle part of the slope. In the fill, a surface level with somewhat higher resistivity values is observed in a discontinuous way, especially in the berm areas and in the lower part of the slope, which suggests areas in which the waterproofing has not been as effective. Bearing in mind that the granulometry variations in this dam are not very significant, ranging between silt and fine sand, the resistivity variations observed in this fill (between 30 and 150  $\Omega\cdot\text{m}$ ) are related to changes in humidity and not with lithological changes, as occurs in other dams in the sector (Martínez et al. 2014; 2016; 2021). On the other hand, the granitic basement is characterized by presenting high resistivities, with important and abrupt decreases in the values (up to 50  $\Omega\cdot\text{m}$ ) that are difficult to explain. These

could be attributed either to alteration zones associated with fractures or even to old mining operations currently filled with mud and water. Therefore, in profile 1, a higher level with a lower degree of humidity could be considered, which could be related to the restoration and waterproofing work carried out. However, this level of medium resistivity (between  $100\text{--}150\ \Omega\cdot\text{m}$ ) is not continuous, being lost at both ends of the mining dam, in contact with the granite. From this it can be deduced that the waterproofing process was not completely achieved in the perimeter area of the pool, in contact with the substrate. For this reason, this perimeter zone continues to be a recharge zone for leachates.

Figure 4 shows the two profiles (P3 and P4) made in the unrestored dam (A and B, apparent resistivity values, C and D real resistivities).

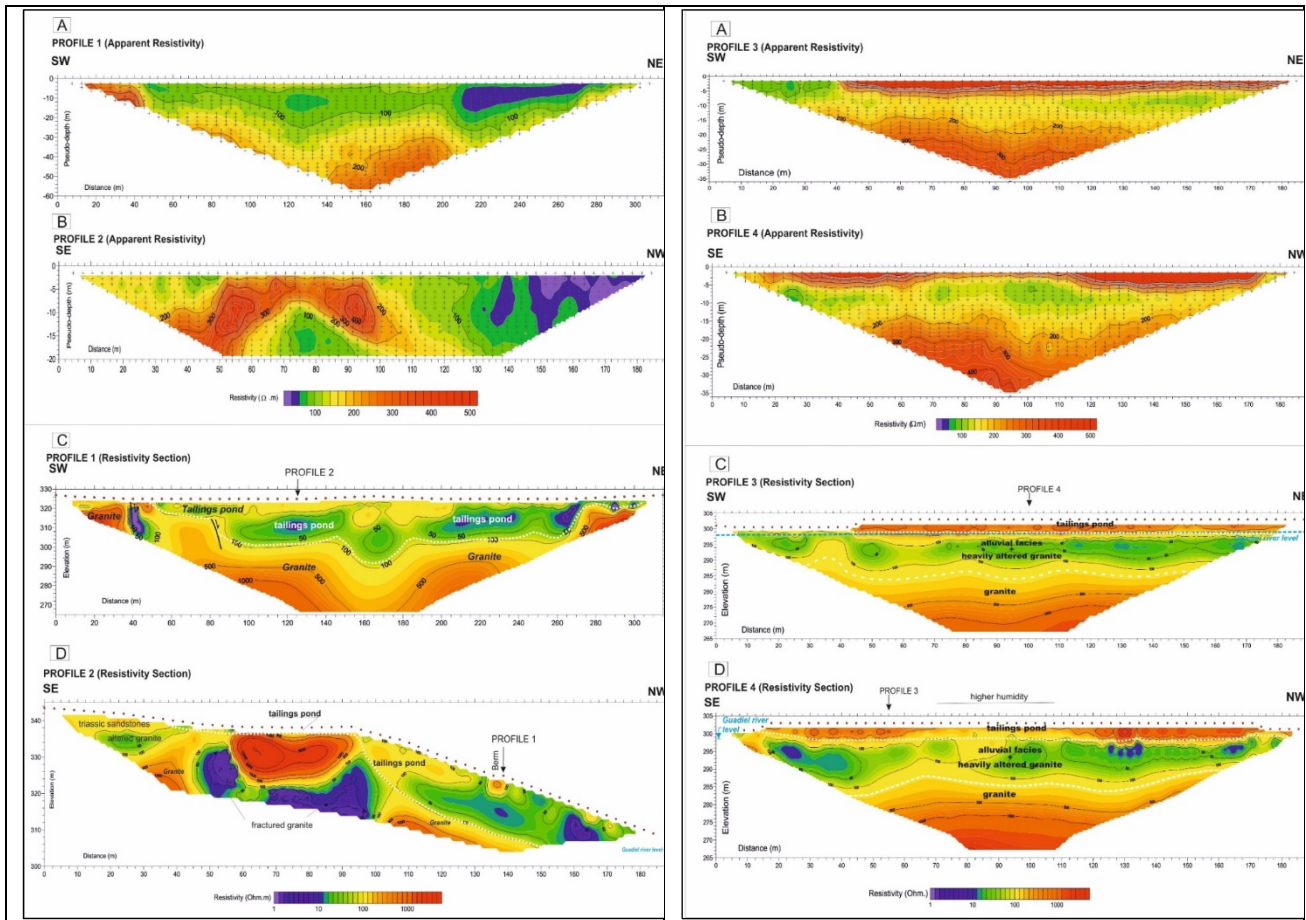


**Fig.3.** Electrical resistivity imaging profiles (profiles 1–2). The position of each profile is shown in Fig. 2. (Cortada et al., 2017).

**Fig.4.** Electrical resistivity imaging profiles (profiles 3–4). The position of each profile is shown in Fig. 2. (Cortada et al., 2017).

Profile 3, SW-NE direction, was made on the mud pond, parallel to the Guadiel River. In it, from the resistivity values, three large sets can be differentiated (C in Fig. 4), one superficial, of about 2-3 m of power, with medium-high values (between  $500\text{--}1500\ \Omega\cdot\text{m}$ ), which is associated with the waste from the sludge dam. The intermediate set, which outcrops in the vicinity of the Guadiel River, offers low resistivity values (between  $50$  and  $100\ \Omega\cdot\text{m}$ ) and is related to the shales associated with the old floodplains of the river. Finally, in the deepest position, granite appears, first very altered (with resistivity values less than  $500\ \Omega\cdot\text{m}$  and healthy in depth (with values that can exceed  $2000\ \Omega\cdot\text{m}$ ). Profile 4 is perpendicular to the previous one and passes right through the center of the old structure (Fig. 2). On this occasion, the presence of the three levels (granite, fluvial shale and mud dam) can also be deduced. However, a difference is noted compared to the previous profile: in the central part of the sludge dam since the resistivity values drop considerably to values of  $150\ \Omega\cdot\text{m}$  (Fig. 4, D). This geoelectric behavior could be associated with the model of construction and growth of the pond since the system discharge was through a perimeter gutter

and the drainage system was centered, with a slightly conical structure morphology. Therefore, the central part of the structure will retain the highest humidity, which translates into the lowest resistivities.

Other works carried out later, in which Electrical Resistivity and Induced Polarization have been measured, at the foot of the restored dam next to the Guadiel River (Rey et al, 2020) (Fig. 5 and 6), reveal the presence of possible leachate that would be taking place at the foot of the structure, as can be seen in figure 6D, where we assimilate the chargeability values between 5 and 8 mv/V measured superficially to these leachates.

In Fig. 6, it is represented: A) real resistivity in a profile 395 meters long (80 electrodes every 5 meters). B) real resistivity of a profile 315 meters long (64 non-polarizable electrodes every 5 meters). C) Chargeability obtained in the Induced Polarization profile (315 meters).

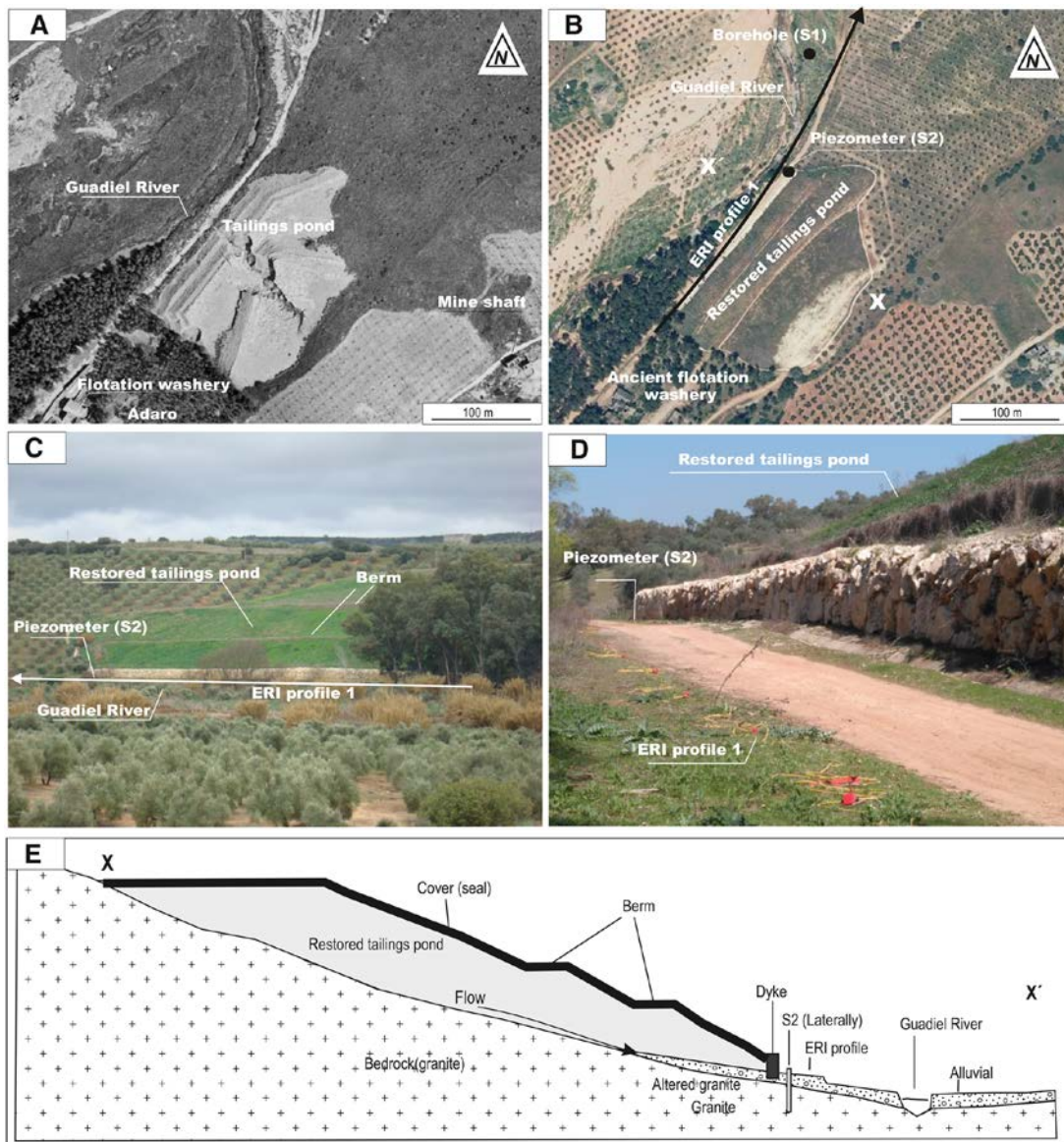


**Fig.5.** Position of the Resistivity and Induced Polarization profile made at the foot of the Adaro dam. A) dam before restoring. B and C) restored dam and profile position. D) Layout of the wiring at the foot of the dam. E) cross-sectional profile of the dam and situation with respect to the Guadiel river (Rey et al, 2020).

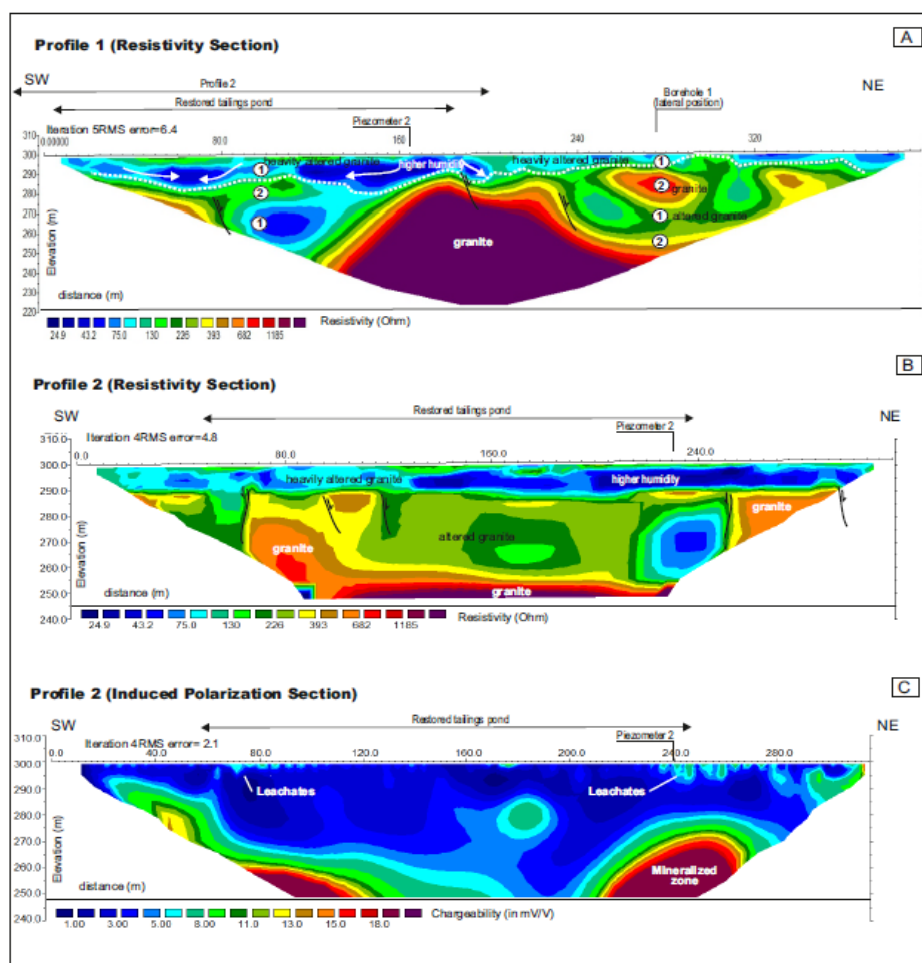


**Fig.6.** A) Real resistivity of the 395 m profile. B) Real resistivity of the 315 m profile. C) Chargeability of the Induced Polarization profile (315 meters) made at the base of the Adaro dam (Rey et al, 2020).

## 5. Conclusions

The hydrochemical study carried out on the surface and groundwater of the Adaro area allows the identification of high contents of sulfates, carbonates and metals(oids) dissolved in the water, with a signal of sulfated hydrofacies. It is significant the high concentrations of Fe, Mn, Pb, Zn and Se. These elements are associated with the oxidation process of metallic sulfides of the mining dams, so they could be related to local processes of generation of leachates from these waste deposits. The comparison of the hydrochemical studies carried out in the sector before and after sealing can also inform us about the effectiveness of the sealing and, therefore, the elimination of contamination vectors. In this way, although the hydrochemical parameters have improved substantially after encapsulation, high metal(oid) values continue to be measured, which are associated with leaks from the sludge deposit associated with local leachate infiltration processes from these residues towards the substrate. all this facilitated by the intense fracturing of the granite plinth. Geophysical prospecting methods, Electrical Resistivity Imaging (ERI), were used in the characterization of mining dams. In this way, the ERI technique allows reconstructing the morphology of these mining structures, it is possible to identify the contact of the residue with the substrate and detect the areas of greatest humidity. Thus, areas with higher humidity could be related to failures in the insulation of the structure during the sealing stage. The possible leakage of leachate at the foot of the structure was also made clear by the results obtained in the Induced Polarization profile carried out.

## References

Azcárate, J.E. (1977). Mapa geológico y memoria explicativa de la hoja 905 (Linares), escala 1:50.000. Instituto Geológico y Minero de España, Madrid.

- Cortada, U., Martínez, J., Rey, J., Hidalgo, C. (2017) Assessment of tailings pond seals using geophysical and hydrochemical techniques. *Eng Geol* 223:59–70
- Cortada, U., Hidalgo, M., Martínez, J., Rey, J. (2019). Dispersion of metal(loid)s in fluvial sediments: an example from the Linares mining district (southern Spain). *Int. J. Environmental Science and Technology*, 16, 469–484. <https://doi.org/10.1007/s13762-018-1687-x>
- Cortada, U. (2021) Ph Thesis. Universidad de Jaén.
- Dahlin, T., Zhou, B. (2004). A numerical comparison of 2D resistivity imaging with 10 electrode arrays. *Geophysical Prospecting* 52(5): 379–398. <https://doi.org/10.1111/j.1365-2478.2004.00423.x>
- De la Torre, M.J., Hidalgo, M.C., Rey, J., Martínez, J. (2012). Mineralogical characterization of tailing dams: incidence of abandoned mining works on soil pollution (Linares, Jaén). *Geophysical Research Abstracts*.
- Griffiths, D.H., Barker, R.D. (1993). Two-dimensional resistivity imaging and modelling in areas of complex geology. *J. Appl. Geophys.* 1993, 29, 211–226.
- Hidalgo, M.C., Benavente, J., El Mabrouki, K., Rey, J. (2006). Estudio hidroquímico comparativo en dos sectores con minas abandonadas de sulfuros metálicos: distrito de Linares-La Carolina (Jaén). *Geogaceta* 39:123–126
- Hidalgo, M.C., Rey, J., Benavente, J., Martínez, J. (2010). Hydrogeochemistry of abandoned Pb sulphide mines: the mining district of La Carolina (southern Spain). *Environ Earth Sci* 61:37–46
- Huang, X., Luo, D., Zhao, D., Li, N., Xiao, T., Liu, J., Wei, L., Liu, Y., Liu, L., Liu, G. (2019). Distribution, Source and Risk Assessment of Heavy Metal(oid)s in Water, Sediments, and Corbicula Fluminea of Xijiang River, China. *International Journal of Environmental Research and Public Health* 16: 1823.
- Lillo, F. J. (1992a). Geology and geochemistry of Linares - La Carolina Pb-ore field (Southeastern border of the hesperian massif).
- Lillo, F. J. (1992b). Vein-type base-metal ores in Linares-La Carolina (Spain) ore-lead isotopic constrains. *Eur. J. Mineral.* 4: 337-343.
- Lillo, F. J. (2002). Hydrothermal alteration in the Linares-La Carolina Ba-Pb-Zn-Cu-(Ag) vein district, Spain: mineralogical data from El Cobre vein. *Trans. Instn. Min. Metall.* 111: 114-118.
- Loke MH, Barker RD (1996). Rapid least-squares inversion of apparent resistivity pseudosections by a quasi-Newton method. *Geophysical Prospecting* 44: 131-152.
- Loke MH, Dahlin T (2002) A comparison of the Gauss-Newton and quasi-Newton methods in resistivity imaging inversion. *Journal of Applied Geophysics* 49: 149-162.
- Loke, M.H., Dahlin, T. (2002). A comparison of the Gauss-Newton and quasi-Newton methods in resistivity imaging inversion. *J. Appl. Geophys.* 2002, 49, 149–162.
- Martínez, J., Rey, J., Hidalgo, M., Garrido, J., Rojas, D. (2014). Influence of measurement conditions on the resolution of electrical resistivity imaging: The example of abandoned mining dams in the la Carolina District (Southern Spain). *International Journal of Mineral Processing*, 133, 67–72. <https://doi.org/10.1016/j.minpro.2014.09.008>
- Martínez, J., Hidalgo, M., Rey, J., Garrido, J., Kohfahl, C., Benavente, J., Rojas, D. (2016). A multidisciplinary characterization of a tailings pond in the Linares-La Carolina mining district, Spain. *Journal of Geochemical Exploration*, 162, 62–71. <https://doi.org/10.1016/j.gexplo.2015.12.013>
- Martínez, J., Mendoza, R., Rey, J., Sandoval, S., Hidalgo, M. C. (2021). Characterization of Tailings Dams by Electrical Geophysical Methods (ERT, IP): Federico Mine (La Carolina, Southeastern Spain). *Minerals*, 11(2). <https://doi.org/10.3390/min11020145>
- Mendoza, R., Martínez, J., Rey, J., Hidalgo, M., Campos, M. (2020). Metal(loid)s Transport in Hydrographic Networks of Mining Basins: The Case of the La Carolina Mining District (Southeast Spain). *Geosciences*, 10(10). <https://doi.org/10.3390/geosciences10100391>
- Rey, J., Martínez, J., Hidalgo, M.C., Mendoza, R., Sandoval, S. (2021). Assessment of Tailings Ponds by a Combination of Electrical (ERT and IP) and Hydrochemical Techniques (Linares, Southern Spain). *Mine Water and the Environment* 40: 298-307. <https://doi.org/10.1007/s10230-020-00709-3>
- Rojas, D., Hidalgo, M., Kohfahl, C., Rey, J., Martínez, J., Benavente, J. (2019). Oxidation Dynamics and Composition of the Flotation Plant Derived Tailing Impoundment Aquisgrana (Spain). *Water, Air & Soil Pollution*, 230, 158. <https://doi.org/10.1007/s11270-019-4190-1>
- Sasaki, Y. (1992). Resolution of resistivity tomography inferred from numerical simulation. *Geoph. Prospecting* 40: 453–464.
- Store, H., Storz, W., Jacobs, F. (2000). Electrical resistivity tomography to investigate geological structures of earth's upper crust. *Geophysical Prospect.* 48, 455-471.
- Telford, W.M., Geldart L.P., Sheriff, R.E. (1990). *Applied Geophysics*, Cambridge University Press. 770 pp.

# Metal sorption processes by clay minerals in soils and sediments. Effect of the alteration of clay minerals

Tibor Németh (1), (2)

(1) Eötvös Loránd University, Department of Mineralogy, Budapest, Hungary

(2) University of Pécs, Department of Geology, Hungary

## *Abstract*

Sorption of metals in soils and sediments are influenced by the properties of the adsorptive and adsorbate, the properties of the adsorbent and the physical and chemical conditions of the environment. The sorption of a metal cation for clay minerals having a layer charge, such as smectites or vermiculites, can take place on the outer planar crystal surface, and in the interlayer space as hydrated cations. Among clay minerals smectites have large metal ion adsorption. Montmorillonites from bentonites adsorb high amount of metals, considerably higher than illite. Heterogeneous composition of soil clays, and the pedogenic clay mineral transformation processes modify sorption properties. The adsorption capacity of soil smectites and vermiculites is closer to that of almost pure montmorillonite, but still lower. During the clay mineral alteration processes, the formation of intermediate phases, whose properties are between the primary clay mineral and the product affect the sorption properties of soils and sediments.

## *Resumen*

La adsorción de metales en suelos y sedimentos está influida por las propiedades de los metales, las propiedades de las fases adsorbentes y las condiciones físicas y químicas del medio ambiente. La adsorción de un catión metálico en minerales arcillosos con carga de capa, tales como esmectitas o vermiculitas, puede tener lugar en la superficie exterior plana del cristal y en el espacio entre capas como cationes hidratados. Entre los minerales arcillosos, las esmectitas tienen una gran capacidad de adsorción de iones metálicos. Las montmorillonitas de las bentonitas adsorben una gran cantidad de metales, considerablemente más que las illitas. La composición heterogénea de las arcillas del suelo y los procesos de transformación de minerales arcillosos pedogénicos modifican las propiedades de adsorción. La capacidad de adsorción de las esmectitas y vermiculitas del suelo es solo ligeramente inferior a la de la montmorillonita casi pura. Durante los procesos de alteración del mineral arcilloso, la formación de fases intermedias, cuyas propiedades se encuentran entre el mineral arcilloso primario y el producto, afectan a las propiedades de adsorción de suelos y sedimentos

*Key-words:* Metal; sorption; clays; alteration

## **1. Introduction**

Thanks to the enormous number of studies the main features of the distribution and migration of toxic and bioessential metals in soils and geological formations are sufficiently well known. One of the basic processes is the adsorption of metals by soils, and the most various soil constituents. It is also well known that clay minerals play an important role in these sorption processes due to their unique physical and chemical characteristics. Plenty of data for various adsorbates and adsorbents are available in the literature, providing us the opportunity to predict the sorption properties and processes for almost any material, under any circumstances. Nevertheless, there is not a general rule describing the relationship between soil properties and metal sorption. Additionally, our knowledge about the metal adsorption capacity of individual constituents of soils and sediment is still incomplete. These components are various: minerals and rock fragments (constituted by minerals), organic matter, and even the association of these two, the organo-mineral complexes. As the phase composition of soils are heterogenous, the characterization of their metal sorption is complicated (Strawn, 2021). Moreover, the soil and sediment components are not stable. They have their typical alteration and transformation pathways according to the physico-chemical environment. Consequently, the soil properties – such as the metal sorption capacity – change over time. And finally,

the peculiarities of the Earth planet's surface, the presence of water and life, never should be disregarded. This lecture gives a brief insight through some examples into the change of metal sorption with the alteration of clay minerals in soils and sediments. This review summarizes only a small segment of the mineralogical aspects of metal sorption in soils. Nevertheless, the author hopes for its usefulness for all researchers (geologists, hydrogeologists, soil scientists, chemists, environmental scientist, etc.) working on metal contamination issues related to soils and sediments.

## 2. Factors influencing the sorption of metals in soils and sediments

Sorption of metals – and thus, their distribution and fate – in soils and sediments are influenced by several factors. These factors can be divided in three groups: factors related to 1. the properties of the adsorptive and adsorbate, 2. the properties of the adsorbent, and 3. the physical and chemical conditions of the environment. An adequate study of the metal sorption requires the characterization each of them. Since sorption of metals in soils and sediments always takes place in aqueous medium, the adsorptive metal and the environment can be considered a solution. Table 1 lists the most important factors for clay minerals (in particular smectites). The factor is considered positive when its rise involves the increase of the sorption. It can be stated that the role of most of them is complex, or variable, depending on other factors. The most important influencing factor from the part of the solution is pH. Chemical species of the adsorbed metal is affected by the pH. In case of ion exchange processes  $H^+$  behaves as a competing cation: adsorption generally increases with pH, because the competition decreases. Moreover, the variable charge of soils is pH dependent, the surface charge becomes more negative with the increasing pH. The sorption sequence of the cations depends on the charge, ionic radius and hydration ability of the cations. The differences in the real sequence series are due to the different and very commonly heterogeneous adsorbents.

**Table 1.** Effect of sorption influencing factors on the metal sorption of clay mineral adsorbent.

<b>Properties of the adsorbent (clay mineral)</b>	
<i>Factor</i>	<i>Effect on the sorption</i>
permanent charge	positive
origin of permanent charge	variable, cation depending
variable charge	pH dependent, positive with increasing pH
surface area	positive
particle size	positive
swelling capacity	positive
<b>Properties of the solution</b>	
pH	variable, complex
metal ion concentration	positive
chemical form of the metal ion	complex
metal ion	
▪ charge	positive
▪ hydration	negative
ionic strength	negative
temperature	variable
<b>Other factors</b>	
time	positive
solid/fluid ratio	positive

## 3. General features of the metal sorption by clay minerals

Among clay minerals smectites have large metal ion adsorption capacity therefore they have high environmental and geochemical importance. According to the respected structural models, smectites are phyllosilicates having pyrophyllite like 2:1 basic structure and extremely small crystallite size, some 100 nm lateral dimension and some nanometres thickness. Due to isomorphic substitution in their lattice, they have a permanent negative charge, the

layer charge. This negative charge is responsible for the high cation exchange and adsorption capacity of the smectites. Smectites can integrate water or other polar organic substances into their interlayer space, and thus expanding it. The swelling capacity is an important feature related to the layer charge. The expanding and sorption capacity of smectites is utilised in the isolating layer of landfills.

The sorption of a metal cation can take place on various sites of a clay mineral (Figure 1). On the outer planar crystal surface (A), and in the interlayer space (B) cations are bond by outer-sphere adsorption, which means that these cations are hydrated. These are the most important sorption sites for clay minerals having a layer charge (permanent charge), such as smectites or vermiculites. The mechanism of this type of sorption is cation exchange. The layer charge resulting in 80–120 cmol/kg cation exchange capacity, associated with the huge specific surface area (~800 m<sup>2</sup>/g) make smectites and vermiculites excellent adsorbents, as demonstrated by some adsorption capacity data in Table 2. On the crystallite edges (C) metals are bond by inner-sphere sorption to the reactive (OH) groups of the octahedral sheet, whose charge is pH dependent (variable charge of the soil). Since clay minerals in soils, particularly smectites and mixed layer clay minerals are very thin in soils (some TOT layers) the ratio of the variable charge is only 10-15% of the total layer charge. Moreover, as the point of zero charge (PZC) of montmorillonite is around pH 6.5 (Tombácz and Szekeres, 2004), this site contributes to the cation uptake at alkaline pH, and they can adsorb anions at acidic conditions. Consequently, 2:1 clay minerals have very restricted adsorption affinity for metals in form of oxyanions (e.g. As, Mo) or for P, the indispensable plant nutrient. Large, generally non-hydrated cations are fixed in the ditrigonal cavities of the silicate tetrahedral sheet (D). This is the typical site of K<sup>+</sup> (or even NH<sub>4</sub><sup>+</sup>) in illite and high charge vermiculite or smectite, giving a significant role to this site and minerals in plant nutrient issues. Radiocaesium is also preferentially sorbed on this site. Dehydrated cations with smaller than ~0.7 Å ionic radius can migrate upon heating from the interlayer space to the octahedral vacancy (E) of a dioctahedral 2:1 clay mineral and neutralizes the charge originating from the octahedral sheet. This is the well-known Hofmann-Klemen effect, which is used with Li in smectite identification, but it is also known for Cu (He et al., 2001; Németh et al. 2005), and Ni (Németh. 2003).

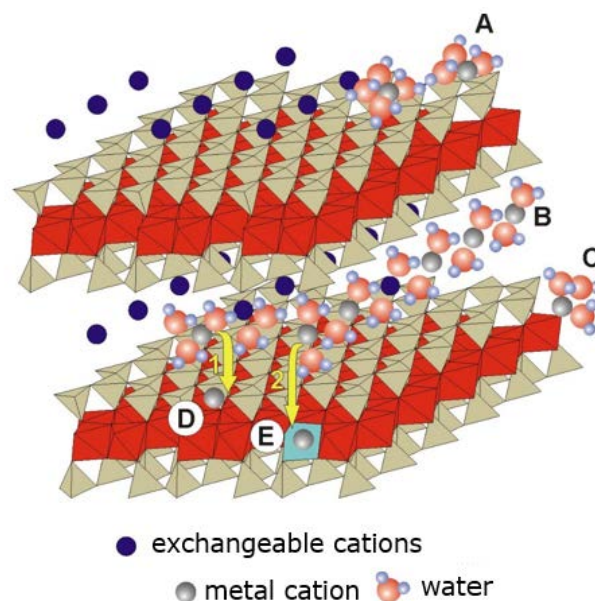


Fig. 1. Possible sorption sites of metal ions in clay minerals (smectites). A: outer planar surface, B: interlayer space, C: edge sites, D: hexagonal/ditrigonal cavity, E: octahedral vacancy.

According to McBride's concept, precipitation is the continuation of the surface adsorption, especially in contaminated medium, where the metal concentration is high (McBride, 2000). The precipitation of cerussite and basic Cu carbonates in calcareous soils is a common way of the immobilization of lead or copper (Sipos et al., 2008; Sipos et al., 2019).

The determination of the adsorption capacity of a sediment or soil can be achieved by batch sorption experiments, but sequential extraction methods also provide a good approach. Table 2 summarizes the maximum adsorption capacity determined from linearized Langmuir isotherms based on batch adsorption experiments (Németh, 2003;

Németh et al. 2005). It can be stated that montmorillonites from bentonites adsorb high amount of metals, considerably higher than illite. However, the adsorption capacity of soil smectites and vermiculites is closer to that of almost pure montmorillonite, but still lower. This is due to the heterogenous composition of soil clays, and the pedogenic clay mineral alteration, transformation processes, which modify the sorption properties.

**Table 2.** *Cu and Zn sorption capacity of various montmorillonites and other clay minerals.*

clay mineral	Cu sorption (mg/kg)	Zn sorption (mg/kg)
montmorillonite SWy-2 (Wyoming, USA)	22240	22880
montmorillonite (Istenmezeje, Hungary)	20970	30720
montmorillonite (Oraşu Nou, Romania)	24150	20920
montmorillonite (Valea Chioarului, Romania)	21610	26150
illite (Füzérradvány, Hungary)	3180	
soil smectite (Luvisol, Hungary)	13980	14380
soil vermiculite (Luvisol, Hungary)	13340	14380

#### 4. Clay mineral alteration, transformation and the change of metal sorption

Clay mineral assemblage of brown forest soils of temperate zone, especially Luvisols, shows variability with depth within a soil profile. The typical clay mineral formation, transformation and alteration processes in Luvisols depending on the parent rock are: formation of smectite with heterogenous charge distribution; decrease of the layer charge and illite to smectite transformation, alteration of low charge smectite to high charge vermiculite, vermiculitization of chlorite, hydroxy interlayering of vermiculite (Németh and Sipos, 2006).

Adsorption isotherm curves in Figure 2 show that copper adsorption capacity of the accumulation (B) horizons of a Luvisol profile is 35% higher than the illuviation (E) horizon.

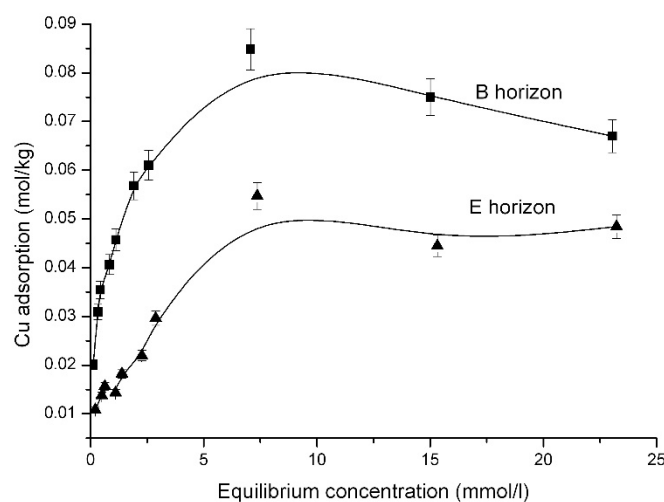


**Fig. 2.** *Copper adsorption isotherms for the E and B horizons of a Luvisol soil profile (Németh et al., 2010).*

The difference arises from the different mineral composition of the horizons. Swelling chlorite/vermiculite mixed layer clay mineral and hydrous iron oxides in the accumulation layer enhances the Cu uptake, while hydroxy-interlayering of vermiculite, and absence of iron oxides decrease the sorption of the eluviated horizon.

Adsorption isotherms reflect the adsorption capacity of the bulk soil material. The contribution of the different soil components can be determined by analytical TEM, which is able to measure the chemical composition of individual particles. The cobalt uptake by soil smectite was found to increase as the total layer charge of the smectite increased.

The layer charge of smectite has considerable effect on the sorption properties. Generally, increasing layer charge increases the metal adsorption capacity within the smectite layer charge range. Transformation of chlorite to vermiculite increases the metal uptake capacity due to the hydration of the interlayer space and thus increased specific area. Hydroxy interlayering has an opposite effect due to the formation of Al-Fe-hydroxyde pillars in the interlayer space. The clay mineral loses its expansion capacity, and the surface area is reduced (Németh et al., 2011). Close association of iron-oxides and clay minerals tend to increase the sorption capacity. Illitization of smectite by potassium fixation decreases the uptake of lead.

Clay mineral alteration processes have significant effect on the sorption of metals by soils and sediments. Sorption capacity is a changing property of soils. During the clay mineral alteration processes intermediate phases form, whose properties are between the primary clay mineral and the product.

## ACKNOWLEDGMENTS

The author thanks the Organizers of the Workshop for the honourable invitation.

## REFERENCES

- He, H. P., Guo, J. G., Xie, X. D., Peng, J. L. (2001): Location and migration of cation in Cu<sup>2+</sup>-adsorbed montmorillonite. *Environment International*, **26**, 347-352.
- McBride, M.B. (2000): Chemisorption and precipitation reactions. In *Handbook of Soil Science* (Ed: Sumner, M.E.) B265-B302. CRC Press, USA.
- Németh T. (2003): Mineralogical, crystal structural and crystal chemical aspects of metal-ion adsorption by montmorillonites. PhD. thesis, Eötvös Loránd University, Budapest, Hungary.
- , Mohai I., Tóth M. (2005): Adsorption of copper and zinc ions on various montmorillonites: an XRD study. *Acta Mineralogica-Petrographica*, **46**, 29-36.
- , Sipos P. Characterization of Clay Minerals in Brown Forest Soil Profiles (Luvisols) of the Cserhát Mountains (North Hungary). *Agrochemistry and Soil Science*, **55**, 39-48.
- , Sipos P., Balázs R., Szalai Z., Mészáros E., Di Gléria M. (2010): Adsorption of copper from dilute brine solution on the illuviation and accumulation horizons of a Luvisol. *Carpathian Journal of Earth and Environmental Sciences*, **5**, 19-24.
- , Jiménez-Millán, J., Sipos P., Abad, I., Jiménez-Espinosa, R., Szalai Z. (2011): Effect of pedogenic clay minerals on the sorption of copper in a Luvisol B horizon. *Geoderma*, **160**, 509-516.
- Sipos P., Németh T., Kovács Kis V., Mohai I. (2008): Sorption of copper, zinc and lead on soil mineral phases. *Chemosphere*, **73**, 461-469.
- , Tóth A., Kovács Kis V., Balázs R., Kovács I., Németh T. (2019): Partition of Cd, Cu, Pb and Zn among mineral particles during their sorption in soils. *Journal of Soils and Sediments*, **19**, 1775-1787.
- Strawn, D.G. (2021): Sorption mechanisms of chemicals in soils. *Soil Systems*, **5**, 13.
- Tombácz E., Szekeres M. (2004): Colloidal behaviour of aqueous montmorillonite suspensions: the specific role of pH in the presence of indifferent electrolytes. *Applied Clay Science*, **27**, 75-94.

# Metal mobility in acid mine drainage-impacted waters: from rivers to oceans

Rafael Pérez-López (1), Sergio Carrero (2), Ricardo Millán-Becerro (1), María D. Basallote (1), Francisco Macías (1), Carlos R. Cánovas (1), José M. Nieto (1)

(1) Department of Earth Sciences & Research Center on Natural Resources, Health and the Environment (RENSMA). University of Huelva, Campus “El Carmen”, E-21071, Huelva, Spain

(2) Institute of Environmental Assessment and Water Research (IDÆA-CSIC), E-08034, Barcelona, Spain

## Abstract

The complete pathway to the oceans for metals contained in acid mine drainages (AMD), from their release to river courses by weathering of sulfide-rich mining wastes, can be elucidated in the Iberian Pyrite Belt (FPI). The Odiel and Tinto rivers drain this vast expanse of massive sulfides, exploited since historical times, discharging a large amount of acidity and pollutants into a common estuary, the so-called Estuary of Huelva. The mixing of acidic river water and alkaline seawater in the estuary leads to a series of geochemical reactions that control the residence time of pollutants along the estuarine transition. This manuscript focuses its attention on that set of geochemical processes that ultimately determine the amount of pollutants that are subsequently transferred to the Atlantic Ocean. In the estuary, a progressive increase in pH is observed from the fluvial to the marine domain due to the water mixing. During the AMD neutralization, flocculation of particulate material occurs: Fe firstly precipitates as schwertmannite and later Al in the form of basaluminite. Other non-conservative elements that are removed from the water column by precipitation processes are Cu, rare earth elements (REE) and Y. The precipitation of schwertmannite produces the retention of As by adsorption at pH below 5.0. However, when schwertmannite particulate matter reach waters with higher pH values, As desorption occurs, which is released back to solution. Arsenic adsorption/desorption processes are associated with the zero-charge point for schwertmannite. Other contaminants such as Zn, Mn, Ni and Co behave conservatively, remaining in solution throughout their estuarine transit and, hence, significantly threatening the environmental conditions of the coastal areas of the Gulf of Cadiz.

## Resumen

El camino completo hasta el océano que siguen los metales contenidos en drenajes ácido de mina (AMD), desde su liberación a los cursos fluviales debido a la meteorización de residuos mineros ricos en sulfuros, puede ser dilucidado en la Faja Pirítica Ibérica (FPI). Los ríos Odiel y Tinto drenan esta vasta extensión de sulfuros masivos, explotados desde tiempos históricos, descargando una gran cantidad de acidez y contaminantes a un estuario común, el Estuario de Huelva. La mezcla de agua fluvial ácida y agua de mar alcalina en el estuario conduce a una serie de reacciones geoquímicas que controlan el tiempo de residencia de los contaminantes en la transición estuarina. El presente manuscrito focaliza su atención en ese conjunto de procesos geoquímicos que en definitiva determinan la cantidad de contaminantes que posteriormente se transfiere al Océano Atlántico. En el estuario, se observa un aumento progresivo del pH desde el dominio fluvial hasta el dominio marino debido a la mezcla de aguas. Durante la neutralización del AMD, se produce la floculación de material particulado: primero precipita el Fe como schwertmannita y posteriormente el Al en forma de basaluminita. Otros elementos no conservativos que son eliminados de la columna de agua por procesos de precipitación son Cu, elementos de tierras raras (REE) e Y. La precipitación de schwertmannita produce la retención por adsorción del As a pH inferiores a 5.0. Sin embargo, cuando el material particulado de schwertmannita entra en contacto con aguas de pH superior se produce la desorción del As que pasa de nuevo a solución. Los procesos de adsorción/desorción de arsénico están asociados al punto de carga cero de schwertmannita. Otros contaminantes tales como Zn, Mn, Ni y Co se comportan conservativamente, permaneciendo en solución durante todo su tránsito estuarino y, por tanto, amenazando significativamente las condiciones ambientales de las áreas costeras del Golfo de Cádiz.

**Key-words:** Acid mine drainage; Estuary of Huelva; Seawater mixing; Geochemical processes; Contaminants mobility

## 1. Introduction

Sulfide minerals have a high potential to react with oxygen and water, and their weathering under atmospheric conditions involves a series of chained geochemical and microbiological reactions that result in the generation of extremely acid drainage with high concentrations of sulfate, metals (Fe, Cu, Pb, Zn, etc.) and metalloids (As, Sb, etc.). Acid leachates originating from oxidation of sulfide minerals located in wastes and facilities from mining activities (e.g., waste piles, tailings ponds and open-pit mines) are called acid mine drainage (AMD). Human activities, especially related to abandoned mining facilities, cause important global environmental changes due to the release of significant concentrations of these metals into rivers that finally flow into the oceans. But before that, estuaries represent the transition zone between river water and seawater, regulating through a series of geochemical processes the flux of metals reaching the coastal areas.

The Estuary of Huelva is formed by the confluence of the Tinto and Odiel rivers (SW Spain). Both rivers cross a region known geologically as the Iberian Pyrite Belt (IPB), which is one of the most important massive sulfide provinces in the world with original reserves on the order of 1700 Mt (Sáez et al., 1999). Intense mining activity in the IPB dates back to about 5000 years (Leblanc et al., 2000). The main environmental problem in the IPB is the AMD from the surface oxidation of sulfides located in the abandoned mining districts. These acidic and metal-rich leachates are drained by the Tinto and Odiel rivers, causing their total degradation (e.g., Olías et al., 2006; Nieto et al., 2013). The transfer of acidity and toxic metals to the Estuary of Huelva has been the focus of numerous investigations (e.g., Elbaz-Poulichet et al., 2001; Borrego et al., 2002; Braungardt et al., 2003; Carro et al., 2011; Hierro et al., 2014). Pollution levels are so extreme that both rivers and their common estuary are considered one of the most polluted aquatic systems in the world. This manuscript focuses on the geochemical processes occurring in the Tinto and Odiel rivers as well as in the Huelva Estuary; however, it is extensible to other mining districts in the world where AMD-affected fluvial courses reach seawater such as King River (Tasmania, Australia; Augustinus et al., 2010), Chonam-ri Creek (Kwangyang, South Korea; Jung et al., 2012), Afon Goch (Anglesey, North Wales; Dean et al., 2013) or Gromolo Torrent (Liguria, North-West Italy; Consani et al., 2017).

## 2. Geochemistry of AMD-impacted rivers

Numerous investigations have focused on the behavior of metals in AMD-affected streams. The AMD contains mostly high concentrations of sulfates and iron (from sulfide oxidation, mainly pyrite) and aluminum (from dissolution of host rock), in addition to other elements, some of them being potentially toxic pollutants. In AMD-affected streams, both hydrochemistry and mineralogy are controlled by the  $\text{SO}_4\text{-Fe(III)}$  and  $\text{SO}_4\text{-Al}$  systems in pH ranges between 2.5-4.0 and 4.5-6.0, respectively (Bigham et al., 1996; Nordstrom & Alpers, 1999). Hydrolysis of Fe and Al during pH increase in AMD results in the precipitation of schwertmannite  $[\text{Fe}_8\text{O}_8(\text{OH})_6(\text{SO}_4)_n\cdot n\text{H}_2\text{O}]$  and basaluminite  $[\text{Al}_4(\text{SO}_4)(\text{OH})_{10}\cdot 4\text{-}5\text{H}_2\text{O}]$ , respectively. Both mineral phases are oxyhydroxysulfates of poorly-crystalline nature.

In mining environments, acid drainage often arises from underground shafts under oxygen-free reducing conditions, where all iron in solution is Fe(II) and the water is almost colorless (Fig. 1a). Under atmospheric conditions, the presence of oxygen and, mainly, the activity of extremophilic microorganisms catalyze the oxidation of Fe(II) to Fe(III). High concentrations of ferric iron and sulfate lead to the spontaneous precipitation of schwertmannite. Iron oxidation and precipitation of schwertmannite turn the water reddish in color (Fig. 1a). In the river network, Fe(III) is the main iron species and schwertmannite is commonly oversaturated in solution. In addition, the increase of pH induced by mixing with pristine waters along the drainage basin or by alkaline addition in passive treatment systems favors the enhanced precipitation of schwertmannite, a process that buffers the pH between 2.5 and 4.0. With the progressive increase in pH, once all the aqueous Fe(III) precipitates, basaluminite precipitation begins and the pH becomes buffered between 4.5 and 6.0. Both phases have high capacity to retain some trace elements in AMD; whereas schwertmannite has strong affinity for As and Cr, basaluminite has for Cu, Si, rare earth elements (REE) and Y. Therefore, their precipitation attenuates pollution naturally along river courses (Fig. 1b; Sarmiento et al., 2009) and artificially in passive treatment systems (Fig. 1c; Macías et al., 2012).

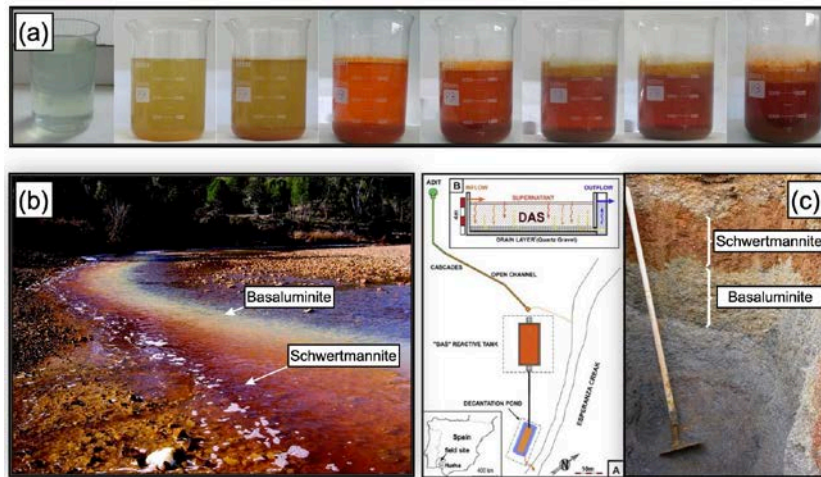


**Fig. 1.** (a) Oxidation of Fe(II) to Fe(III) and spontaneous precipitation of schwertmannite in an oxygen-free AMD sample. (b) Precipitation of schwertmannite and basaluminite by mixing of AMD and unpolluted Odiel river. (c) Reactive filling of a treatment system for AMD and detail of the precipitation horizons of both mineral phases.

In the AMD-affected fluvial systems of the IPB, Al precipitation as basaluminite is a minor process because Fe concentrations are so high that the system is controlled primarily by schwertmannite precipitation or even jarosite if acidic conditions are extreme. In fact, schwertmannite minerals cover the bed of most AMD-affected fluvial courses. The affinity of schwertmannite to retain preferentially oxyanions such as As and Cr and its ability to buffer pH lead to that other metal cations typically behave conservatively in streams at pH below 4.0; i.e., their concentrations mainly decrease by dilution instead of mineral precipitation (Braungardt et al., 2003). On the other hand, schwertmannite structure is metastable and recrystallizes spontaneously to more crystalline phases with time (Acero et al., 2006). In the IPB, iron precipitates capping riverbeds affected by AMD upon slight consolidation and ageing create terrace levels along the channels. The current terraces frequently define a laminated sequence where this recrystallization is observed gradually, from fresh schwertmannite at surface to goethite at depth (Fig. 2a). In addition, there are fossil analogues of current terraces that are isolated from the stream courses due to the river migration over time. In the older terraces, goethite, originating from precursor schwertmannite, has partially recrystallized to hematite by diagenetic processes (Fig. 2b; Pérez-López et al., 2011). The mineral transformation could be accompanied by the release of part of the contaminants, mainly arsenic, previously retained in the solid. Therefore, the search for stability in this poorly crystalline oxyhydroxysulfate could determine the flux of contaminants over time, and what is now considered a sink could become a source of contamination in the medium or long term.

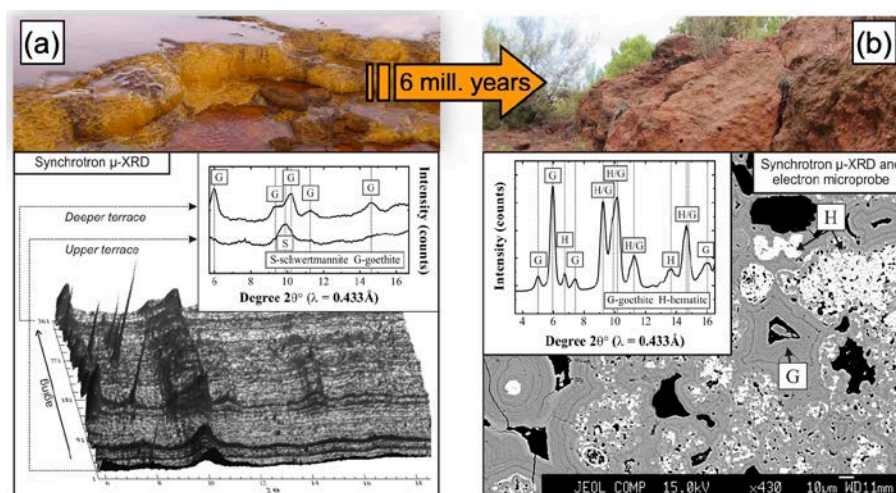


**Fig. 2.** Synchrotron  $\mu$ -XRD analysis on samples from (a) current terrace and (b) fossil terrace of the Tinto-Odiel fluvial system affected by AMD.

Fluvial contribution of metals to the Estuary of Huelva is currently well known for different periods and under different climatic conditions. For example, Olías et al. (2006) calculated the discharge for the period 1995 to 2003 and estimated that both rivers contribute to the estuary more than 50% of the Zn and 10% of the Cu of the total of these metals transferred globally from the continents to the oceans (Table 1). Thus, IPB is a local anomaly but with global repercussions from an environmental point of view.

**Table 1.** Average values of the pollutant load transported by the Tinto and Odiel rivers (Olías et al., 2006), and their comparison with the global flow transported by rivers to the oceans (GESAMP, 1987).

	Río Tinto ton/yr	Río Odiel ton/yr	Tinto-Odiel ton/yr	Global gross flux ton/yr	Fraction (%)
<b>As</b>	12	23	36	10,000	0.4
<b>Cd</b>	4	7	11	340	3.3
<b>Cu</b>	469	1252	1721	10,000	17.2
<b>Fe</b>	5075	2847	7922	1,400,000	0.6
<b>Mn</b>	163	1452	1615	280,000	0.6
<b>Pb</b>	15	12	27	2000	1.3
<b>Zn</b>	863	2612	3475	5800	59.9
<b>Co</b>	9	62	71	1700	4.2
<b>Ni</b>	2	34	36	11,000	0.3

In rivers affected by AMD, geochemical processes have been widely described in the scientific literature and, therefore, this section can be considered as background for this text. The following section aims to highlight an integrated study between river discharges and the geochemical processes that take place during mixing with seawater in the Estuary of Huelva. These processes will reveal the net flux of pollutants that really reaches the Atlantic Ocean. This information is novel in the scientific literature, and for that reason, these results will be explained in more detail.

### 3. Geochemistry of AMD-impacted estuaries

The geochemical processes controlling the mobility of contaminants in estuarine systems can be very complex, including removal from solution into newly-formed solid phases or release to solution by dissolution, desorption or even mineral transformation processes (Morris et al., 1986; Bowers & Yeats, 1989; Baeyens et al., 1998; Zhou et al., 2003). Freshwater inflows and oceanic saltwater mixing is addressed in typical estuaries as salt-induced mixing. However, other geochemical processes occur in estuaries receiving AMD-affected streams, as there is a gradient of pH from values between 2.5-3.5 at the mouth to values close to 8.0 in the marine domain. Such a wide variation in pH in a very short space can cause metals, which are mostly conservatives in fluvial courses, to undergo strong geochemical processes related to acid neutralization that can affect their mobility in marine environments. Such processes will be unpacked below from laboratory to a real field scale.

#### 3.1. AMD - seawater mixing

Evaluation of the hydrochemical and mineralogical processes taking place during interaction of AMD with water of the Estuary of Huelva can be simplified at the laboratory scale by mixing experiments. The dropwise addition of seawater over AMD from the main course of Tinto and Odiel rivers just at the mouth to the estuary causes a progressive increase in pH, revealing the acid neutralization during estuarine mixing (Fig. 3a,b). The pH increases slowly even with large amounts of seawater. Approx. 8.8 mL and 11 mL of seawater were necessary to raise the pH to 7 for each 1 mL of AMD from Tinto and Odiel, respectively.

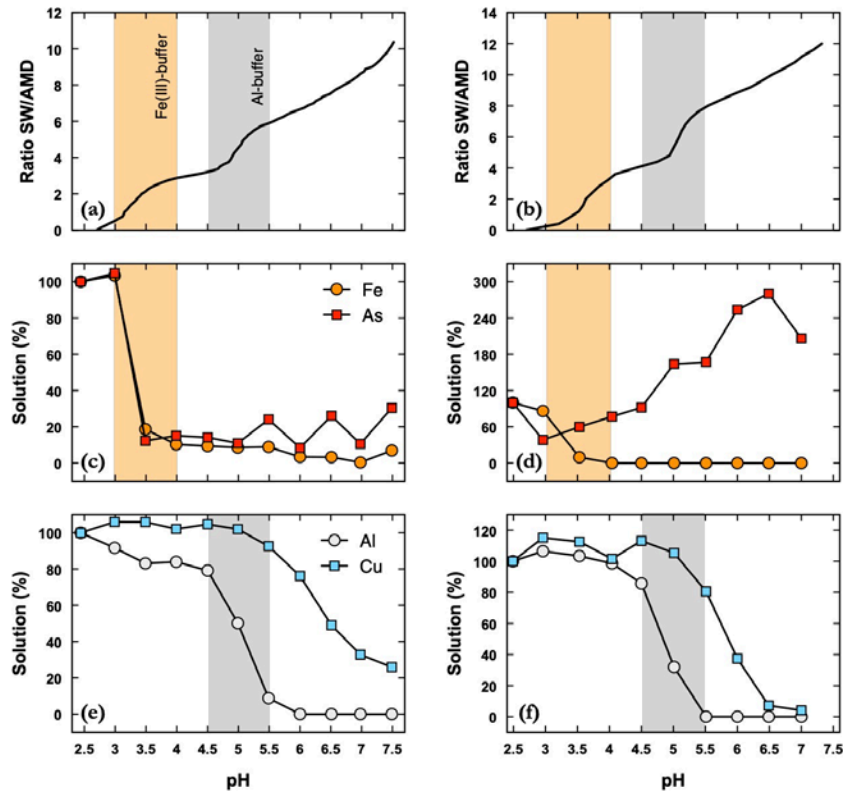


**Fig. 3.** Evolution of pH and percentages of Fe, As, Al and Cu during the addition of seawater to AMD from (a,c,e) Tinto and (b,d,f) Odiel rivers. Orange and grey areas represent different buffers for Fe(III) and Al, respectively. Percentages refer to the relationship between the experimental concentrations and the values calculated from the theoretical mixing of the end-members.

As the pH increases, two buffer zones are observed which are closely related to the formation of two newly-formed mineral phases whose precipitation involves the release of protons. The first buffer, at pH between 3.0 and 4.0, corresponds with the precipitation of Fe(III) as schwertmannite; while the second buffer, at pH between 4.5 and 5.5, corresponds with the precipitation of Al as basaluminite (Fig. 4).

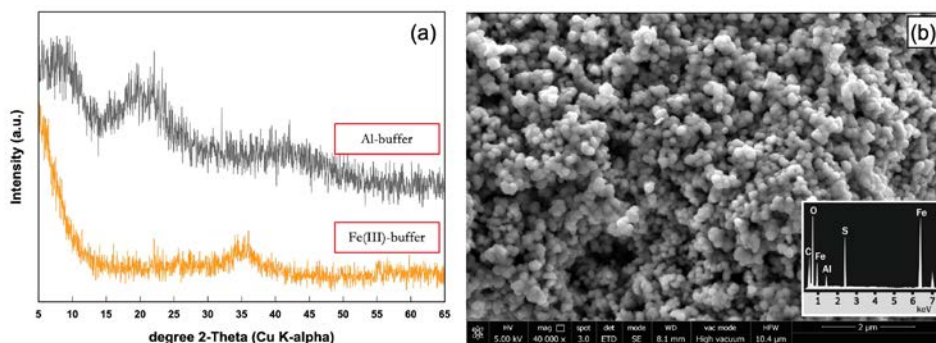


**Fig. 4.** (a) XRD spectra revealing schwertmannite precipitation in Fe(III)-buffer and basaluminite in Al-buffer. (b) SEM image and EDS analysis of schwertmannite. Note the poorly-crystalline nature of both schwertmannite and basaluminite, as suggested by their typical XRD spectra. For comparison purposes, XRD spectra for pure schwertmannite and basaluminite can be found in Sánchez-España et al. (2011).

These findings show for the first time the progressive sequential precipitation of schwertmannite and basaluminite during the mixing of an AMD with seawater, as also observed in fluvial systems. Schwertmannite precipitation, at pH between 3.0 and 4.0, removes Fe(III) from solution. Concomitant with the removal of Fe(III) is the depletion of As (Fig. 3c,d). On the other hand, basaluminite precipitation, at pH between 4.5 and 5.5, removes Al from solution, in addition to Cu (Fig. 3e,f), REE and Y. Hence, both mineral phases also exert a control on the same

elements as in fluvial courses. However, in the estuary there is a wide pH range so that Al precipitation as basaluminite is expected to be of greater importance than in AMD-affected rivers. Moreover, the affinity of schwertmannite for As is only observable at low pH values during the estuarine mixing since an increase in As concentration is observed at higher pH (Fig. 3c,d). This As increase could be associated with possible changes in the superficial properties of schwertmannite in the marine environment, as will be discussed in the next subsection. Other contaminants such as S, Zn, Cd, Ni and Co reveal a conservative behavior throughout the experiments, i.e., their experimental concentrations can be deduced from the theoretical mixing of the end-members (Fig. 5).

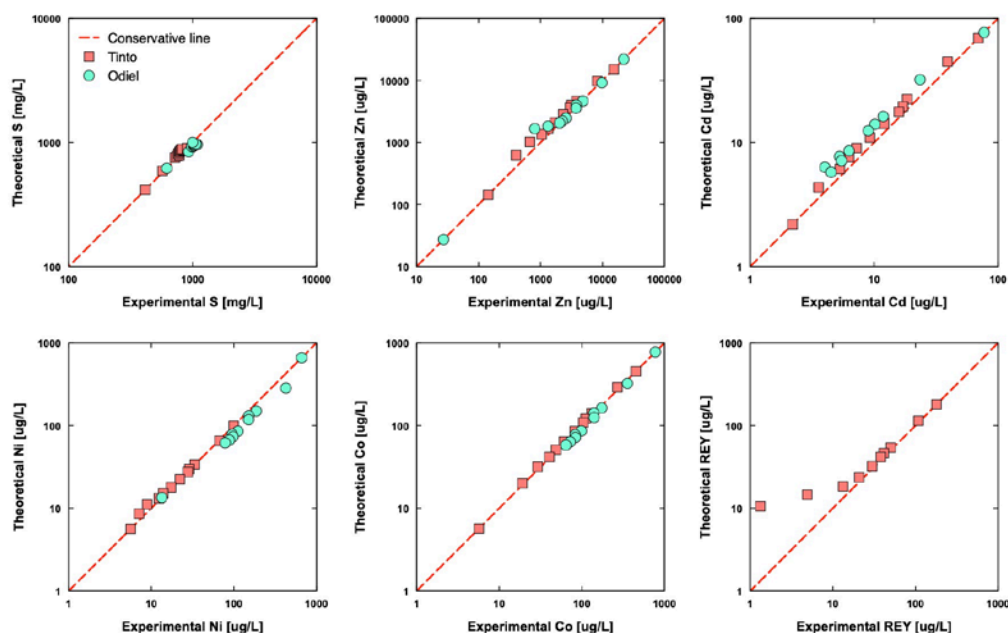


**Fig. 5.** Comparison between experimental concentrations and values calculated from the theoretical mixing of end-members for AMD from Tinto and Odiel rivers. Red line marks the conservative behavior, i.e., those elements plotting on the conservative line do not precipitate during acid neutralization.

### 3.2. The role of particulate matter

According to the previous experiments, high amounts of schwertmannite should flocculate in the Estuary of Huelva during the neutralization of the Tinto and Odiel rivers by seawater mixing. In addition, elevated concentrations of suspended particulate matter consisting mainly of schwertmannite must be transported by both rivers to the estuary, especially during flood events associated with strong rainfalls. The stability of schwertmannite under estuarine conditions, as well as its role on contaminant mobility, can also be simplified in the laboratory. The continuous schwertmannite-seawater interaction at different contact times (from 0 to 336 h) causes a decrease in pH from seawater values (pH = 7.7) to values of around 2.7, 3.7 and 4.6 for the solid:liquid ratios of 1:40, 1:200 and 1:400, respectively (Fig. 6). The higher the amount of schwertmannite, the lower pH values are reached. This response confirms the high potential of schwertmannite to buffer pH.

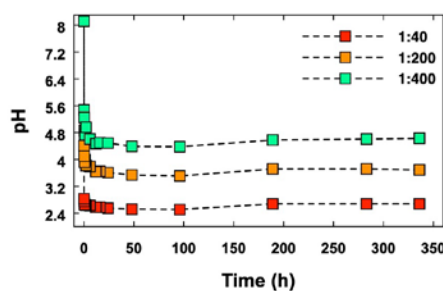


**Fig. 6.** Time evolution of pH in the schwertmannite-seawater interaction experiments.

During the interaction time of schwertmannite with seawater, other contaminants are increasingly released into solution until reaching a steady-state. In addition, the concentrations reached at the steady-state are higher at increasing amounts of starting schwertmannite. Figure 7 shows, as an example, the behavior of Fe, Zn and Mn, although it can be extended to other metals studied such as Al, Cu, REE or Y.

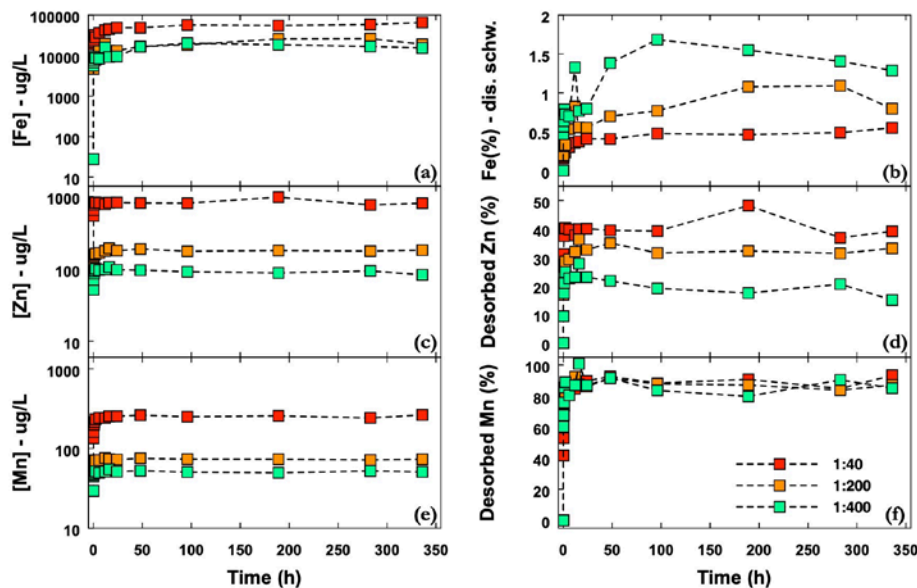


**Fig. 7.** Time evolution of Fe, Zn and Mn: (a,c,e) concentrations in solution and (b,d,f) percentages exclusively released by desorption in the schwertmannite-seawater interaction experiments. In the case of Fe, the percentage would indicate the amount of schwertmannite dissolved in the experiments.

Considering the following assumptions as starting points: (1) the initial sample consists only of schwertmannite, (2) the release of Fe is due exclusively to schwertmannite dissolution during the interaction with seawater and (3) the rest of the metals are also hosted in the schwertmannite by the same structural mechanism, it is possible to calculate the amount of metals released to solution by desorption using the following equation:

$$[M]_{desorbed} = ([M]_{solution} - [M]_{seawater}) - \frac{[M]_{schw}}{[Fe]_{schw}} \times ([Fe]_{solution} - [Fe]_{seawater})$$

The metal concentrations released by desorption ( $[M]_{desorbed}$ ) would correspond to the concentrations in solution ( $[M]_{solution}$ ) minus those in the initial seawater ( $[M]_{seawater}$ ) and minus the concentrations theoretically released by mineral dissolution. The latter concentrations can be calculated from the ratio of metal/Fe in the starting solid ( $[M]_{schw}/[Fe]_{schw}$ ) by the concentration of Fe in solution released only by mineral dissolution, i.e., by deducting the Fe in solution ( $[Fe]_{solution}$ ) minus the Fe in the initial seawater ( $[Fe]_{seawater}$ ). The concentrations released by desorption with respect to the total concentrations that the solid could release by complete dissolution, expressed as a percentage, can be also seen in Figure 7.

As shown in Figure 7, the metals define a positive desorption isotherm with higher percentages released at higher amounts of initial schwertmannite. The contact of schwertmannite with seawater causes the release by desorption of up to 40% of Zn and 100% of Mn with respect to the total existing in the solid; in addition to other elements such as 30% of Al, 20% of Cu and 100% of La. This behavior demonstrates the potential of this mineral to easily release the previously retained elements. The amount of schwertmannite dissolved in the experiments ranges from 0.5% for the 1:40 ratio to 1.5% for the 1:400 ratio. However, the behavior of As is different from that of the other elements previously indicated. Although the total concentrations of As in solution increase with time (Fig. 8a), the percentage released by desorption does not define a positive isotherm as with the other elements. At pH values of 2.7 (1:40 ratio), the percentage of desorbed As defines negative values as an “inverse desorption isotherm” (Fig. 8b). This inverse isotherm reflects the ability of schwertmannite at extremely acidic pH to re-adsorb the As that is

released to solution during the dissolution of the mineral itself. At pH values of 3.7 (ratio 1:200), the As concentrations released by desorption are still slightly negative; however at pH values of 4.6 (ratio 1:400), some As release by desorption is already observed (Fig. 8c). This behavior could indicate that the zero-charge point for schwertmannite in seawater is found at pH values close to 4.6.

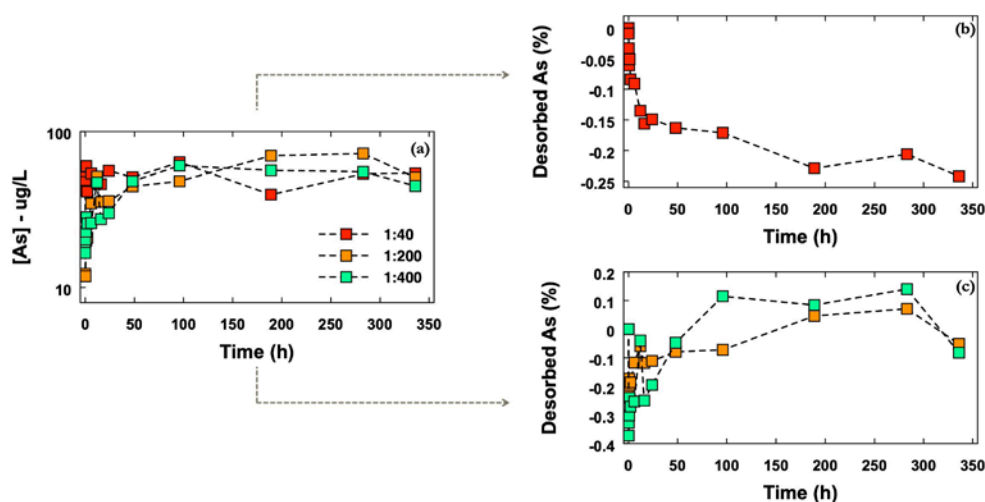


**Fig. 8.** Time evolution of As: (a) concentration in solution, (b) percentage exclusively released by desorption for the ratio 1:40 and (c) percentage exclusively released by desorption for the ratios 1:200 and 1:400 in the schwertmannite-seawater interaction experiments.

The surface of schwertmannite is found positively charged at acid pH values; while the main aqueous As species for the entire pH range is a negatively-charged oxyanion ( $H_2AsO_4^-$ ) according to thermodynamic models. Both aspects would explain the high affinity of As for schwertmannite through adsorption in acid environments. The remaining elements present as positively-charged metal cations would undergo electrostatic repulsion with the mineral surface and thus be released easily into solution. At pH values above the zero-charge point (ca. 4.6 in seawater), the schwertmannite surface becomes negatively charged and desorption of As is also expected (Fig. 9). This desorption process would also explain the increase in the As concentration observed at high pH values in the mixing experiments of the previous section (Fig. 3c,d). Moreover, schwertmannite controls in the same way as for arsenic the mobility of other elements such as Cr, V, Mo or Sb occurring as oxyanions as the main species in solution.

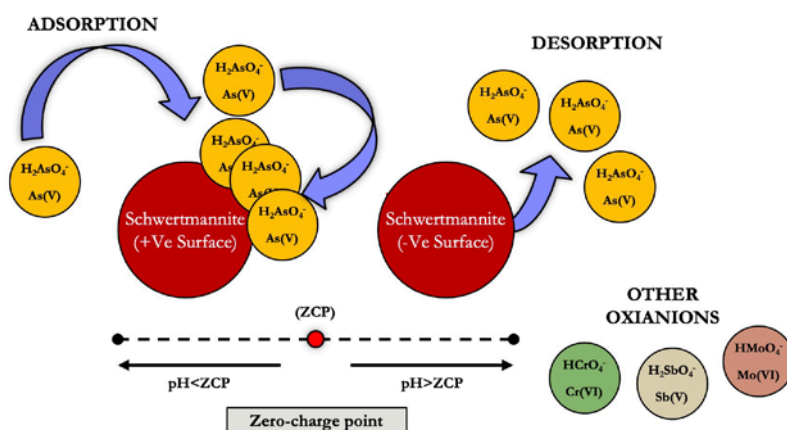


**Fig. 9.** Illustration of adsorption-desorption processes associated with the zero-charge point in schwertmannite.

### 3.3. Hydrochemical study of the Estuary of Huelva

A field study was required to provide a complete picture of the geochemical processes controlling metal mobility during mixing of AMD solutions and particulate matter with seawater observed in the laboratory. Thus, water samples during several sampling campaigns were collected by boat through the Estuary of Huelva, from the fluvial to the marine environment (Fig. 10). Samplings in the estuarine zone allowed us to locate the areas of neutralization

of the acid discharges and flocculation of precipitates. Water samplings were carried out using a Van Dorn bottle at 10 m depth to avoid possible contamination by the ship, except for surface waters where the sampling depth was around 5 m. To understand the behavior of metals during mixing, both total and dissolved contaminants were analyzed through the analysis of both filtered and unfiltered samples, the difference being those associated with particulate matter. Note that a non-conservative element tends to precipitate, and its concentration would pass from dissolved to particulate fraction; while a conservative element does not precipitate, so the concentrations in the particulate fraction would be negligible.

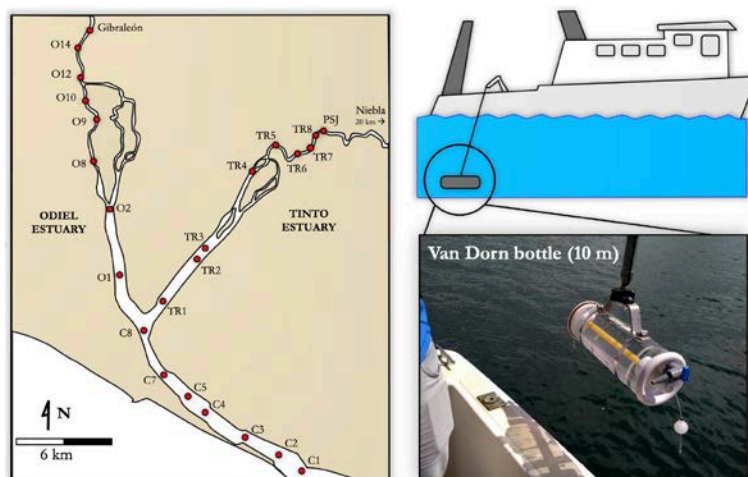


**Fig. 10.** Location of sampling points in the Estuary of Huelva: O points refer to Odíel river estuary, TR points to Tinto river estuary, and C points to the common estuarine channel, which is directed until the Atlantic Ocean.

In the Estuary of Huelva, an increase in pH from acidic fluvial values to alkaline values typical of the sea was observed. In the mixing zone (orange band; Fig. 11), the increase in pH is accompanied by a decrease in dissolved Fe concentrations. Arsenic concentrations first tend to decrease along with the decrease in Fe concentration. However, at pH values above 5.0-6.0 (vertical green dashed line), As concentrations again increase in solution while Fe continues to decrease. The concentration of Fe in solution decreases by mineral precipitation since Fe passes from being 100% in the dissolved fraction to 100% in the particulate fraction. Arsenic first precipitates together with Fe; however, at pH values close to neutrality the percentage of As associated with the dissolved fraction begins to increase until reaching 100% (Fig. 11).

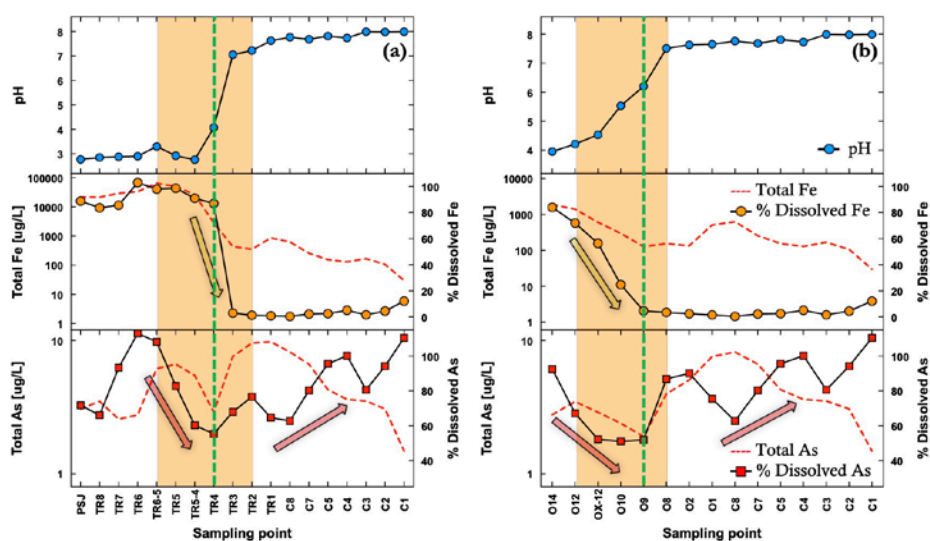


**Fig. 11.** Evolution of pH and total concentrations (principal Y-axis) and dissolved percentages (secondary Y-axis) of Fe and As along the estuaries of (a) Tinto and (b) Odíel rivers in a sampling conducted in May 2018.

Elements such as Al, REE, Y and, to a lesser extent, Cu seem to have also a non-conservative behavior in the estuary. The decrease in their total concentrations (dashed lines; Fig. 12) is due not only to dilution by seawater but also to mineral precipitation. This non-conservative behavior due to mineral precipitation is deduced since the percentages associated with the dissolved fraction with respect to the total (gray columns; Fig. 12) decrease during water mixing because these elements precipitate passing to the particulate matter fraction.

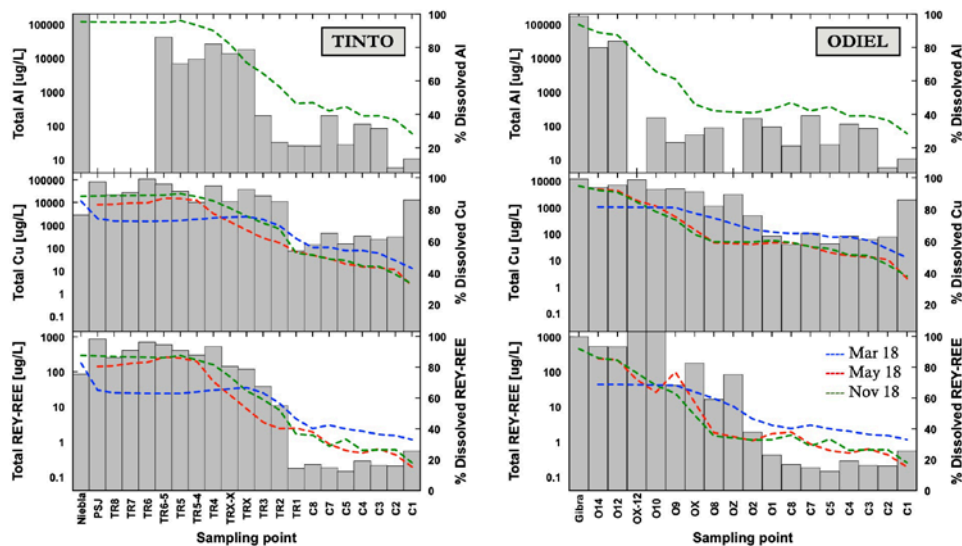


**Fig. 12.** Evolution of total concentrations (principal Y-axis) and dissolved percentages (secondary Y-axis) of Al, Cu, REE and Y along the estuaries of Tinto and Odiel rivers in three samplings conducted in March, May and November 2018 upon different hydrological conditions.

Iron chiefly precipitates during water mixing as schwertmannite; whereas Al precipitates as basaluminite (Fig. 13). However, the increase in dissolved As concentrations seems to be related to the release of As retained originally in schwertmannite precipitates at acidic conditions when pH values above their zero-charge point are reached in the estuary. These results support and further confirm previous laboratory results.

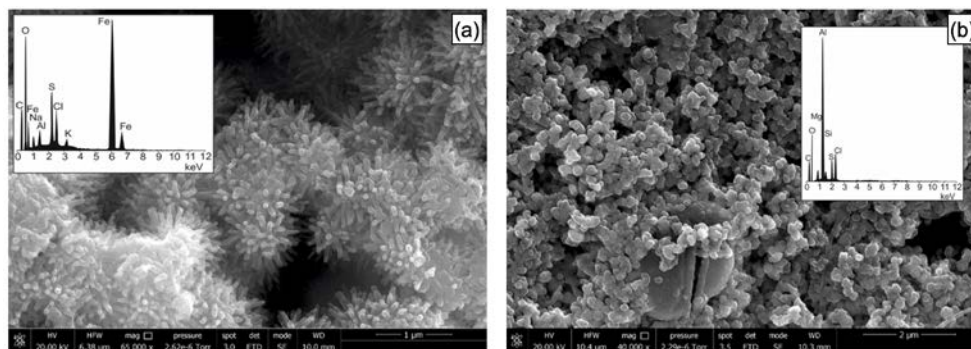


**Fig. 13.** SEM images and EDS analyses of (a) schwertmannite and (b) basaluminite precipitates found in particulate material from the Estuary of Huebra.

Other elements such as Zn, Cd, Co and Ni seem to have a quasi-conservative behavior in the estuary. The decrease in their total concentrations may be exclusively due to a dilution effect by seawater. No precipitation occurs during estuarine mixing as most of the total concentration of these elements is dominated by the dissolved fraction throughout the estuary (Fig. 14), also confirming the processes deduced in the laboratory.

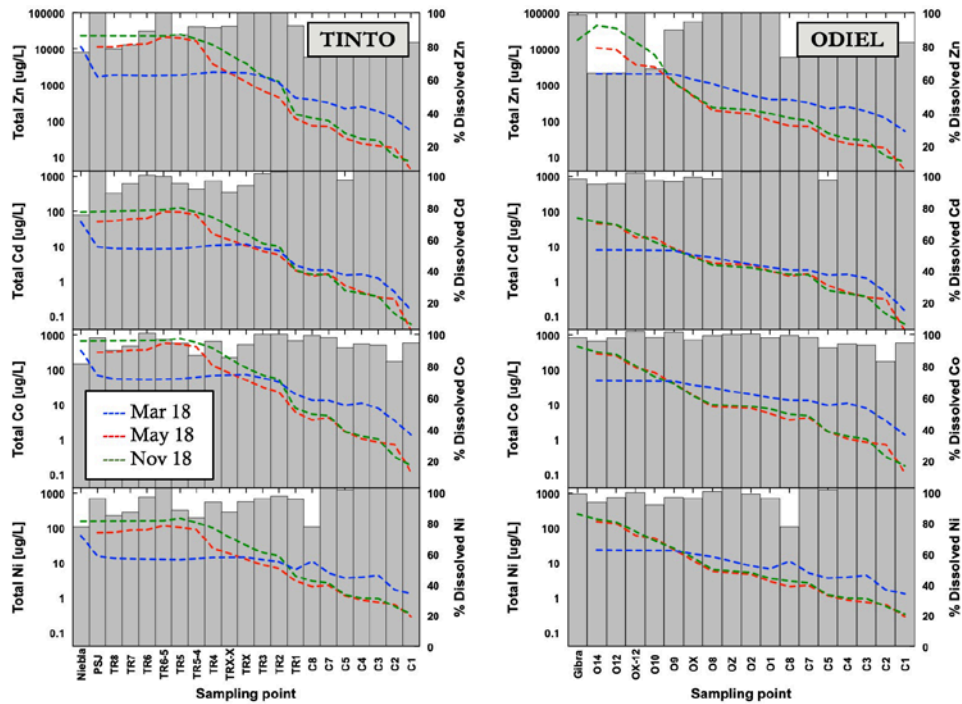


Fig. 14. Evolution of total concentrations (principal Y-axis) and dissolved percentages (secondary Y-axis) of Zn, Cd, Co and Ni along the estuaries of Tinto and Odiel rivers in three samplings conducted in March, May and November 2018 upon different hydrological conditions.

#### 4. Transference of potentially toxic elements to oceans

The seawater of the Gulf of Cadiz shelf is particularly enriched in dissolved metals, mainly Zn, Cd, As and Cu, compared to other coastal waters. These enrichments were first observed and analyzed during the 1980s by an oceanographic expedition organized by the Woods Hole Oceanographic Institution of Massachusetts (Spivack et al., 1983; Boyle et al., 1985; Sherrell & Boyle, 1988). In fact, the pollution plume circulates and dominates the chemical composition of the Atlantic entrance to the Mediterranean Sea through the Strait of Gibraltar (Van Geen et al., 1988). Initially, after analyzing the main rivers draining this part of the region (e.g., Guadalquivir and Guadiana rivers), these authors ruled out the fluvial input and explained this enrichment by a process of upwelling from deep ocean areas and sequestration of metals in the Gulf of Cadiz (Van Geen et al., 1991). Some years later, Elbaz-Poulichet & Leblanc (1996) were the first authors to focus the source of the metals in two secondary fluvial courses in relation to the rest: the Tinto and Odiel rivers, which was confirmed a year later by the same authors who detected the anomaly in the ocean (Van Geen et al., 1997).

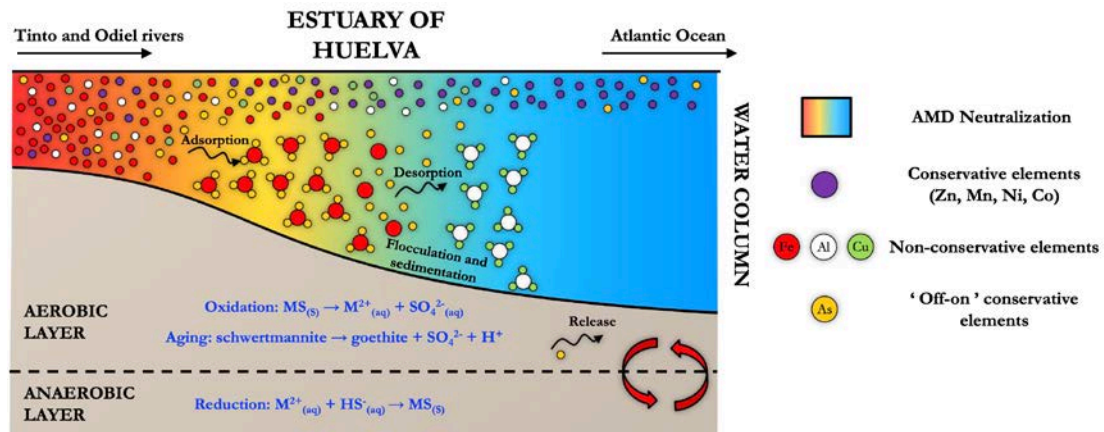


Fig. 15. Conceptual model of metal partitioning, indicating the processes that affect particulate matter from its flocculation to its sedimentation in the Estuary of Huelva during the mixing between AMD and seawater.

Currently, there is no scientific dispute regarding the fact that the metals circulating through the Gulf of Cadiz are discharged by the Tinto and Odiel rivers. This manuscript is dedicated to the geochemical processes that take place in the Estuary of Huelva, since it is the transition zone between the acidic fluvial discharges and the Atlantic Ocean. These processes would reveal the behavior of metals that are discharged into the Estuary of Huelva through the Tinto and Odiel rivers (Table 1). Special attention should be paid to conservative elements such as Cd, Zn, Co or Ni since the total amount discharged by both rivers would practically reach oceanic waters. Other elements such as As would have an OFF-ON behavior; that is, the schwertmannite that flocculates in the estuary adsorbs As (OFF) below a pH value close to 5.0, however, the As would be desorbed (ON), passing again to solution, when these precipitates reach the estuarine zones with pH values above 5.0. All these geochemical processes have been represented as conclusions in the conceptual model shown in Figure 15.

## ACKNOWLEDGMENTS

I would like to thank Dr. Juan Jiménez Millán (University of Jaen, Department of Geology) and the Spanish Society of Mineralogy (SEM) for their kind invitation to present this talk at the workshop “Continental sediment metal contamination by agricultural, industrial and mining activities: mineral processes and bioavailability” (Baeza, June 28<sup>th</sup>, 2022). This work was supported by the Spanish Ministry of Science and Innovation under the research project TRAMPA (PID2020-119196RB-C21).

## REFERENCES

- Acero, P., Ayora, C., Torrentó, C., Nieto, J.M. (2006): The behavior of trace elements during schwertmannite precipitation and subsequent transformation into goethite and jarosite. *Geochim. Cosmochim. Acta*, **70**, 4130-4139.
- Augustinus, P., Barton, C.E., Zawadzki, A., Harle, K. (2010): Lithological and geochemical record of mining-induced changes in sediments from Macquarie Harbour, southwest Tasmania, Australia. *Environ. Earth Sci.*, **61**, 625-639.
- Baeyens, W., Elskens, M., Gillain, G., Goeyens, L. (1998): Biogeochemical behaviour of Cd, Cu, Pb and Zn in the Scheldt estuary during the period 1981–1983. *Hydrobiologia*, **366**, 15-44.
- Bewers, J. & Yeats, P.A. (1989): Transport of river-derived trace metals through the coastal zone. *Neth. J. Sea Res.*, **23**, 359-368.
- Bigham, J.M., Schwertmann, U., Traina, S.J., Winland, R.L., Wolf, M. (1996): Schwertmannite and the chemical modeling of iron in acid sulfate waters. *Geochim. Cosmochim. Acta*, **60**, 2111-2121.
- Borrego, J., Morales, J.A., de la Torre, M.L., Grande, J.A. (2002): Geochemical characteristics of heavy metal pollution in surface sediments of the Tinto and Odiel river estuary (southwestern Spain). *Environ. Geol.*, **41**, 785-796.
- Boyle, E.A., Chapnick, S.D., Bai, X.X., Spivack, A.J. (1985): Trace metal enrichments in the Mediterranean Sea. *Earth Planet. Sc. Lett.*, **74**, 405-419.
- Braungardt, C.B., Achterberg, E.P., Elbaz-Poulichet, F., Morley, N.H. (2003): Metal geochemistry in a mine-polluted estuarine system in Spain. *Appl. Geochem.*, **18**, 1757-1771.
- Carro, B., Borrego, J., López-González, N., Grande, J.A., Gómez, T., de la Torre, M.L., Valente, T. (2011): Impact of acid mine drainage on the hydrogeochemical characteristics of the Tinto-Odiel Estuary (SW Spain). *J. Iberian Geol.*, **37**, 87-96.
- Consani, S., Carbone, C., Dinelli, E., Balić-Žunić, T., Cutroneo, L., Capello, M., Salviulo, G., Lucchetti, G. (2017): Metal transport and remobilisation in a basin affected by acid mine drainage: the role of ochreous amorphous precipitates. *Environ. Sci. Pollut. Res.*, **24**, 15735-15747.
- Dean, A.P., Lynch, S., Rowland, P., Toft, B.D., Pittman, J.K., White, K.N. (2013): Natural wetlands are efficient at providing long-term metal remediation of freshwater systems polluted by acid mine drainage. *Environ. Sci. Technol.*, **47**, 12029-12036.
- Elbaz-Poulichet, F. & Leblanc, M. (1996): Transfert de métaux d'une province minière à l'océan par des fleuves acides (Rio Tinto, Espagne). *C.R. Acad. Sci. Paris*, **322**, 1047-1052.
- , Braungardt, C., Achterberg, E., Morley, N., Cossa, D., Beckers, J.M., Nomérange, P., Cruzado, A., Leblanc, M. (2001): Metal biogeochemistry in the Tinto-Odiel rivers (Southern Spain) and in the Gulf of Cadiz: a synthesis of the results of TOROS project. *Cont. Shelf Res.*, **21**, 1961-1973.

- GESAMP (1987): Land/sea boundary flux of contaminants: contributions from rivers. Reports and Studies No. 32. IMO/FAO/UNESCO/WMO/WHO/IAEA/UN/UNEP Group of Experts on the Scientific Aspects of Marine Pollution. Paris.
- Hierro, A., Olías, M., Ketterer, M.E., Vaca, F., Borrego, J., Cánovas, C.R., Bolívar, J.P. (2014): Geochemical behavior of metals and metalloids in an estuary affected by acid mine drainage (AMD). *Environ. Sci. Pollut. Res.*, **21**, 2611-2627.
- Jung, H.B., Yun, S.T., Kwon, J.S., Zheng, Y. (2012): Role of iron colloids in copper speciation during neutralization in a coastal acid mine drainage, South Korea: Insight from voltammetric analyses and Surface complexation modeling. *J. Geochem. Explor.*, **112**, 244-251.
- Leblanc, M., Morales, J.A., Borrego, J., Elbaz-Poulichet, F. (2000): A 4500 years old mining pollution in Spain. *Econ. Geol.*, **95**, 655-662.
- Macías, F., Caraballo, M.A., Rötting, T.S., Pérez-López, R., Nieto, J.M., Ayora, C. (2012): From highly polluted Zn-rich acid mine drainage to non-metallic waters: Implementation of a multi-step alkaline passive treatment system to remediate metal pollution. *Sci. Total Environ.*, **433**, 323-330.
- Morris, A.W., Bale, A.J., Howland, R.J., Millward, G.E., Ackroyd, D.R., Loring, D.H., Rantala, R.T.T. (1986): Sediment mobility and its contribution to trace metal cycling and retention in a macrotidal estuary. *Water Sci. Technol.*, **18**, 111-119.
- Nieto, J.M., Sarmiento, A.M., Cánovas, C.R., Olías, M., Ayora, C. (2013): Acid mine drainage in the Iberian Pyrite Belt: 1. Hydrochemical characteristics and pollutant load of the Tinto and Odiel rivers. *Environ. Sci. Pollut. Res.*, **20**, 7509-7519.
- Nordstrom, D.K. & Alpers, C.N. (1999): Geochemistry of acid mine waters. In "The Environmental Geochemistry of Mineral Deposits", G.S. Plumlee & M.J. Logsdon, eds. *Rev. Econ. Geol.*, **6**, 133-160.
- Olías, M., Cánovas, C.R., Nieto, J.M., Sarmiento, A.M. (2006): Evaluation of the dissolved contaminant load transported by the Tinto and Odiel rivers (South West Spain). *Appl. Geochem.*, **21**, 1733-1749.
- Pérez-López, R., Asta, M.P., Román-Ross, G., Nieto, J.M., Ayora, C., Tucoulou, R. (2011): Synchrotron based X-ray study of iron oxide transformations in terraces from the Tinto-Odiel river system: Influence on arsenic mobility. *Chem. Geol.*, **280**, 336-343.
- Sáez, R., Pascual, E., Toscano, M., Almodóvar, G.R. (1999): The Iberian type of volcano-sedimentary massive sulphide deposits. *Miner. Depos.*, **34**, 549-570.
- Sánchez-España, J., Yusta, I., Díez-Ercilla, M. (2011): Schwertmannite and hydrobasaluminite: A re-evaluation of their solubility and control on the iron and aluminium concentration in acidic pit lakes. *Appl. Geochem.*, **26**, 1752-1774.
- Sarmiento, A.M., Nieto, J.M., Olías, M., Cánovas, C.R. (2009): Hydrochemical characteristics and seasonal influence on the pollution by acid mine drainage in the Odiel river Basin (SW Spain). *Appl. Geochem.*, **24**, 697-714.
- Sherrell, R.M. & Boyle, E.A. (1988): Zinc, chromium, vanadium, and iron in the Mediterranean Sea. *Deep-Sea Res.*, **35**, 1319-1334.
- Spivack, A.J., Huested, S.S., Boyle, E.A. (1983): Copper, nickel and cadmium in surface waters of the Mediterranean. In "Trace Metals in Seawater", C.S. Wong, E. Boyle, K.W. Bruland, J.D. Burton, E.D. Goldberg, eds. NATO Conference Series, vol 9. Springer, Boston, MA, 505-512.
- Van Geen, A., Rosener, P., Boyle, E.A. (1988): Entrainment of trace metal-enriched Atlantic shelf-water in the inflow Mediterranean Sea. *Nature*, **331**, 423-426.
- , Boyle, E.A., Moore, W. (1991): Trace metal enrichments in waters of the Gulf of Cadiz, Spain. *Geochim. Cosmochim. Acta*, **55**, 2173-2191.
- , Adkins, J.F., Boyle, E.A., Nelson, C.H., Palanques, A. (1997): A 120 yr record of widespread contamination from mining of the Iberian Pyrite Belt. *Geology*, **25**, 291-294.
- Zhou, J.L., Liu, Y.P., Abrahams, P.W. (2003): Trace metal behavior in the Conwy estuary, North Wales. *Chemosphere*, **51**, 429-440.

# Industrial trace element contamination in wetlands: the effect of the precipitation of biogenic sulfides

**Beata Smieja-Król**

Institute of Earth Sciences, Faculty of Natural Sciences, University of Silesia in Katowice, 60 Będzińska Str., 41-200 Sosnowiec, Poland, e-mail: beata.smieja-krol@us.edu.pl

## *Abstract*

Wetlands are conducive to precipitating and maintaining biogenic metal sulfide mineralization. The transformation of oxidized industrial contaminants into authigenic sulfides is widespread in contaminated wetlands, occurring even close (a few cm) to the surface and at only occasionally waterlogged sites. The characteristic feature of the authigenic sulfides is their strong spacial association with organic tissues. They commonly form micro-sized globular aggregates, more massive botryoidal or bulbous crusts on plant fragments, infillings in plant voids and cells, and pseudomorphs after microbial cells. Hidden in plant tissues or encapsulated in microbial biofilms, sulfides have increased resistance to oxidation and mechanical displacement. Most authigenic sulfides are nanocrystalline. Impurities, substitutions, solid solutions, and multi-sulfide submicrometre aggregates are common in addition to single-metal sulfide minerals. The trace elements sequestration into stable hardly-soluble secondary phases limits their mobility and toxicity, giving a chance for a safer environment if the wetlands are adequately managed. Additionally, contaminated wetlands can be used to understand the geochemical and biological evolution of the Earth and to reconstruct ancient ore deposits' genesis and mechanisms of formation.

## *Resumen*

Los humedales son ambientes propicios para la precipitación y el mantenimiento de las mineralizaciones de sulfuros metálicos biogénicos. La transformación de contaminantes industriales oxidados en sulfuros autigénicos es muy común en los humedales contaminados, produciéndose, incluso, cerca (unos pocos centímetros) de la superficie y solo ocasionalmente en lugares inundados. El rasgo característico de los sulfuros autigénicos es su fuerte asociación espacial con tejidos orgánicos. Por lo general, forman agregados globulares de tamaño micrométrico, costras botrioidales o bulbosas más masivas en fragmentos de plantas, rellenos en huecos y células de plantas, y pseudomorfos de células microbianas. Ocultos en tejidos vegetales o encapsulados en biopelículas microbianas, los sulfuros tienen una mayor resistencia a la oxidación y al desplazamiento mecánico. La mayoría de los sulfuros autigénicos son nanocristalinos. Además de los sulfuros de un solo metal, son comunes las impurezas, las sustituciones, las soluciones sólidas y los agregados submicrómetros de sulfuros múltiples. El secuestro de elementos traza en fases secundarias estables y poco solubles limita su movilidad y toxicidad, lo que brinda la posibilidad de conseguir un medio ambiente más seguro si los humedales se manejan adecuadamente. Además, los humedales contaminados se pueden utilizar para comprender la evolución geoquímica y biológica de la Tierra y para reconstruir la génesis y los mecanismos de formación de los antiguos depósitos de minerales..

**Key-words:** *metal sulfides; wetland; Recent Earth's surface processes, trace elements immobilization, sulfate reduction*

## **1. Introduction**

Sulfides are a large group of minerals from which several can precipitate under low pressure and temperature conditions of the Earth's surface (e.g., Baas Becking and Moore, 1961). Iron sulfides (pyrite, mackinawite, greigite) dominate due to the overwhelming abundance of Fe relative to other chalcophile metals in both marine and terrestrial sediments (Rickard et al., 2017). Larger accumulations of the less common sulfides in modern natural environments are rare (e.g., Lett and Fletcher, 1980; Yoon et al., 2012; Awid-Pascual et al., 2015). Conversely, they seem quite common in industry-affected regions. Biogenic sulfides were found in freshwater canal and river sediments, wetlands, soils, and flooded mines (Sobolewski, 1996; Gammons and Frandsen, 2001; Large et al., 2001;

Sonke et al., 2002; Moreau et al., 2004; Smicja-Król et al., 2015; Ciszewski et al., 2017; Mantha et al., 2019; Myagkaya et al., 2020; Quevedo et al., 2020). Human activities create unique geochemical conditions favorable for metal sulfide precipitation by modifying trace elements cycling on local and global scales. Mine drainage, for example, is often responsible for high sulfate concentrations in wetlands, i.e., a condition otherwise not encountered in freshwater wetlands.

Wetlands, which cover about 5 to 8% of the land surface, are especially well suited for contaminants immobilization and are often called "the kidneys of the landscape" because they function as the downstream receivers of water and wastes from both natural and human sources. They can be loosely defined as constantly or periodically waterlogged ecosystems that accumulate organic plant material that decomposes slowly and support various plants and animals adapted to saturated conditions (Mitsch and Gosselink, 2007). Several metal sequestration processes are envisaged in both natural and artificially constructed wetlands, occurring simultaneously or separated spatially and temporally (Figure 1). In addition to sulfide precipitation, these include particle sedimentation, plant uptake, sorption onto organic matter (mainly Cu, Ni, U, Pb), oxidation and hydrolysis (Fe, Al, Mn), carbonate precipitation (Fe, Cu, Ni), reduction to non-mobile forms (Cu, U, Cr, Se), and sorption onto metal hydroxides (As, Pb, Co, Ni, Zn, Cu, U), making wetlands extremely complex geochemical systems (Sobolewski, 1996; Sheoran and Sheoran, 2006).

The article summarizes the current state of knowledge on the biogenic sulfide formation in wetlands and its role in metal sequestration. Methods of sulfide identification, the textural and structural organization of the mineral phases, and precipitation conditions are presented. Finally, the implications of sulfide formation in the water-saturated contaminated sites are indicated.

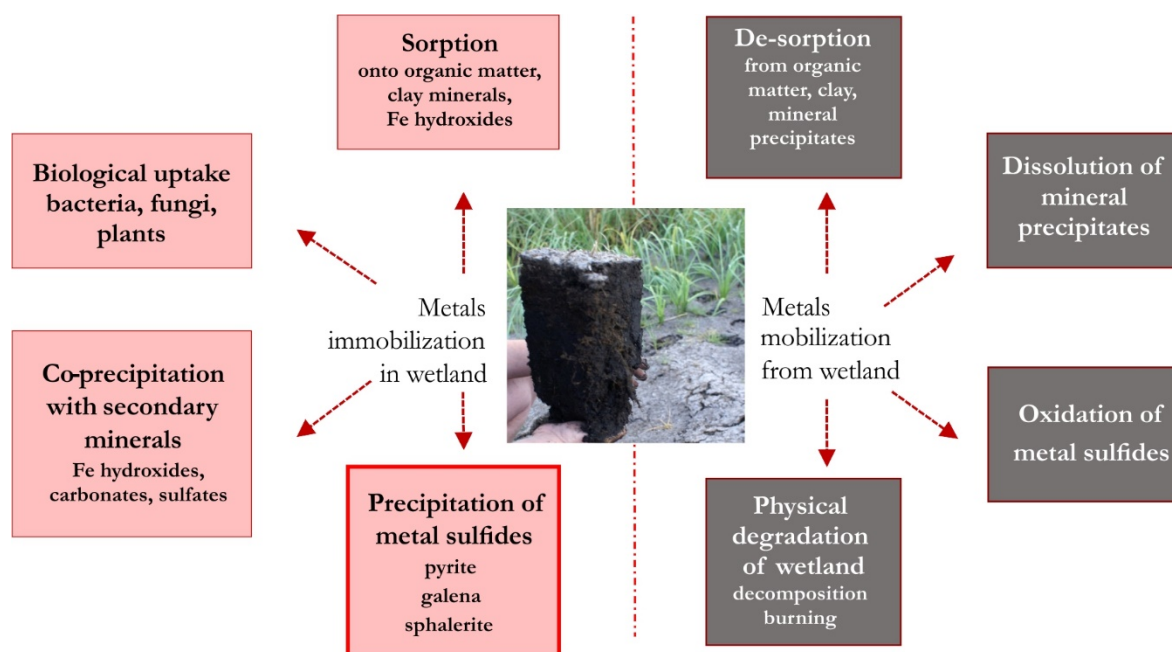


Fig. 1. Processes controlling metals behavior in contaminated wetlands.

## 2. Methods used for sulfide identification

Metal sulfide investigation in wetlands is challenging. The wetland sediment is a crumbling inhomogeneous mixture of organic and inorganic matter. Furthermore, it is water-saturated, redox-sensitive, and prone to alteration due to sample excavation and handling. Consequently, studies directly confirming the *in situ* precipitation of sulfide minerals are rare.

In the majority, the removal of metals by precipitation with sulfide is elaborated by monitoring changes in the aqueous chemistry of wetlands, e.g., the metal removal rates during sulfate reduction/sulfide generation (Machemer and Wildeman, 1992; Christensen et al., 1996; Webb et al., 1998; Batty et al., 2006). Also, seasonal changes in water sulfur isotopic composition ( $\delta^{34}\text{S}$ ) are indicative of active sulfide formation (Wu et al., 2011). Bacterial reactions

favor the lighter isotope ( $^{32}\text{S}$ ) so that fractionation is produced in going from a sulfate reactant to sulfide products (Konhauser, 2007).

Indirect methods used to estimate the fraction of metals incorporated into sulfide phases include acid-volatile sulfide (AVS) and chromium-reducible sulfides (CRS) extraction/distillation methods of Canfield et al. (1986) for monosulfide and disulfide minerals, respectively (Debusk et al., 1996; Moreau et al., 2013). Sequential extraction techniques involve using specific reagents to selectively dissolve phases in sediment with which metals may be associated. The technique is used to provide a quantitative measure of sulfides in wetlands (e.g., Sobolewski, 1999). All the methods are "operationally defined" and not always 100% selective. Most sequential extraction procedures (e.g., the Tessier scheme) significantly underestimate the content of metals associated with sulfide phases or do not distinguish organically bound metals from sulfides in organic-rich wetland sediments (Peltier et al., 2005).

Both optical and electron-beam microscopy provide direct evidence of sulfide occurrence in organic sediments. The size, shape, aggregation, relation to organic tissues, and semi-quantitative determination of chemical composition are best accomplished by analyzing whole mineralized plant remains using scanning electron microscopy (SEM). Several chemical fixation and dehydration techniques are used to preserve the organic part of the sample (plant cells, fungal hyphae, microbial cells, and exudates) and learn more about organic-mineral interactions (e.g., Fratesi et al., 2004). Quantitative chemical composition and trace substitutions are determined using mounts or thin sections and electron microprobe (EMPA). However, the small size and intermixture with organic components commonly result in low analytical totals (Moreau et al., 2013). Specific characterization at the nanometric level can be done using transmission electron microscopy (TEM). Selected area electron diffraction (SAED) is a crystallographic technique performed using TEM, which allows for identifying crystal structures, polycrystalline materials, and the measurement of crystal parameters, i.e., d-spacing even in very small crystallites. High-angle annular dark-field (HAADF) is a powerful method in the scanning transmission electron microscope (STEM) system providing Z-contrast images. HAADF allows recognizing subtle changes in chemical composition at nanometric distances, nanometer-sized inclusions, and detecting nanoporosity. A combination of focused ion beam (FIB) technology with TEM enables the extraction of desired mineral aggregate from the organic matter substance and conducting in-depth nanoscale observation (Wirth, 2009; Mantha et al., 2019; Smieja-Król et al., 2022a).

Synchrotron-based spectroscopy and diffraction analyses are perspective tools to quantify and determine the elemental speciation of metals and metalloids in wetlands (Yoon et al., 2012). They extend the range of structural and chemical investigation possible, allowing studies at low concentrations and with a redox-sensitive material.

### 3. Inventory of nonferrous sulfides identified in wetlands

Only a few sulfide minerals have been uniquely identified. Zinc sulfide is the best-elaborated and probably most common nonferrous sulfide formed in wetlands. It was found in peatlands contaminated through atmospheric deposition (Sonke et al., 2002; Smieja-Król et al., 2010; Smieja-Król et al., 2015), even at low bulk Zn contents in the organic sediment ( $\sim 200$  ppm). Zn sulfides were documented in natural wetlands receiving acid mine drainage (Moreau et al., 2013; Myagkaya et al., 2020) and anaerobic treatment wetland purifying storm waters in an industrially affected region (Butte, Montana; Gammons and Frandsen, 2001). Sphalerite (cubic ZnS) was confirmed using TEM in Pb-Zn smelter-contaminated peatland in Upper Silesia (Smieja-Król et al., 2022b). Wurtzite (hexagonal ZnS) was identified using synchrotron-based XRD to dominate over sphalerite in naturally metal-enriched peatland in western New York (Yoon et al., 2012).

Galena (PbS) forms in wetlands affected by Zn-Pb industry, although the phase is much less common than sphalerite despite comparable bulk Zn and Pb concentrations in the sediment (Smieja-Król et al., 2022a). Galena is easily identified by chemical composition and characteristic cuboidal shape using SEM. Its atomic structure was confirmed by STEM and TEM-SAED techniques (Smieja-Król et al., 2022b).

HgS was described by Myagkaya et al. (2020) to co-occur with ZnS. Polhemusite (Zn,Hg)S was suggested but not identified unambiguously.

The knowledge about Cu sulfide mineralogy in redox-sensitive ecosystems is derived mainly from laboratory experiments (Weber et al., 2009; Hofacker et al., 2013; Hoffmann et al., 2020). Chalcopyrite ( $\text{CuFeS}_2$ ) rims on pyrite framboids and idiomorphic covellite (CuS) grains, identified by reflected light microscopy and SEM, are known from an early work of Lett and Fletcher (1980) to precipitate in naturally copper-rich peatland in British Columbia. Sonke et al. (2002) identified chalcopyrite contours on plant cells by EMPA in the subsurface (0-8 cm) of contaminated peatland in Maatheide Natural Reserve.

## 4. Sulfide characteristics

The characteristic feature of the authigenic sulfides is their strong spatial association with organic tissues (Figure 2a and 2b): plant remains, bacterial cells, microbial biofilms, and fungal hyphae. They commonly form micro-sized globular aggregates, more massive botryoidal or bulbous crusts on plant fragments, infillings in plant voids and cells, and pseudomorphs after microbial cells or biogenic Ca oxalate crystals (e.g., Smieja-Król et al., 2014; Awid-Pascual et al., 2015; Myagkaya et al., 2020). Most authigenic sulfides are nanocrystalline. ZnS nanoparticles are within the range <3 to 80 nm (Yoon et al., 2012; Myagkaya et al., 2020; Smieja-Król et al., 2022a; Smieja-Król et al., 2022b). With time (counted in tens of years), the crystallinity of ZnS tends to increase. An aging mechanism was described as leading to the formation of submicrometre highly-defected platy crystals through an oriented attachment mechanism for sphalerite (Smieja-Król et al., 2022b). Galena forms slightly larger, defect-free crystals, between 10 nm to hundreds of nm, often with well-developed faces (Figure 2c). Large (up to 2.5  $\mu\text{m}$ ) spheroidal aggregates of nanometer-sized PbS particles were found inside fungal hypha and encrusting fungal spores (Smieja-Król et al., 2015). Individual PbS nanocrystals also reside inside ZnS aggregates (Smieja-Król et al., 2022a; Smieja-Król et al., 2022b).

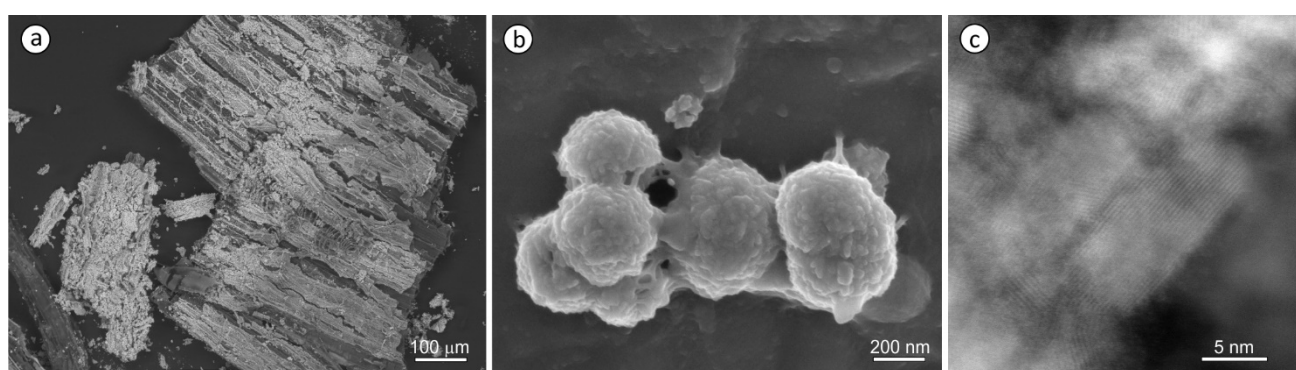


**Fig. 2.** Biogenic metal sulfides. (a) SEM BSE image of ZnS mineralized tissues of Equisetaceae; (b) spheroidal aggregates of ZnS attached to plant tissue by microbial biofilm (SEM SE); (c) TEM HAADF image of two galena nanocrystals.

The electron-beam techniques (SEM, TEM/STEM, EMPA) reveal impurities, substitutions, solid solutions, and multi-sulfide submicrometre aggregates to occur in wetland sediments in addition to single-metal sulfide minerals. Traces (up to a few wt%) of As, Se, Cu, Cd, Fe, and Ni were documented in authigenic ZnS (Sonke et al., 2002; Moreau et al., 2013; Myagkaya et al., 2020). Cu was shown to incorporate preferably in galena when only ZnS and PbS are present in organic sediment (Smieja-Król et al., 2015; Smieja-Król et al., 2022b). Due to the nanometer size of individual crystallites, distinguishing between a solid solution and a multi-metal sulfide aggregate is challenging even while using high-resolution TEM. Aggregates of  $\sim 10\text{nm}$  particles unresolvable in terms of a solid solution of sphalerite-metacinnabarite or a mixture of pure ZnS and HgS nanoparticles are a good example (Myagkaya et al., 2020). Aggregates of nanoparticles ( $<5\text{ nm}$ ) forming a true Zn-Cd sulfide solid solution in a cubic polytype (sphalerite-hawleyite) over a whole Zn/Cd range were documented using TEM-SAED and STEM-HAADF techniques. An intricate core-shell structure was revealed in which high-Zn outer layers encapsulate Cd-rich sulfide core. PbS inclusions (3-15 nm) occurred between the Cd-rich and Cd poor sulfide within nano sites of increased porosity (Smieja-Król et al., 2022a).

## 5. Controls of sulfide precipitation in wetlands

The critical requirement for sulfide precipitation at metal polluted sites is the availability of sulfide ions. In the low-temperature range ( $< \sim 80^\circ\text{C}$ ), sulfides are generated through sulfate reduction in a fully biologically mediated process. Due to high activation energy, the abiotic reaction is kinetically inhibited at low temperatures (Cross et al., 2004). Two main biological paths are recognized. The sulfide ions (or hydrogen sulfide) are produced during anaerobic respiration of some types of bacteria and archaea (so-called sulfate-reducing microorganisms; SRM) in excess of biodegradable organic matter serving as an electron donor. The process is known as dissimilatory sulfate reduction. Living organisms also reduce sulfur for incorporation into the principal organic sulfur compounds (e.g., amino acids, coenzymes, vitamins) within cells in a process known as assimilatory sulfate reduction. Assimilatory

sulfate reduction is an energy-requiring process and is assumed to be of lesser importance in terms of sulfide mineral formation (Konhauser, 2007).

Anaerobic condition is a commonly stated pre-requisite for maintaining SRM activity and sulfide mineral formation and persistence (Konhauser, 2007). Some studies even suggest that any oxygen ingress into the anaerobic zone is detrimental to metal sulfide precipitation (e.g., Dvorak et al., 1992; Johnson and Hallberg, 2005). However, wetlands are open systems and stay only mildly reducing, allowing for constant gas exchange with the atmosphere, i.e., ingress of oxygen (e.g., through plant roots), much enhanced during low water table, and liberation of reduced species (H<sub>2</sub>S, methane). Sulfide ions and dissolved oxygen co-occur in wetlands porewater (e.g., Smieja-Król et al., 2015). Still, the transformation of oxidized industrial contaminants into authigenic sulfides was detected close (a few cm) to the wetland surface and in wetlands only occasionally waterlogged (Sonke et al., 2002; Smieja-Król et al., 2022a). This can be explained by a diffusion-limited solute exchange in the complex network of wetland pores and the coexistence of diverse groups of microorganisms, which create steep redox gradients between aerated and oxygen-depleted microsites. A close association of the sulfide minerals with decaying vascular plant roots and litter is observed in wetland sediments (Sonke et al., 2002; Smieja-Król et al., 2015; Smieja-Król et al., 2022a).

The organic matter's high affinity to some metals and precipitation of other minerals, mainly Fe hydroxides, controls the chemical composition and mineral assemblage of the sulfides. Especially Cu and Pb ions are agreed to be effectively bound by organic matter, in both solid and dissolved form, limiting the availability of free Pb and Cu ions to react with the sulfide. In contrast, Zn and Cd adsorb rather weakly on organic matter, silicate clays, and oxides at the usual wetland pH, favoring the precipitation of Zn and Cd over Pb and Cu sulfides. Additionally, Fe tends to precipitate as Fe hydroxides (goethite, ferrihydrite) in wetlands with fluctuating water table levels or is stabilized in the ferric form (Fe<sup>3+</sup>) by complexation with organic matter (Syrovetsnik et al., 2007; Bhattacharyya et al., 2018). The preferred preservation of iron in the ferric state in wetlands suppresses the Fe(II) ions activity and allows for the precipitation of the less common sulfides.

## 5. Implications of sulfide precipitation in wetlands

Trace elements are effectively sequestered into sulfide phases in contaminated wetlands limiting their mobility and toxicity. The wetlands' primary role is to sustain SRM activity by delivering biodegradable organic matter and limiting oxygen penetration. Precipitation inside plant tissues or encapsulation in microbial biofilms increases sulfides resistance to oxidation and mechanical displacement during flooding or short-term water table lowering. Based on thermodynamic data, metal sulfides are extremely insoluble phases, which means they can precipitate at very low ions concentrations in solution (theoretically <1 µg/l), lowering the dissolved metal and sulfide ion concentrations in water well below the environmentally permissible thresholds. On the other hand, the heavily contaminated wetlands constitute a danger of changing from net sinks to net sources of trace elements and sulfate, causing water-quality degradation (Figure 1; Sobolewski 1999; Eimers et al., 2003; Adkinson et al., 2008). The release of the contaminants into water is possible in unfavorable conditions of a prolonged drought, cessation of mine water discharges, or a change of land use. Hardly soluble, sulfides are prone to oxidative dissolution (Barrett and McBride, 2007). Consequently, a safer environment is the ultimate benefit of the in-depth research into the mechanisms that govern sulfide formation and preservation in wetlands, allowing for long-term rational management of the contaminated sites and more efficient designs for artificially constructed wetlands. From a broader perspective, sites extremely polluted by human activities undergo extensive transformation by Earth's surface processes, becoming similar to metal accumulations known from geological records. Vast amounts of metals that transform over time into stable secondary sulfide phases in some wetlands can be considered human-induced ore deposits, adding to the list of significant anthropogenic impacts on Earth's geology, leading recently to the recognition and formalization of the Anthropocene. A concept of human-made deposits has already been introduced by Saryg-ool et al. (2017). Finally, contaminated wetlands can be used to understand the geochemical and biological evolution of the Earth and to reconstruct ancient ore deposits' genesis and mechanisms of formation.

## References

- Adkinson, A., Watmough, S.A., Dillon, P.J. (2008): Drought-induced metal release from a wetland at Plastic Lake, central Ontario. *Can. J. Fish. Aquat. Sci.*, **65**, 834-845.
- Awid-Pascual, R., Vadim, S., Kamenetsky, V.S., Goemann, K., Allen, N., Noble, T.L., Lottermoser, B.G., Rodemann, T. (2015): The evolution of authigenic Zn–Pb–Fe-bearing phases in the Grieves Siding peat, western Tasmania. *Contrib. Mineral. Petrol.*, **170**, 17.
- Baas Becking, L.G.M. & Moore, D. (1961): Biogenic sulfides. *Econ. Geol.*, **56**, 259-272.

- Barrett, K.A., McBride, M.B., (2007): Dissolution of zinc-cadmium sulfide solid solutions in aerated aqueous suspension. *Soil Sci. Soc. Am. J.*, **71**, 322-328.
- Batty, L.C., Baker, A.J.M., Wheeler, B.D. (2006): The effects of vegetation on porewater composition in a natural wetland receiving acid mine drainage. *Wetlands*, **26**, 40-48.
- Bhattacharyya, A., Schmidt, M.P., Stavitski, E., Martinez, C.E. (2018): Iron speciation in peats: Chemical and spectroscopic evidence for the co-occurrence of ferric and ferrous iron in organic complexes and mineral precipitates. *Org. Geochem.*, **115**, 124-137.
- Canfield, D.E., Raiswell, R., Westrich, J.T., Reaves, C.M., Berner, R.A. (1986): The use of chromium reduction in the analysis of reduced inorganic sulfur in sediment sand shales. *Chem. Geol.*, **54**, 149-155.
- Christensen, B., Laake, M., Lien, T. (1996): Treatment of acid mine water by sulfate-reducing bacteria; results from a bench-scale experiment. *Water Res.*, **30**, 1617-1624.
- Ciszewski, D., Kucha, H., Skwarczek, M. (2017): Authigenic minerals and sediments in the hyporheic zone of the Biala Przemsza River polluted by metal ore mining. *Przegląd Geologiczny*, **65**, 650-660.
- Cross, M.M., Manning, D.A.C., Bottrell, S.H., Worden, R.H. (2004): Thermochemical sulphate reduction (TSR): experimental determination of reaction kinetics and implications of the observed reaction rates for petroleum reservoirs. *Org. Geochem.*, **35**, 393-404.
- Debusk, T.A., Laughlin, R.B., Schwartz, L.N. (1996): Retention and compartmentalization of lead and cadmium in wetland microcosms. *Water Res.*, **30**, 2707-2716. DOI:10.1016/s0043-1354(96)00184-4
- Dvorak, D.H., Hedin, R.S., Edenborn, H.M., McIntyre, P.E. (1992): Treatment of metal-contaminated water using bacterial sulfate reduction: results from pilot scale reactors. *Biotechnol. Bioeng.*, **40**, 609-616.
- Eimers, M.C., Dillon, P.J., Schiff, S.L., Jeffries, D.S. (2003): The effects of drying and re-wetting and increased temperature on sulphate release from upland and wetland material. *Soil Biology and Biochemistry* **35**, 1663-1673.
- Fratesi, S.E., Lynch, F.L., Kirkland, B.L., Brown, L.R. (2004): Effects of SEM preparation techniques on the appearance of bacteria and biofilms in the carter sandstone. *J. Sediment. Res.*, **74**, 858-867.
- Gammons, C. H. & Frandsen A.K. (2001): Fate and transport of metals in H<sub>2</sub>S-rich waters at a treatment wetland. *Geochem. Trans.* **1**, 1–15.
- Hofacker, A.F., Voegelin, A., Kaegi, R., Weber, F.-A., Kretzschmar R. (2013): Temperature-dependent formation of metallic copper and metal sulfide nanoparticles during flooding of a contaminated soil. *Geochim. Cosmochim. Acta* **103**, 316-332.
- Hoffmann, K., Bouchet, S., Christl, I., Kaegi, R., Kretzschmar, R. (2020): Effect of NOM on copper sulfide nanoparticle growth, stability, and oxidative dissolution. *Environ. Sci.: Nano*, **7**, 1163-1178.
- Hsu, S.C., Maynard, J.B. (1999): The use of sulfur isotopes to monitor the effectiveness of constructed wetlands in controlling acid mine drainage. *Environ Eng. and Policy* **1**, 223-233.
- Johnson, D.B., Hallberg, K.B. (2005): Acid mine drainage remediation options: a review. *Sci. Total Environ.* **338**, 3-14.
- Konhauser, K., (2007): *Introduction to Geomicrobiology*. Blackwell Publishing, UK. 425 p.
- Large, D.J., Fortey, N.J., Milodowski, A.E., Christy, A.G., Dodd J. (2001): Petrographic observations of iron, copper, and zinc sulfides in freshwater canal sediment. *J. Sediment. Res.*, **71**, 61-69.
- Lett, R.E.W., & Fletcher, W.K. (1980): Syngenetic Sulphide Minerals in a Copper-rich Bog. *Mineral. Deposita*, **15**, 61-67.
- Machemer, S.D., & Wildeman, T.R. (1992): Adsorption compared with sulfide precipitation as metal removal processes from acid mine drainage in a constructed wetland. *J. Contam. Hydrol.*, **9**(1-2), 115-131. DOI:10.1016/0169-7722(92)90054-i
- Mantha, H., Schindler, M., Hochella, M.F. (2019): Occurrence and Formation of incidental metallic Cu and CuS nanoparticles in organic-rich contaminated surface soils in Timmins, Ontario. *Environ. Sci.: Nano* **6**, 163.
- Mitsch W.J. & Gosselink J.G. (2007): *Wetlands*. J. Wiley and Sons, Inc., New Jersey. 582 p.
- Moreau, J.W., Fournelle, J.H., Banfield, J.F. (2013): Quantifying heavy metals sequestration by sulfate-reducing bacteria in an acid mine drainage-contaminated natural wetland. *Front. Microbiol.* **4**, 1-10.
- , Webb, R.I., Banfield, J.F. (2004): Ultrastructure, aggregation-state, and crystal growth of biogenic nanocrystalline sphalerite and wurtzite. *Am. Mineral.*, **89**, 950-960.
- Myagkaya, I.N., Lazareva, E.V., Zhmodik, S.M., Zaikovskiy, V.I. (2020): Interaction of natural organic matter with acid mine drainage: authigenic mineralization (case study of Kursk sulfide tailings, Kemerovo region, Russia). *J. Geochem. Explor.*, **211**, 106456.
- Peltier, E., Dahl, A.L., Gaillard, J.F. (2005): Metal Speciation in Anoxic Sediments: When Sulfides Can Be Construed as Oxides. *Environ. Sci. Technol.*, **39**, 311-316.

- Quevedo, C.P., Jiménez-Millán, J., Cifuentes, G.R., Jiménez-Espinosa, R. (2020): Electron microscopy evidence of Zn bioauthigenic sulfides formation in polluted organic matter rich sediments from the Chicamocha river (Boyacá-Colombia). *Minerals*, **10**, 1–17.
- Rickard, D., Musmann, M., Steadman, J.A. (2017): Sedimentary Sulfides. *Elements*, **13**, 117-122.
- Saryg-ool, B.Y., Myagkaya, I.N., Kirichenko, I.S., Gustaytis, M.A., Shuvaeva, O.V., Zhmodik, S.M., Lazareva, E.V. (2017): Redistribution of elements between wastes and organic-bearing material in the dispersion train of gold-bearing sulfide tailings: Part I. Geochemistry and mineralogy. *Sci. Total Environ.*, **581-582**, 460-471.
- Sheoran, A.S., Sheoran, V. (2006): Heavy metal removal mechanism of acid mine drainage in wetlands: a critical review. *Miner. Eng.*, **19**, 105-116.
- Smieja-Król, B., Fialkiewicz-Kozielec, B., Sikorski, J., Palowski B. (2010): Heavy metal behaviour in peat - a mineralogical perspective. *Sci. Total Environ.*, **408**, 5924-5931.
- , Janeczek, J., Bauerek, B. and Thorseth, I.H. (2015): The role of authigenic sulfides in immobilization of potentially toxic metals in the Bagno Bory wetland, southern Poland. *Environ. Sci. Pollut. Res.*, **22**, 15495-15505.
- , —, Wiedermann, J. (2014): Pseudomorphs of barite and biogenic ZnS after phyto-crystals of calcium oxalate (whewellite) in the peat layer of a poor fen. *Environ. Sci. Pollut. Res.* **21**, 7227-7233.
- , Pawlyta, M., Galka, M. (2022a): Ultrafine multi-metal (Zn, Cd, Pb) sulfide aggregates formation in periodically water-logged organic soil. *Sci. Total Environ.*, **820**, 153308.
- , —, Kądziołka-Gaweł, M., Fialkiewicz-Kozielec, B. (2022b): Formation of Zn and Pb sulfides in a redox-sensitive modern system due to high atmospheric fallout. *Geochim. Cosmochim. Acta*, **318**, 126-143.
- Sobolewski, A. (1999): A Review of Processes Responsible for Metal Removal in Wetlands Treating Contaminated Mine Drainage. *Int. J. Phytoremediation*, **1:1**, 19-51, DOI: 10.1080/15226519908500003
- Sonke, J.E., Hoogewerff, J.A., van der Laan, S.R., Vangronsveld, J. (2002): A chemical and mineralogical reconstruction of Zn-smelter emissions in the Kempen region (Belgium), based on organic pool sediment cores. *Sci. Total Environ.*, **292**, 101-119.
- Syrovetnik, K., Malmström, M.E., Neretnieks, I. (2007): Accumulation of heavy metals in the Oostriku peat bog, Estonia: Determination of binding processes by means of sequential leaching. *Environ. Pollut.*, **147**, 291-300.
- Webb, J.S., McGinness, S., Lappin-Scott, H. (1998): Metal removal by sulphate-reducing bacteria from natural and constructed wetlands. *J. Appl. Microbiol.*, **84**(2), 240-248.
- Weber, F.-A., Voegelin, A., Kretzschmar R. (2009): Multi-metal contaminant dynamics in temporarily flooded soil under sulfate limitation. *Geochim. Cosmochim. Acta*, **73**, 5513-5527.
- Wirth, R. (2009): Focused ion beam (FIB) combined with SEM and TEM: advanced analytical tools for studies of chemical composition, microstructure and crystal structure in geomaterials on a nanometre scale. *Chem. Geol.*, **261** (3-4), 217-229.
- Wu, S., Jeschke, C., Dong, R., Paschke, H., Kusch, P., Knoller, K. (2011): Sulfur transformations in pilot-scale constructed wetland treating high sulfate-containing contaminated groundwater: A stable isotope assessment. *Water Res.*, **45**, 6688-6698.
- Yoon, S., Yáñez, C., Bruns, M.-V., Martínez C.E. (2012): Natural zinc enrichment in peatlands: Biogeochemistry of ZnS formation. *Geochim. Cosmochim. Acta*, **84**, 165-176.



Sociedad Española de Mineralogía  
© Museo Geominero del Instituto Geológico  
y Minero de España  
Ríos Rosas, 23  
28003 Madrid

# SEM



Universidad  
de Jaén



CEACTEMA  
CENTRO DE ESTUDIOS AVANZADOS  
EN CIENCIAS DE LA TIERRA,  
ENERGÍA Y MEDIO AMBIENTE

un  
i Universidad  
Internacional  
de Andalucía  
A



Fundación  
CAJA RURAL JAÉN



SEM  
Sociedad Española de Mineralogía



Universidad de Jaén



Junta de Andalucía  
Categoría de Transformación Económica,  
Industria, Conocimiento y Universidades



Unión Europea  
Fondo Europeo  
de Desarrollo Regional



Andalucía  
se mueve con Europa

Proyecto de Investigación FEDER UJA 2020. Solubilidad, agregación y fijación mineral de contaminantes agrícolas nanoparticulados de metales: papel de los sedimentos de ambientes lacustres salinos. (Referencia 1380934)



Universidad  
de Jaén  
Escuela de Doctorado

Programa de Doctorado en  
Ciencia y Tecnología de la Tierra y  
del Medio Ambiente